Integrated hydrologic modeling as a key for sustainable development planning of urban water resources in the semi-arid watersheds of the Gaza Strip

Dissertation

zur

Erlangung des Doktorgrades (Dr. rer. nat.)

der

Mathematisch-Naturwissenschaftlichen Fakultät

der

Rheinischen Friedrich-Wilhelms-Universität Bonn

vorgelegt von

Tamer Eshtawi

aus

Gaza, Palästina

Bonn, 2015

1. Gutachter: Prof. Dr. M. Evers

2. Gutachter: Prof. Dr. B. Diekkrüger

Tag der Promotion: 07.07.2015

Erscheinungsjahr: 2015

Acknowledgements

First and foremost, thanks be to Allah for all my blessings.

I would like to express my sincere gratitude to my supervisor Prof. Mariele Evers for her continuous support, advice, and motivation throughout my time as her doctoral student.

Besides my supervisor, I would like to thank my second supervisor Prof. Bernd Diekkrüger and my academic advisor at the Center for Development Research (ZEF) Dr. Bernhard Tischbein for their encouragement and insightful comments. Thanks also go to the rest of my thesis committee.

I would like to express my deepest thanks to the German Federal Ministry for Economic Cooperation and Development (BMZ) for the PhD scholarship via the German Academic exchange service (DAAD). Thanks also to the Fiat Panis Foundation for supporting this research during the period of data collection.

I am grateful for the academic, logistics and social support I received at ZEF during my PhD study in Bonn; I was very pleased with courses, seminars, scientific and social events I attended there. Special mention goes to Dr. Günther Manske, coordinator of the doctoral program at ZEF, for his interesting support.

I would also like to thank the Palestinian Water Authority (PWA) and Coastal Municipalities Water Utility in Palestine (CMWU) for their support during the period of data collection. Special thanks go to Eng. Jamal Eldadah for his support through invaluable data and up-to-date reports.

Finally, but by no means least, thanks go to my mother and father for consistent support with their wishes and prayers. Special mention goes to my beloved wife for standing by me throughout my study period. I dedicate this thesis to my children Asad, Alma, and Kenan and to my sister, brother, and friends.

Abstract

This study demonstrates the strength of using integrated hydrologic modeling in a sustainable urban water planning process. It provides a complete view of the urban water system of the Gaza Strip, quantifies the urban water budget interaction with sufficient spatial and temporal details, and supports realistic scenarios inferred from the decision-making agenda. This study comprises three main parts. The first part aims to quantify the impact of urban area expansion on groundwater recharge and surface runoff by developing surface water modeling and investigating the response of watersheds to urban development. The second part provides a spatial-temporal assessment of potential impacts of urban area expansion on groundwater level concerning the link between surface and groundwater models. The third part promotes an integrated hydrologic modeling as a key for sustainable urban water resources considering the coupling of surface water, groundwater flow, and solute transport models.

In the first part, a new spatial evaluation for assessing the impact of urbanization was applied for the semi-arid watersheds intersecting with the Gaza coastal aquifer. The SWAT model was calibrated and validated in a semi-automated approach for stream flow in the main watersheds. The results show that the model could simulate water budget components adequately within the complex semi-arid watersheds. Linear relationships between the change in urban area and the corresponding change in surface runoff or percolation were concluded for the urbanized subbasins. The urban-surface runoff index (USI) and the urban-percolation index (UPI) were developed to represent a micro-level evaluation of different urban change scenarios in the subbasins. The global urban-surface runoff index (GUSI) and the global urban-percolation index (GUPI) were derived as macro-level factors reflecting the influence on the overall Gaza coastal aquifer due to urban area expansion.

In the second part, a 3-D groundwater flow model was developed using MODFLOW-USG to investigate the groundwater levels within the Gaza coastal aquifer. Recharge estimation is based on a comprehensive approach including the connection to the surface water model (SWAT) for determining percolation from rainfall as well as detailed approaches regarding further recharge components. An unstructured grid (Voronoi cells) generated by MODFLOW-USG engine was used to reduce run time within complicated aquifer boundary conditions. The results indicate a very good fit between measured and simulated heads. Long-term forecasting (2004–2030) of the groundwater levels was carried out as an essential step to support realistic and sustainable water resources planning and decision making. The increasing built-up area was linked to the potential impacts of urban expansion relating to water supply quantities and groundwater recharge components. The percolation was reduced temporally and spatially in the forecasting period based on the projected built-up area as well as the urban-percolation index. Considering the current management situation, the annual groundwater level correlated negatively with the increasing built-up area; the regression line slope was -0.056 m/km^2 for the average groundwater levels while it became steeper at -0.23 m/km^2 in sensitive locations in the southern part of the Gaza Strip. The groundwater-level trend index was developed as a spatial indicator for the appropriate management alternatives that can achieve less negative trend index.

In the last part of this study, a coupling of surface water (SWAT), groundwater (MODFLOW) and solute transport (MT3DMS) models was performed to quantify surface-groundwater and quantity-quality interactions under urban area expansion. The results indicate a good fit between measured and simulated nitrate and chloride concentrations. The response of groundwater level, nitrate concentrations (related to human activities) and chloride concentrations (related to seawater intrusion) to urban area expansion and corresponding changes in the urban water budget were examined on a macro-scale level (the Gaza coastal aquifer domain). The potentials of non-conventional water resources scenarios, namely desalination, stormwater harvesting and treated wastewater reuse as well as an infrastructure performance scenario were investigated. In a novel analysis, groundwater improvement and deterioration under each scenario were defined and discussed in spatial-temporal and statistical approaches. The quality deterioration cycle index was estimated as the ratio between the amounts of low and high quality recharge components within the Gaza Strip boundary predicted for year 2030. The improvement index for groundwater level (IIL) and the improvement index for groundwater quality (IIQ) were developed for the scenarios as measures of the effectiveness toward sustainable groundwater planning.

Table of contents

Figures

Tables

CHAPTER 1

1 General introduction

1.1 Motivation for research

Hydrology was concisely defined by Penman (1961) as the science needed to answer the question "what happens to the rain?" Hydrologic models have been developed to answer Penman's question at different spatial scales (micro to macro) and varied purposes (Singh and Woolhiser, 2002). The integrated hydrologic modeling has become a hot topic illustrating a significant temporal flux and storage connection between surface water and groundwater (Ross *et al*., 2004). The impacts of human activities on water resources have directed integrated hydrologic models toward answering more complicated questions than Penman's. "What happens to the urban water system?" could be a state-of-the-art research question in hydrology, where the urban water system concept fully integrates human activities and biophysical processes in the urbanized watersheds. Different studies applied integrated hydrologic modeling to general problems of water resources (Castronova *et al*., 2013; Bhatt *et al*., 2014; McNider *et al*., 2014; Srivastava *et al*., 2014; Panagopoulos *et al*., 2015). Based on science research websites, it can be said that relatively few studies to date have applied integrated hydrologic modeling in the context of urban water system planning, in particular in the context of potential non-conventional water resources in relation to sustainable water resources. Improving the information base and providing appropriate management indicators are essential steps to support proper development planning processes. The quantitative evaluation of the impacts of human activities on water resources is the focus of present research in hydrology (Chu *et al*., 2010).

Water is the most important natural resource, especially in the arid or semi-arid zones that face high population growth, scarcity of freshwater, irregularity of rainfall, excessive land-use change and increasing vulnerability to risks such as drought, desertification and pollution (Fadil *et al*., 2011). The Gaza Strip (Fig. 1.1) is a narrow coastal strip located on the

south-eastern coast of the Mediterranean Sea with a land area covering 365 km^2. Gaza has a water crisis and faces serious challenges for the future sustainability of its water resources. Gaza has a sub-aquifer, which is a part of the larger coastal aquifer. Different governmental reports and scientific studies (PWA, 2013; HWE, 2010) estimated the abstracted water from the Gaza coastal aquifer at around 150–170 Mm^3/y. The total replenishment of the aquifer from the natural (such as rainwater) and anthropogenic (agricultural return flow and waste water) sources is around 100 Mm^3/y. These results reveal that Gaza has a current water deficit of approximately 50–70 Mm^3/y. In addition to the lack of water, mainly a consequence of the semi-arid climate, the overall water quality is also poor, and the Gaza aquifer is polluted by high levels of nitrates and chlorides. Chloride (a seawater intrusion indicator) and nitrate (a human activities indicator) are the main indicators for the groundwater quality in the Gaza coastal aquifer. The Gaza aquifer has mostly nitrate levels over 100 mg/l and chloride levels averaging 1000 mg/l (CMWU, 2013). Salinity caused by seawater intrusion has increased over time. In many areas of the Gaza Strip, the total dissolved solids have exceeded 1000 mg/l and even 3000 mg/l in some areas (Al-Khatib *et al*., 2009). Pollution of the water resources poses a threat to the sustainability of the urban water system in the Gaza Strip.

Therewith, Gaza is a typical example of a coastal region under pressure of land use changes. Additional challenges result from a high population density; a dependency on groundwater as the only water resource; a high water demand for agricultural, domestic and industrial use. Thus, proper development planning is urgently needed to solve these problems and to ensure a sustainable water environment in the future. In order to do so, it is essential to improve the information base and provide appropriate management indicators.

The previous studies focused on the evaluation of the current situation of the water environment of the Gaza strip region and mainly considered specific questions or single components of the urban water system. This study overcomes the shortage of previous studies on considering the interrelations between surface water and groundwater in the context of sustainable water resources in the urban water system. It applies an innovative approach by quantifying the spatial trade-offs and synergies between the urban water system components of the Gaza Strip considering the potential for use of non-conventional water resources in addition to or in order to replace groundwater use and, as a consequence, support a sustainable water environment.

This study answers the question "how can integrated hydrologic modeling assist decision-makers toward achieving sustainable urban water resources in the semi-arid watersheds of the Gaza Strip?"

Figure 1.1 Gaza Strip (Wikipedia, 2013; UN-ESCWA and BGR, 2013)

1.2 Research objectives

This study is directed to assist decision makers to advance towards achieving sustainable urban water planning in the Gaza Strip by improving integrated hydrologic modeling of the water resources system and developing a multidimensional analysis within the urban water system. It demonstrates the potential use of non-conventional water resources by quantifying their impacts in the context of groundwater sustainability. The main objective of this study is addressed in three main parts and eight specific objectives.

1.2.1 Research objectives (part 1)

The first part aims to quantify the impact of urban area expansion on groundwater recharge and surface runoff by developing surface water modeling and investigating the response of watersheds to urban development.

This part is innovative as it considers all watersheds intersecting with the Gaza aquifer domain and also calibrates the Soil and Water Assessment Tool (SWAT) model parameters to quantify the impact of urban area expansion on the coastal aquifer recharge and surface runoff in a spatial approach. The specific objectives of this part are (1) calibration and validation of the SWAT model in terms of stream flow for three gauges in the main watersheds intersecting with the Gaza costal aquifer, and (2) spatial evaluation and quantification of the impact of urban land-use change on percolation and surface runoff at the subbasin and Gaza coastal aquifer level.

1.2.2 Research objectives (part 2)

The second part aims to develop a spatial-temporal assessment of potential impacts of urban area expansion on groundwater level focusing on the link between surface and groundwater models.

The specific objectives of this part are (1) develop a 3-D groundwater flow model to investigate the groundwater levels within the Gaza coastal aquifer considering the connection to the SWAT model as well as a high-precision estimation of other recharge components, (2) assess the long-term trend of groundwater levels and determine the distribution across the Gaza Strip.

1.2.3 Research objectives (part 3)

The third part promotes an integrated hydrologic modeling as a key for sustainable urban water resources considering the coupling of surface water, groundwater flow, and solute transport models under different scenarios of non-conventional water resources.

The specific objectives include: (1) provide a complete view of the urban water budget components (vertical and horizontal) based on a comprehensive approach including the connection to the SWAT model; (2) develop a 3-D groundwater flow and transport model to investigate groundwater levels, nitrate concentration, and chloride concentration within the Gaza coastal aquifer; (3) investigate the groundwater quality deterioration cycle concerning

the urban water system; (4) develop sustainability measures to quantify the effectiveness trend of non-conventional water resources scenarios, namely desalination, stormwater harvesting and treated wastewater reuse as well as an infrastructure performance scenario aiming at sustainable groundwater management.

1.3 Data used

Data used in this study comprises the followings (source: local government data, global data, and scientific reports (more details are in the next chapters)):

- Study area boundaries (watersheds and aquifer);
- Daily rainfall records (2004–2010) of 19 rainfall stations;
- Five climate stations (2004–2010) with daily minimum and maximum temperature records, in addition to monthly solar radiation, dew point, pan evaporation, and wind speed;
- Three flow gauges within the study area (monthly records (2004–2010));
- Digital elevation model (DEM) (30 m resolution);
- Soil types, textures, and other different properties;
- Aerial images (0.5 m resolution);
- Regional plan of the Gaza Strip (2020);
- Population data;
- Lithological variations within the aquifer, aquifer thickness and lateral extent;
- Water wells abstraction (monthly records of more than 4000 water wells (2004–2010));
- Water table elevation (monthly records of 138 water wells (2004–2010));
- Chloride levels (Annual records of 114 water wells (2004–2010));
- Nitrate levels (Annual records of 96 water wells (2004–2010));
- Water supply network efficiency as well as wastewater network coverage and efficiency;
- Agricultural areas (patterns and water requirements);

- Artificial infiltration ponds for stormwater and treated wastewater;
- Future plans regarding desalination, stormwater harvesting, and treated wastewater reuse.

1.4 Research methodology

In addition to the data collection step outlined in the previous section, the following steps represent the way to systematically achieve research objectives of each part of this study. These steps, including approaches, methods, and techniques could be conceptually transferred and applied in investigations of other combinations of urban water system. Table 1.1 depicts the methodological framework comprising inputs, processes, methods, and outputs.

1.4.1 Research methodology (part 1)

This part of the research methodology is related to the research objectives (part 1) and includes the followings:

1. Manual digitization using ArcGIS 10.0 to delineate main watersheds and develop soil, land-use, rainfall stations, climate stations, and topography maps;
2. Image classification using ERDAS 9.3 (a remote sensing software) to extract land-use map of the study area from aerial images;
3. Sensitivity analysis, calibration, and validation of the SWAT model using the SWAT-Calibration Uncertainty Procedure (SWAT-CUP);
4. Quantification of water budget components;
5. Development of scenarios regarding urban area changes then simulation of the hydrologic response to these changes;
6. Development of the urban-surface runoff index (USI) and the urban-percolation index (UPI) to represent a micro-level evaluation of different urban change scenarios in the subbasins;
7. Derivation of the global urban-surface runoff index (GUSI) and the global urban-percolation index (GUPI) as macro-level factors reflecting the influence on the overall Gaza coastal aquifer due to urban area expansion.

1.4.2 Research methodology (part 2)

The second part of the research methodology is related to the research objectives (part 2) and contains the following steps:

1. Maps digitization using ArcGIS 10.0 regarding initial and observed groundwater heads, pumping wells, delineated watersheds within the aquifer domain, urban area within the Gaza governorates, agricultural areas in and out the Gaza Strip, and artificial recharge ponds;
2. Verification of percolation results by the SWAT model using the water table fluctuation method (WTF);
3. Development of aquifer-conceptual model as well as estimation of recharge components;
4. Calibration and validation of a 3-D groundwater flow model using MODFLOW-USG (an unstructured grid version of MODFLOW), in which Voronoi cells were used to reduce run time within complicated aquifer boundary conditions;
5. Model forecasting comprising the projection of built-up area, population, pumping water, and recharge components (the percolation was reduced temporally and spatially in the forecasting period based on the projected built-up area as well as the urban-percolation index (from Part 1));
6. Trend analysis of groundwater levels (2004–2030);
7. Investigation of the relationship between the forecasted groundwater levels and the projected built-up area;
8. Development of the groundwater-level trend index as a spatial indicator of potential impacts of urban area expansion on groundwater level.

1.4.3 Research methodology (part 3)

The last part of the research methodology related to the research objectives (part 3) consists of the following steps:

1. Manual digitization using ArcGIS 10.0 to exhibit observed chloride and nitrate levels as well as targeted urban and agricultural areas by different scenarios;

2. Identification of urban water system; in particular, urban water budget components (vertical and horizontal fluxes);
3. Characterization of groundwater quality in the Gaza costal aquifer;
4. Calibration and validation of a 3-D groundwater solute transport model using MODFLOW-2005 (the most recent release of MODFLOW model) considering the calibrated groundwater flow model (from Part 2);
5. Model forecasting regarding nitrate and chloride levels in the recharge components, in parallel with the previous forecasting step in Part 2;
6. Scenarios characterization considering the recent planning agenda of using non-conventional water resources (desalination, stormwater harvesting, and treated wastewater reuse) as well as an infrastructure performance scenario aiming at sustainable groundwater management;
7. Investigation of the scenarios based on the forecasted model concerning recharge components (quantity and quality) as well as pumping water;
8. Estimation of the deterioration cycle index (DCI) as a ratio between the amounts of low and high quality recharge components within the Gaza Strip boundary;
9. Development of the improvement index for groundwater level (IIL) and the improvement index for groundwater quality (IIQ) for the scenarios as measures of the effectiveness toward sustainable groundwater planning.

Table 1.1 Research methodological framework

Integrated hydrologic modeling in a context of urban water system

Data inputs
Study area boundaries, daily rainfall records, climatic records, stream-flow gauges, DEM, soil, aerial images, regional plans, population data, lithological data, water wells abstraction, water table elevation, chloride levels and nitrate levels in the groundwater, water supply network efficiency, wastewater network coverage and efficiency, agricultural areas (patterns and water requirements), artificial infiltration ponds, future plans regarding desalination, stormwater harvesting, and treated wastewater reuse.

Part 1	(Processes and methods)	Main outputs (1)
Quantifying the impact of urban area expansion on groundwater recharge and surface runoff	- Data preparation for modeling process - Sensitivity analysis, calibration, and validation of the SWAT model - Analysis of urban area changes	- Water budget components - Urban-surface runoff index (USI) - Urban-percolation index (UPI) - Global urban-surface runoff index (GUSI) - Global urban-percolation index (GUPI)

Part 2	(Processes and methods)	Main outputs (2)
Potential impacts of urban area expansion on groundwater level: a spatial-temporal assessment	- Data preparation for modeling and forecasting process - Verification of percolation results by the SWAT using WTF - Aquifer conceptualization - Calibration and validation of a 3-D groundwater flow model using MODFLOW-USG - Model forecasting and urban area analysis	- Aquifer water balance - Simulated and forecasted Groundwater levels - Groundwater-level trend index - A relationship between groundwater levels and built-up area

Part 3	(Processes and methods)	Main outputs (3)
Integrated hydrologic modeling as a key for sustainable urban water resources planning	- Data preparation for modeling and forecasting process - Identification of urban water system - Characterization of groundwater quality - Calibration and validation of a 3-D groundwater transport model using MODFLOW-2005 - Model forecasting regarding groundwater levels, nitrate and chloride concentrations - Scenarios characterization and investigation as well as effectiveness measurement based on the forecasted model	- Urban water budget components (quality and quantity) - Simulated and forecasted nitrate and chloride concentrations - Deterioration cycle index (DCI) - Improvement index for groundwater level (IIL) - Improvement index for groundwater quality (IIQ)

CHAPTER 2

2 Quantifying the impact of urban area expansion on groundwater recharge and surface runoff

2.1 Introduction

Water is the most important natural resource especially in the arid or semi-arid zones that face high population growth, scarcity of freshwater, irregularity of rainfall, excessive land-use change and increasing vulnerability to risks such as drought, desertification and pollution (Fadil *et al*., 2011). Assessing the impact of land-use change on hydrological parameters is considered an important step in water resources management and a prerequisite for ecological restoration as well as for their sustainable management. The quantitative evaluation of the impacts of human activities on water resources at watershed level is in the focus of the present research in hydrology (Chu *et al*., 2010). The spatial approach of quantifying the impact of land-use change at the spatial level of hydrological response units (HRUs) contributes to the understanding of the variation of hydrologic attributes in a basin and its sensitivity; especially land-use changes towards urban areas influence the water balance. In this study, based on surface water modeling, a new spatial evaluation for assessing the impact of urbanization was applied to the semi-arid watersheds intersecting with the Gaza Strip and the Gaza costal aquifer.

In 2010, the estimated total population in the Gaza Strip was 1.64 million (Rahman *et al*., 2013). The area covers 365 km^2, making it one of the most densely populated regions (ca. 4500 inhabitants/km^2) in the world (PCBS, 2006). The Gaza Strip faces serious water crises (CMWU, 2010). The groundwater aquifer is considered the main water supply source for all kinds of human use (domestic, agricultural and industrial), and can basically only be fed by rainfall and lateral aquifer flow from the east (CMWU, 2010). The impervious areas resulting

from the urban expansion pose a threat to the sustainability of the Gaza coastal aquifer in terms of aquifer replenishment.

In contrast to the number of groundwater studies, considerably less research with regard to surface water has been undertaken in the Gaza Strip. Some of these studies focused on the Gaza boundary and neglected the natural extent of the watersheds through historical Palestine and were without calibration for model parameters. Other studies estimated the groundwater recharge without considering the spatial dimension. Laronne and Alexandrov (2004) studied the characterization and utilization of surface water in the Near East, respectively exemplified by Wadi Gaza and Wadi Samoa reservoirs in historical Palestine. Khalaf *et al*. (2006) assessed the rainwater runoff based on the proposed regional plan for the Gaza Strip applying a rational method for runoff calculations, Horton's equation for estimating infiltration, and the geographical information system (GIS) as an analytical tool. Hamdan *et al*. (2007) applied the rational runoff formula using GIS as a tool to estimate runoff amounts from different land-use categories. Aish *et al*. (2010) used the WetSpass model, which is integrated within GIS ArcView, to evaluate groundwater recharge in the Gaza Strip. Ajjur and Mogheir (2012) evaluated the effect of climate change on groundwater in the Gaza Strip and studied the temporal relation between rainfall and recharge in three locations. Hamad *et al*. (2012) evaluated three different urbanization scenarios using the Automated Geospatial Watershed Assessment (AGWA) tool, which works under the umbrella of GIS.

The SWAT (Soil and Water Assessment Tool) model is used in different semi-arid regions to simulate water budget, sediment yield, and nutrient transport (SWAT, 2013). It is a flexible model that can be used under a wide range of different environmental conditions (Zhang, 2005). Recently, SWAT has been widely used in assessing land-use change at different levels. Wang *et al. (*2013) applied the model for analyzing individual and combined impacts of land use/cover (LULC) and climate change on hydrologic processes in a coastal watershed in Alabama, USA. Kim *et al.* (2013) employed the SWAT model to backcast long-term hydrologic behaviour of watersheds in North Carolina with different land-use/cover conditions. Dong *et al*. (2013) used long-term observational data as a basis for examining the effects of human activities and climate change on the runoff variation of Jinghe River Basin, a typical arid inland basin in northwest China. Karcher *et al.* (2013) proposed a modification to the SWAT model to enable the identification of areas where the implementation of best management practices would likely result in the most significant improvements in terms of

downstream water quality. Valdivieso and Sendra (2013) studied SWAT performance although they only had scarce information; the model showed a relatively satisfactory reproduction of the historical record of flows with certain limitations in the calculation of sediment production. Memarian *et al.* (2014) investigated the impact of LUCC on the hydrological conditions of the Hulu Langat basin in Malaysia using the SWAT model. Singh *et al.* (2014) evaluated the model and the data-driven Radial Basis Neural Network (RBNN) model for simulating the sediment load of the Nagwa watershed in India, where soil erosion is a severe problem.

This study is innovative as it considers all watersheds intersecting with the Gaza aquifer domain and also calibrates the SWAT model parameters to quantify the impact of urban area expansion on the coastal aquifer recharge and surface runoff in a spatial approach.

Objectives of this chapter are (1) calibration and validation of the SWAT model in terms of stream flow for three gauges in the main watersheds intersecting with the Gaza costal aquifer, and (2) spatial evaluation and quantification of the impact of urban land-use change on percolation and surface runoff at the subbasin and Gaza coastal aquifer level.

2.2 Study area

Palestine belongs to the sub-tropical zone. Along the coast (Gaza Strip) and in the highlands (West Bank), the climate is of the Mediterranean type with a long hot and dry summer, and short cool and rainy winter (Dudeen, 2001). The study area forms a transitional zone between the sub-humid coastal zone in the north, the semi-arid loess plains in the northern Negev Desert in the east and the arid Sinai Desert in Egypt in the south (Isaac *et al.*, 2006). The Gaza Strip (Fig. 1.1) is a narrow coastal strip located on the south-eastern coast of the Mediterranean Sea with a land area covering 365 km^2 and has a semi-arid climate with a short and mild rainy season and dry summer (CMWU, 2010). Although the Gaza Strip and Israeli side share the biggest surface water basin in historical Palestine (Wadi Gaza Basin), the natural flow extent of this basin to Gaza Strip is cut by Israeli reservoirs. Gaza has a sub-aquifer that is part of the larger coastal aquifer which extends from Karmel Mountain in the north to the Sinai Desert in the south with a variable width and depth (Baalousha, 2008). The aquifer domain boundary extends beyond the political boundaries of the Gaza Strip towards the north, and towards the east where the coastal aquifer pinches out the surface, and towards the south in Egypt and finally towards the west to the Mediterranean Sea (HWE, 2010).

The study area includes the watersheds intersecting with the Gaza Strip as well as the Gaza coastal aquifer domain. The Israeli reservoirs were considered in the watershed delineation especially in the Wadi Gaza watershed (the largest watershed in historical Palestine). Figure 2.1 displays the watersheds considered in the modeling process and clarifies that the Wadi Gaza watershed is not totally included in the study area.

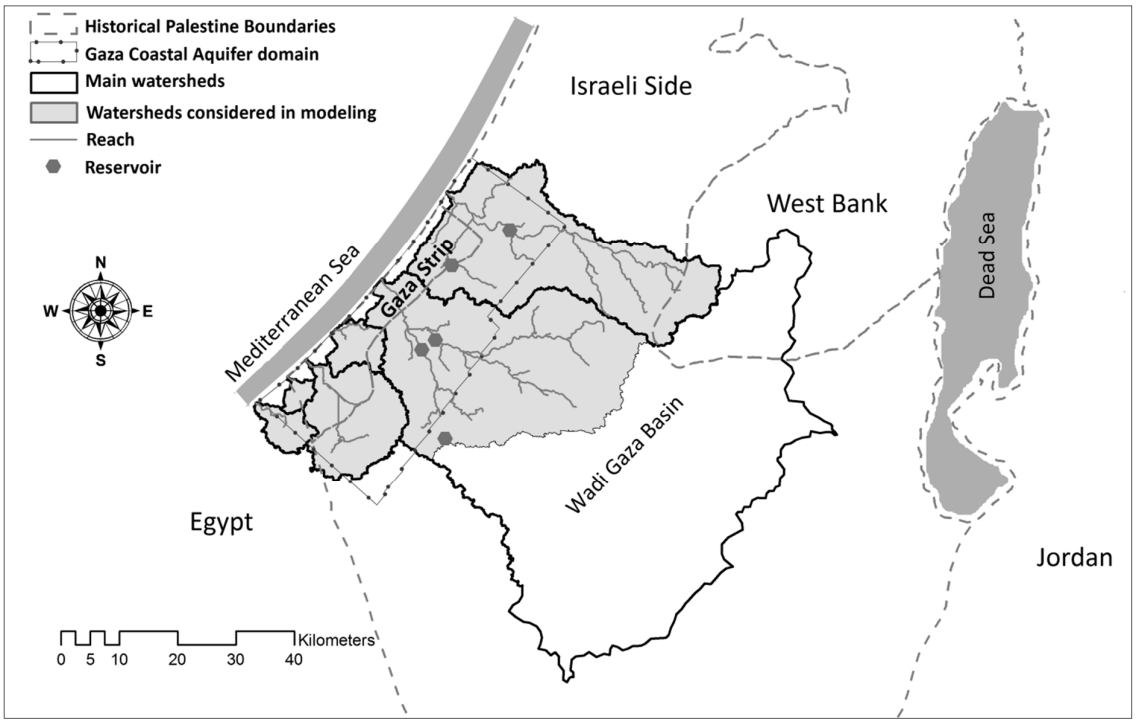

Figure 2.1 Study area (developed based on a digital elevation model (DEM) (USGS, 2012))

2.3 Data and Methods

2.3.1 Data processing

Topography

The general topography of the study area ranges from 0 to 840 meter elevation. Through 40 km from the west to the east, the elevation gradient is moderate (from 0 to 300 m) and then it becomes steep (from 300 to 840 m) over a distance less than 10 km. The digital elevation model of the study area (30 m DEM) is shown in Figure 2.2 (USGS, 2012), and is considered as the base of the main watershed delineation.

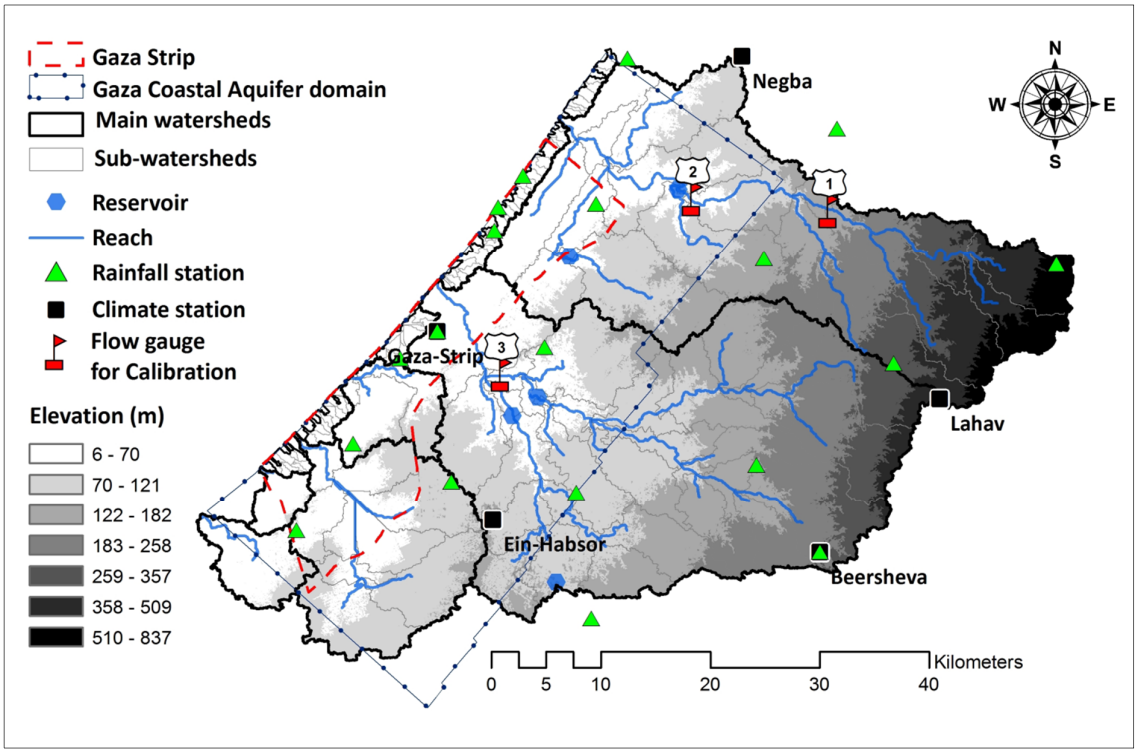

Figure 2.2 Study area - rainfall, climate, and flow stations (Meteorological Service database, 2013; PWA, 2013) and 30-m digital elevation model (DEM (USGS, 2012))

Climate

The climate of the study area is relatively heterogeneous in terms of rainfall, temperature, solar radiation and evaporation. Table A.1 (Appendix A) shows the climate parameters for five stations distributed throughout the study area. Figure 2.2 depicts the location of these climate stations used in this study. The average annual rainfall (2004–2010) varies from 163 mm in Beersheva to 393 mm in Negba, while Gaza city receives 315 mm. The annual pan evaporation ranges from 1620 mm in Gaza city to 1950 mm in Beersheva, and the mean temperature varies between 8–14 C° in January and 21–28 C° in August (Meteorological Service database, 2013; PWA, 2013).

Soil

There are different types of topsoil in the study area, and their spatial distribution was digitized using ArcGIS 10 based on the available soil data (Figure 2.3; Hamad *et al.*, 2012; Dan *et al.*, 1976). *Brown Lithosols and Loessial arid brown soil* consist mainly on steep, rocky and eroded slopes. The underlying rocks may be chalk, marl, limestone or conglomerate, most of which are covered by a hard lime crust. *Brown Lithosols and Loessial*

Serozems comprise shallow brown Lithosols with numerous rock outcrops and Rendzinic desert Lithosols on steep hillslopes and loessial Serozems in broad valleys, terraces, and on large plateaux. The underlying rocks are mainly chalk, Nan lime crust, limestone, dolomite and flint. *Brown Rendzinas soil* consists of shallow brown Rendzinas with numerous outcrops of limestone or calcareous crust. The underlying rocks are soft chalk and marl covered partly by Nan lime crust. *Dark Brown Soils* have developed from fine aeolian sediments, coastal sand calcareous sandstone (kurkar), and medium to fine-textured alluvial deposits. *Loessial Serozems* developed from loessial sediments, some sandy sediments and gravel. *Pararendzinas* cover most of the slopes and developed from calcareous sandstone or caicrete that covers this sandstone. *Sandy Regosols* are shallow (0.5–1.5 m) young sandy deposits covering almost the whole landscape. They developed from sand deposits or loessial deposits mixed partly with sand. *Regosols* cover the steep, eroded slopes and the parent material is sand, clay or loess. Moderate slopes are covered mostly by *loessial soils*. Mainly these soils developed from loessial sediments; in sandy, eroded areas (in the west) or gravel, conglomerates and chalk (in the east) (Dan *et al*., 1976). Soils textural classes are tabulated in Table 2.1.

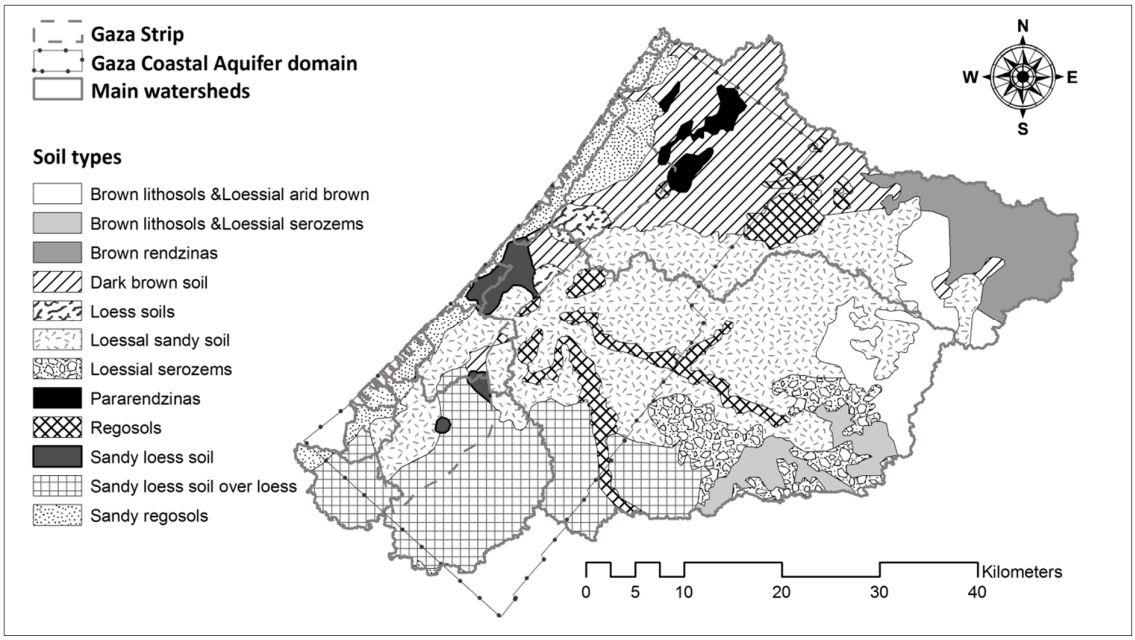

Figure 2.3 Study area - soil types based on Dan et al. (1976) and Ministry of Planning (2007)

Table 2.1 Soil texture in the study area

Soil Type	Layer	Hydrologic group [d]	Soil textural classes %			K_s *	AWC **	Soil texture
			Clay	Silt	Sand			
Brown Lithosols & Loessial Arid Brown [a]	1	C	20	40	40	13	0.32	Loamy
	2		30	35	35	2.3	0.25	Loam to clay loam
	3		40	30	30	0.6	0.19	Clay loam to clay
Brown Lithosols & Loessial Serozems [a]	1	C	15	38	52	26	0.26	Sandy loam to loam
	2		30	35	35	2.3	0.25	Loam to clay loam
Brown Rendzinas [a]	1	C	35	35	30	2.3	0.18	Clay loam with high granular content
Dark Brown Soils [b]	1	B	25.3	12.8	61.9	4.3	0.18	Sandy loam to sandy clay loam
Loess Soils [b]	1	A	6	34	58	26	0.2	Sandy loam
Loessial Sandy [b]	1	A	18	25	57	26	0.2	Sandy loam
Loessial Serozems [c]	1	C	16	48.8	35.2	13	0.32	Loamy
	2		36	44	20	2.3	0.18	Clay loam
Pararendzinas [a]	1	A	4	4	92	210	0.1	Sandy
	2		10	25	65	26	0.2	Sandy loam
Regosols [a]	1	A	10	25	65	26	0.2	Sandy loam
Sandy Loess [b]	1	C	23.2	20.3	56.5	4.3	0.2	Sandy clay loam
Sandy Loess Soil Over Loess [b]	1	A	17.5	16.3	66.2	26	0.2	Sandy loam
Sandy Regosols [b]	1	A	8.5	1.8	89.7	210	0.1	Sandy

(a) Soil texture (Dan *et al.*, 1976), Soil textural classes (FAO, 2006)
(b) Soil texture and soil textural classes (Hamad *et al.*, 2012)
(c) Soil texture (Dan *et al.*, 1976), Soil textural classes (Geron *et al.*, 1985)
(d) (Shadeed and Almasri, 2010), (McCuen, 2004)
(*) Saturated hydraulic conductivity (mm/hr) (Levick *et al.*, 2004)
(**) Available water capacity of soil (mm H_2O/mm soil) (NRCCA, 2013)

Land use

The land-use map (Fig. 2.4) was extracted through the processing of aerial images (resolution: 0.5 m) (Ministry of Planning, 2007) and historical data from Google Earth. The supervised classification technique was used, based on ERDAS 9.3, to distinguish the main land-use classes in the study area. Manual digitization using ArcGIS 10.0 was performed to define the urban area and the layer was merged with the classified land-use image. Five main land-use classes were identified. The dominant categories are rangeland (50.2%), agricultural land (26.1%), barren land (13.8%) and forest land (5.3%). The urbanized areas represent 4.5% of the study area and 20% of the Gaza Strip.

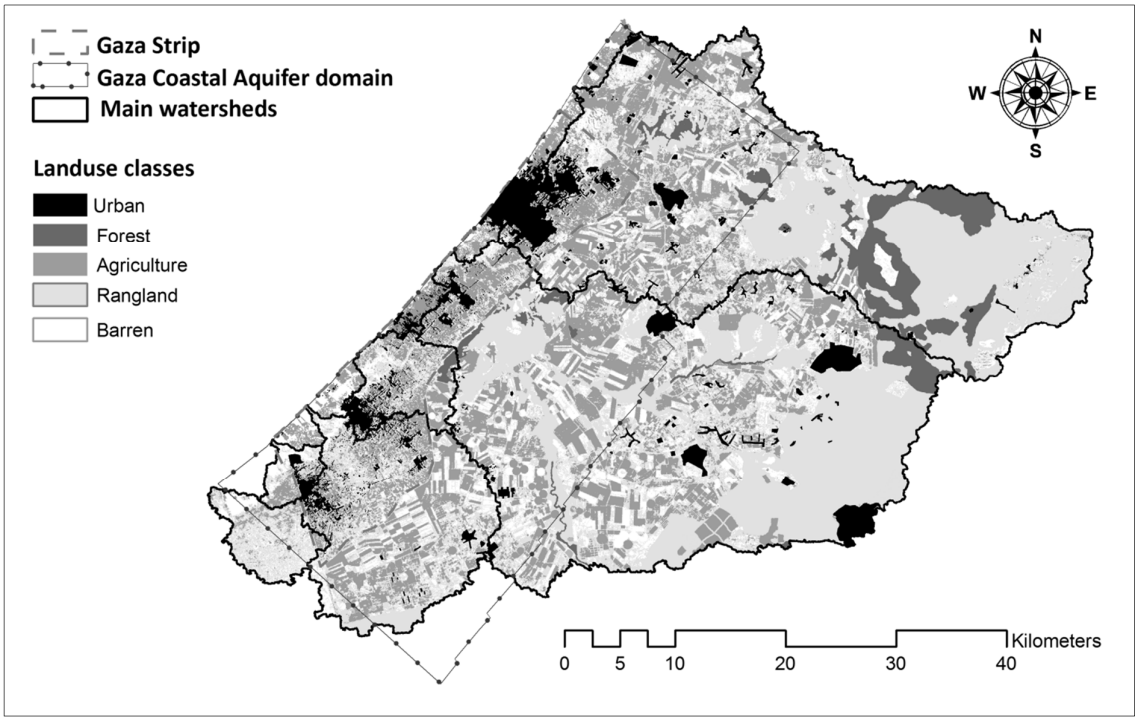

Figure 2.4 Study area - land use (developed based on aerial images (Ministry of Planning, 2007) and historical data from Google Earth)

2.3.2 SWAT model

The ArcSWAT model was used for the surface water modeling processes. ArcSWAT (ArcGIS Extension) is a graphical user interface for the SWAT model (SWAT, 2013). SWAT is a river basin, or watershed-scale model developed to predict the impact of land management practices on water, sediment, and agricultural chemical yields in large, complex watersheds with varying soils, land use, and management conditions over long periods of time (Neitsch *et al.*, 2011).

SWAT uses the water balance approach to simulate watershed hydrologic partitioning as described by Neitsch *et al.* (2011) in equation 2.1.

$$SW_t = SW_o + \sum_{i=1}^{t}\left(R_{day} - Q_s - E_a - w_{seep} - Q_{gw}\right) \quad (2.1)$$

where SW_t is the final soil water content (mm), SW_o is the initial soil water content on day i (mm), t is the time (days), R_{day} is the amount of precipitation on day i (mm), Q_s is the amount of surface runoff on day i (mm), E_a is the amount of evapotranspiration on day i (mm), w_{seep} is the amount of water entering the vadose zone from the soil profile on day i (mm), and Q_{gw} is the amount of return flow on day i (mm).

SWAT provides two methods for estimating surface runoff volume, namely the Soil Conservation Service (SCS) Curve Number procedure (1972) and the Green and Ampt equation (1911). In the SCS method, the runoff for a given rainfall depth is calculated assuming a certain curve number (CN) for the surface related to the land use and the soil hydrologic group. The SCS method is based on an empirical formula that was developed from observations of several years of rainfall and runoff data obtained from a variety of combinations of soil, land use, topography and climate. SWAT defines percolation as the water that drains through the root zone into the aquifer. Downward flow occurs when the soil moisture exceeds the field capacity level of a soil layer. The downward flow rate is governed by the saturated hydraulic conductivity (K_s) of the soil layer. The lateral subsurface flow in the soil profile is calculated simultaneously with percolation. The lateral flow and surface runoff of all HRUs are summed for each subbasin and then routed through the stream network (Ouessar *et al*., 2009).

In this study, the SCS procedure was used to estimate the surface runoff. The Penman-Monteith equation was applied to estimate potential evapotranspiration. Manning's equation was employed to define the rate and velocity of flow. Water was routed through the channel network using the variable storage routing method. A detailed description of different model components can be found in Neitsch *et al*. (2011).

2.3.3 Model running process

Under the umbrella of ArcSWAT, the spatial variability of soil, land use and land slope are accounted for by discretization of the watershed into subbasins based on the topography and stream network. Each subbasin consists of multiple HRUs representing characteristic combinations of soil, land cover and land slope properties. Figure 2.2 shows the discretization of the watersheds into 72 subbasins, which contain 255 HRUs. In addition to the climatic data (Table A.1), daily rainfall data from 19 stations were used to represent the rainfall distribution throughout the study area during the modeling period from 1 November 2004 to 31 October 2010 (Fig. 2.2). Daily minimum and maximum temperature data from 5 climate stations were used during the modeling period (Fig. 2.2) (Governmental portal, 2013; PWA, 2013). To satisfy the Penman-Monteith equation requirements (Neitsch *et al*., 2011) in the SWAT model, wind data taken from the climatic stations at heights of 10 m aboveground were converted to 2 m aboveground according to the equation (Potchter and Ben-Shalom, 2013): $V_h = V_{10}\left(0.233 + 0.656 \times \log\left(h + 4.75\right)\right)$.

2.3.4 Auto-calibration program

The SWAT-Calibration Uncertainty Procedure (SWAT-CUP) was used to perform calibration, validation, and sensitivity analysis. SWAT-CUP contains the uncertainty analysis routine, namely Sequential Uncertainty Fitting–version 2 (SUFI-2), which is a semi-automated inverse modelling procedure for a combined calibration-uncertainty analysis (Abbaspour *et al.*, 2004). In SUFI-2, parameter uncertainty accounts for all sources of uncertainties such as uncertainty in driving variables (e.g., rainfall), conceptual model parameters, and measured data. It is possible to choose the uncertain parameters and the range of their physical values. The degree to which all uncertainties are accounted for is quantified as the percentage of measured data bracketed by the 95% prediction uncertainty (95PPU). The 95PPU is calculated at the 2.5% and 97.5% levels of the cumulative distribution of an output variable obtained through Latin hypercube sampling, disallowing 5% of the very bad simulations. In each running step in SWAT-CUP, previous parameters ranges are updated in such a way that the new ranges are always smaller than the previous ranges, and converge to the best simulation while considering a defined objective function (Abbaspour *et al.*, 2004; Yang *et al.*, 2008; Tang *et al.*, 2012;).

Considering the uncertainty analysis routine and a defined objective function in SWAT-CUP, model calibration and sensitivity analysis were performed. The flexibility of manual modification of the parameters as well as the number of running steps between the auto-calibration runs reflects the semi-automated approach of SWAT-CUP.

2.3.5 Model sensitivity analysis

Using SWAT-CUP, an initial sensitivity analysis was conducted to identify the most critical model parameters before starting the calibration process. The possible physical ranges of the parameters values were used in the initial sensitivity analysis to avoid excluding any sensitive parameter due to its nonlinear behavior. Parameter sensitivities are determined by calculating the multiple regression system ($g = \alpha + \sum_{i=1}^{m} \beta_i b_i$), which regresses parameters generated by the Latin hypercube against the objective function values (g), where b_i is the i-th parameter, m is the total number of parameters, β_i is the partial slope coefficient, and α is the intercept (Abbaspour *et al.*, 2007). The relative sensitivity values in SWAT-CUP are measured by t-tests and the corresponding p-values. The t-test provides a measure of sensitivity (larger absolute values are more sensitive), and p-value determines the significance of the sensitivity

(lower *p*-value denotes more significance of the sensitivity measure).

2.3.6 Model calibration and validation

The simulated stream flow values were calibrated at the monthly time scale with the observed stream flow values for three discharge stations (WAI, 2013) for the years 2004/05, 2007/08, and 2008/09 and validated at the monthly time scale for year 2009/10 (Fig. 2.2).

Generally, the main components of the calibration process include objective function(s) as a measure of goodness of fit between measured and simulated variable as well as optimization procedures. An auto-calibration process was performed using SWAT-CUP, which offers the possibility of selecting an objective function from the nine different available options. bR^2, which was used as the objective function, reflected the best matching between simulated and observed flow, where b is the slope of the regression line between measured and simulated variable and R^2 is the coefficient of determination. The objective function is expressed in equation 2.2 (Krause and Boyle, 2005).

$$\text{Maximize: } \begin{cases} |b| \cdot R^2 & \text{if } b \leq 1 \\ |b|^{-1} \cdot R^2 & \text{if } b > 1 \end{cases} \tag{2.2}$$

R^2 as well as b should be close to 1 in a high-performance model, and consequently the objective function (equation 2.2) should be close to 1. A manual calibration was conducted to refine the auto-calibration, so that an appropriate balance was achieved regarding peak and low flow.

2.4 Model Results and Analysis

2.4.1 Sensitivity analysis, calibration and validation

Table 2.2 shows the initial ranking of the sensitive parameters related to flow calibration based on 100 runs of the SWAT model. Spruill *et al*. (2000), White and Chaubey (2005), Niraula *et al*. (2012), and Wu and Liu (2013) agreed that these parameters were the most sensitive ones in their studies. The initial sensitivity analysis illustrates three sensitive packages (package is a set of parameters), namely soil package, land-use and subbasin parameters package, and groundwater package. The soil package was the most sensitive package, i.e., had the most sensitive parameters in the model. Understanding the interrelations between parameters within a package is worthwhile in order to obtain the optimum solution during the calibration process especially if there is a high level of

uncertainty. A manual sensitivity analysis was conducted to evaluate different relative changes of soil parameters at station 01 (Fig. 2.5). This analysis illustrates that soil parameters in the wet year 2004/05 have a higher sensitivity than in normal or dry years, which could be helpful in investigating the optimal model parameters.

Table 2.2 Initial estimation of sensitive parameters in SWAT model

Parameter	Description	Type of change	Range of parameter values	t-Stat	P-value	Rank
GWQMN	Threshold depth of water in the shallow aquifer required for return flow to occur (mm)	Replaced by value	0–5000 [a]	2.07	0.04	1
SOL_K	Saturated Hydraulic Conductivity (mm/hr)	Relative change	-0.9–1 [a]	1.95	0.05	2
SOL_AWC	Available Water Capacity of the soil layer (mm H_2O/mm soil)	Relative change	-0.5–0.5 [b]	-1.54	0.13	3
CN2	Initial SCS curve number for moisture condition II– pervious areas	Relative change	-0.3–0.2 [b]	1.04	0.3	4
REVAPMN	Threshold depth of water in the shallow aquifer for "revap" to occur (mm)	Replaced by value	0–500 [a]	-0.92	0.36	5
ALPHA_BF	Baseflow alpha factor (days)	Replaced by value	0–1 [a]	-0.78	0.44	6
ESCO	Soil evaporation compensation factor	Replaced by value	0–1 [a]	-0.49	0.63	7
SURLAG	Surface runoff lag coefficient	Replaced by value	0.05–24 [a]	0.48	0.63	8
GW_REVAP	Groundwater "revap" coefficient	Replaced by value	0.02–0.2 [a]	-0.31	0.76	9
SOL_Z	Depth from soil surface to bottom of layer mm	Relative change	-0.5–0.5 [b]	0.19	0.85	10
OV_N	Manning's "n" value for overland flow	Replaced by value	0.01–3 [a]	-0.19	0.85	11
GW_DELAY	Groundwater delay time (days)	Replaced by value	0–500 [a]	0.07	0.95	12
CH_N2	Manning's "n" value for the main channel	Replaced by value	0–0.3 [a]	0.04	0.97	13
CH_K2	Effective hydraulic conductivity in main channel (mm/hr)	Replaced by value	0–25 [a]	0.04	0.97	14

(a) Documented in SWAT input data manual (SWAT, 2013)
(b) Identified based on the authors' experience in the study area

Tables 2.3 to 2.5 show the calibrated parameters for groundwater package, land-use and subbasins package, and soil package. Calibration and validation statistics are summarized in Table 2.6. Considering all flows at the three stations through the calibration period, model efficiency measures for the monthly simulation R^2, bR^2 and E (Nash-Sutcliffe efficiency) are 0.87 (Fig. 2.6), 0.83 and 0.85, respectively which indicate a very good fit between measured and simulated flow.

Through the validation period, it was found that the model has good predicative capability with R^2, bR^2 and E values of 0.90, 0.76 and 0.82, respectively, for all flows at the three stations. Statistical model efficiency criteria (Table 2.6) attained the requirement of $R^2 >$

0.6 and $E > 0.5$, which is recommended by the SWAT developers (Santhi *et al*., 2001). As E values in calibration and validation periods are above 0.75, the performance rating of the model is very good (Moriasi *et al*., 2007).

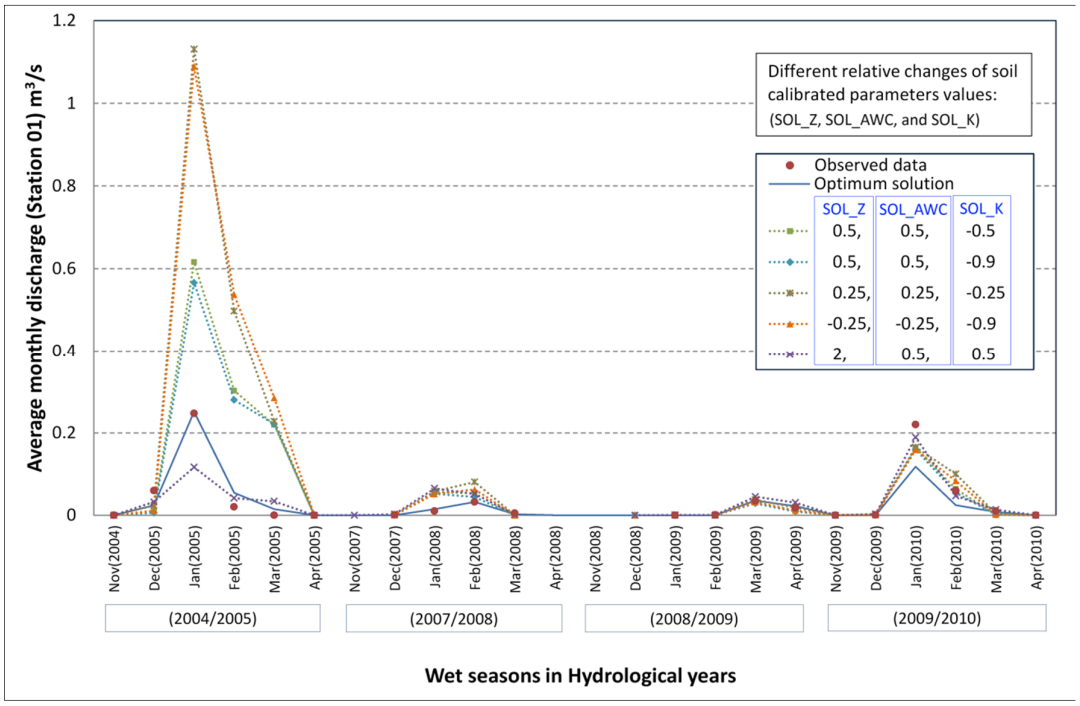

Figure 2.5 Sensitivity analysis of varied relative change in soil parameters

Table 2.3 Calibrated parameters – groundwater package

Parameter	Description	Calibrated value
GWQMN	Threshold depth of water in the shallow aquifer required for return flow to occur (mm)	1000
REVAPMN	Threshold depth of water in the shallow aquifer for "revap" to occur (mm)	325
ALPHA_BF	Baseflow alpha factor (days)	0.6
GW_REVAP	Groundwater "revap" coefficient	0.025
GW_DELAY	Groundwater delay time (days)	160

Table 2.4 Calibrated parameters – land-use and subbasins package

Parameter	Description	Type of change
CN2	Initial SCS curve number for moisture condition II	No change for urban land use, No change for rangeland except rangeland on brown Rendzinas soil, CN2 increases by 6.5% For other land use, CN2 decreases by 5%
ESCO	Soil evaporation compensation factor	Replaced by 0.765
SURLAG	Surface runoff lag coefficient	Replaced by 9
OV_N	Manning's "n" value for overland flow	No change (ranges from 0.1 to 0.15)

Table 2.5 Calibrated parameters – soil package

Soil type	Layer	Calibrated value of soil parameters		
		Sol_K (mm/hr)	Sol_AWC (mm H_2O/mm soil)	Sol_Z (mm)
Brown Lithosols & Loessial arid brown	1	1	0.305	70
	2	0.8	0.24	210
	3	0.4	0.18	350
Brown Lithosols & Loessial Serozems	1	26	0.25	500
	2	2.3	0.25	1000
Brown Rendzinas	1	0.6	0.29	870
Dark Brown Soils	1	4	0.2	650
Loess Soils	1	12	0.1	1000
Loessial Sandy	1	12	0.1	1000
Loessial Serozems	1	13	0.32	750
	2	2.3	0.18	1500
Pararendzinas	1	210	0.1	250
	2	210	0.1	500
Regosols	1	12	0.1	1000
Sandy Loess	1	4.3	0.2	1000
Sandy Loess Soil Over Loess	1	12	0.1	1000
Sandy Regosols	1	210	0.07	750

Table 2.6 Summary of calibration and validation statistics

Calibration results (monthly base)			
	Observed	Simulated	
Average flows (m^3/s)	0.105	0.099	
Standard deviation of flows (m^3/s)	0.21	0.19	
Average of the highest 25% flows (m^3/s)	0.4	0.37	
Average of the lowest 50% flows (m^3/s)	0.0041	0.0054	
	Coefficient of determination, R^2	bR^{2*}	Nash-Sutcliffe efficiency, E
Station 01	0.95	0.89	0.95
Station 02	0.86	0.86	0.84
Station 03	0.89	0.85	0.86
All stations	0.87	0.83	0.85
Validation results (monthly base)			
	Coefficient of determination, R^2	bR^2	Nash-Sutcliffe efficiency, E
Station 01	0.98	0.61	0.82
Station 02	0.95	0.90	0.94
Station 03	0.82	0.54	0.96
All stations	0.90	0.76	0.82

(*) b is the slope of the regression line between measured and simulated flow and it was modified according to equation 2.2

Table 2.7 Final sensitivity analysis of sensitive parameters

Parameter	Description	t-Stat	p-Value	Final Rank
SOL_AWC	Available Water Capacity of the soil layer (mm H_2O/mm soil)	6.0	0.00	1
SOL_Z	Depth from soil surface to bottom of layer mm	4.6	0.00	2
ESCO	Soil evaporation compensation factor	-2.8	0.01	3
CN2	Initial SCS curve number for moisture condition II	-2.3	0.03	4
OV_N	Manning's "n" value for overland flow	1.4	0.17	
GW_DELAY	Groundwater delay time (days)	-1.4	0.17	
SURLAG	Surface runoff lag coefficient	1.1	0.31	
SOL_K	Saturated Hydraulic Conductivity (mm/hr)	-1.0	0.35	
GW_REVAP	Groundwater "revap" coefficient	-0.8	0.43	
GWQMN	Threshold depth of water in the shallow aquifer required for return flow to occur (mm)	-0.7	0.47	
REVAPMN	Threshold depth of water in the shallow aquifer for "revap" to occur (mm)	0.5	0.62	
ALPHA_BF	Baseflow alpha factor (days)	0.0	0.98	

The monthly flow records contain mostly one or two flood events which can be considered as the real calibration level. Figure 2.7 shows that, through the calibration and the validation period, the observed and simulated flow at stations 01, 02, and 03 (Fig. 2.2) matched well. Few flow peaks are overestimated or underestimated by the model. The observed flow at station 03 in January 2005 is obviously higher than the simulated; an external flow from the reservoir upstream in a flood event through that month could be the main reason.

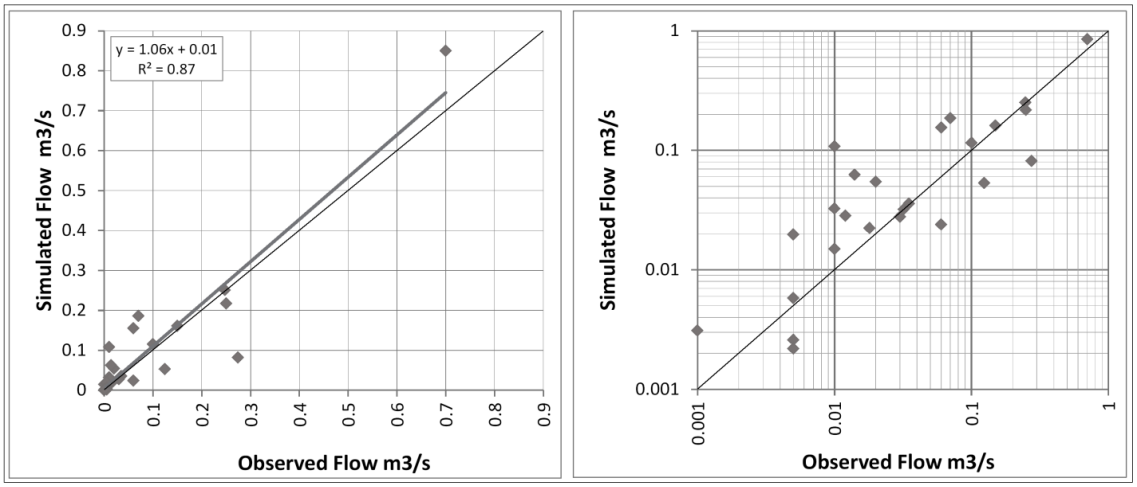

Figure 2.6 Scattered plots between observed and simulated flow for three flow stations (Fig. 2.2) in m^3/s (as average monthly values)

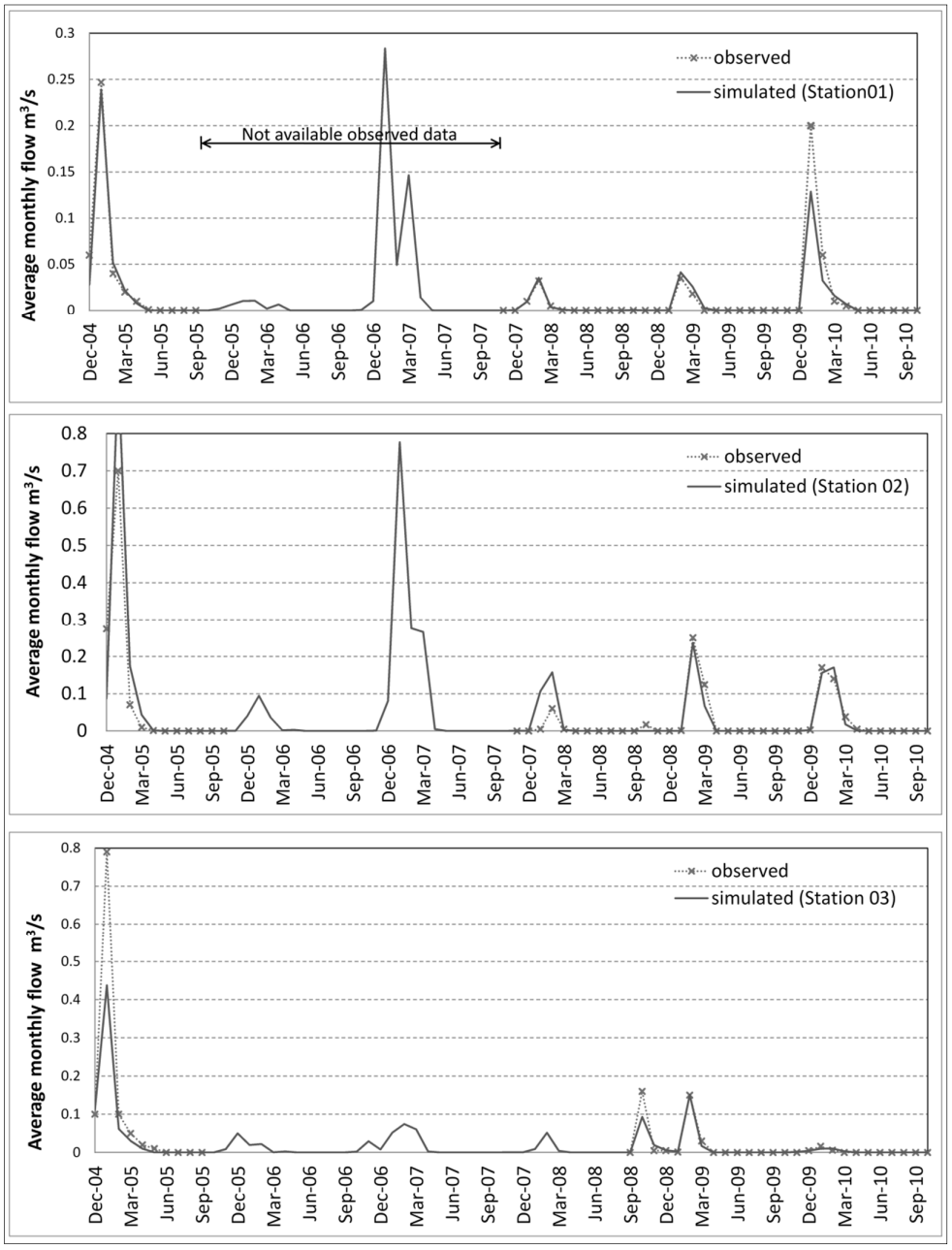

Figure 2.7 Comparison between observed and simulated flow at stations 01, 02, and 03 (Fig. 2.2)

A final sensitivity analysis was carried out to probe the real ranking of the sensitive parameters considering a range within ±10% change of the calibrated value. At 0.05 as the significant level, available water capacity of the soil layer (SOL_AWC), depth from soil surface to bottom of layer (SOL_Z), soil evaporation compensation factor (ESCO), and initial SCS curve number for moisture condition II (CN2) have the highest t-test values and are thus the most sensitive parameters (Table 2.7). Table 2.8 shows the average values of the most sensitive parameters considering the land-use classes within the study area.

Table 2.8 Average values of the most sensitive model parameters, as calculated by SWAT for landuse classes within the study area

Average within:	**The most sensitive model parameters** [a]	
	Land-use parameters: **CN** (curve number)	**Soil parameters** [b]**:** **AWC** (available water capacity of the soil layer, mm H_2O/total soil depth) [c]
Agricultural land	68.0	122.1
Barren land	79.1	115.1
Rangeland	53.3	144.4
Forest land	53.1	126.1
Urban land (pervious and impervious land)	80.5	102.8
The overall study area	61.4	132.0
The Gaza Strip boundary	67.2	98.4

(a) ESCO, a highly sensitive parameter (table 2.7), has a constant value among the HRUs (0.765)
(b) Even though the sensitivity analysis illustrates that the saturated hydraulic conductivity (K_s) of soil is not a highly sensitive parameter, it may be valuable in understanding the watershed conditions. Within the study area, the average calibrated K_s was 18 mm/hr which ranged between 0.6 and 210 mm/hr (see table 2.5)
(c) AWC is a function of (SOL_AWC and SOL_Z)

2.4.2 Water budget components

Spatial variability was investigated in the study area by connecting the model output files and the watershed themes in the ArcGIS environment. Figure 2.8 shows the spatial distribution of the rainfall and the water budget components throughout the study area. The average annual rainfall decreases gradually from north to south as well as from west to east. The average annual surface runoff varies from 0 mm in the south-east to 89 mm in the north-west. The maximum average annual percolation (124 mm) is in the northern part of the study area. The average annual actual evapotranspiration varies between subbasins within a broad range (132–265 mm). Figure 2.8 displays the differences between the northern and southern watersheds in surface water yield as well as the effects of reservoirs on the natural extents of the watersheds. The maximum average annual flow-volume was 15.7 Mm^3 in the largest northern watershed. Simulated percolation, surface runoff and evapotranspiration represent on average 22.4%, 11.7%, and 65.0%, respectively, of the rainfall quantities within the Gaza Strip boundary, whereas these values are 17.9%, 6.5%, and 74.5%, respectively, considering the aquifer domain boundary. Table 2.9 shows the average annual values of the water balance components and their ranges among subbasins.

Table 2.9 Average annual values of water balance components and their ranges among subbasins (2004–2010)

Water balance components	Within the study area		Within the Gaza Strip boundary	
	Average (mm)	Range among subbasins (mm)	Average (mm)	Range among subbasins (mm)
Precipitation	258.4	139.9–377.2	277.4	216.8–340.0
Surface runoff	12.6	0.0–89.2	32.5	0.2–89.2
Lateral flow	4.3	0.01–37.2	2.3	0.03–6.2
Baseflow*	≅ 0.0	0.0–0.3	0.0	0.0
Percolation	38.6	0.0–124.5	62.2	24.3–117.2
Evapotranspiration	201.7	132.4–265.1	180.4	146.2–227.8
Potential evapotranspiration	1517.4	1368.8–1712.4	1414.2	1368.8–1520.8
Change in soil water storage	1.2	0.0–17.8	0.8	0.0–12.7

(*) Although there are some small springs in specific subbasins, they are not sufficient to generate significant baseflow.

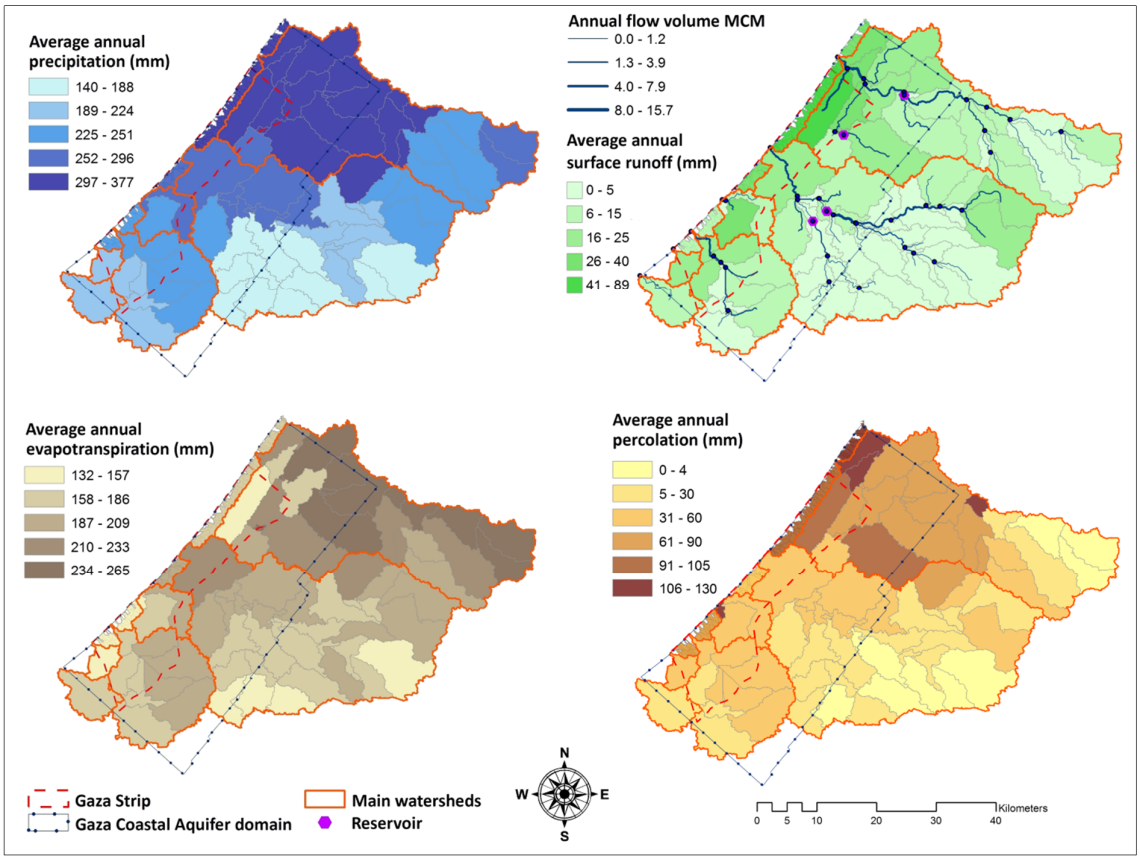

Figure 2.8 Average annual rainfall distribution and water budget components (2004–2010)

2.4.3 Urban area analysis

Urbanization is a major driver of additional pressures (both qualitative and quantitative) on the environment (Rozos and Makropoulos, 2012). Traditionally, the response of watersheds to urban development has been measured in terms of changes in the flow regime and groundwater recharge. There are two patterns of urbanization within the study area, namely Gaza Strip cities and Israel colonies. Great concerns have emerged in recent years about uncontrolled urban expansion in the Gaza Strip (Isaac *et al*., 2006). Urban development and infrastructure encroach upon agricultural land and rangelands creating additional pressure on the limited water resources of the Gaza Strip. The Gaza Strip cities have a high residential density (impervious area represents about 60% of the total urban area). The Israeli colonies or cities in the study area have low to moderate residential density (impervious area represents 12–38% of the total urban area) and are located outside the Gaza Strip. There were scattered Israeli colonies in the Gaza Strip, but the Israeli government evacuated them in 2005 (Isaac *et al*., 2006). Figure 2.9 shows the variety of the urban areas in terms of high or medium residential density at subbasin level. The hydrologic response to the urban area change was simulated in this study. The impacts of 10, 20, 30, and 50% increase in the residential high density area (urban area in the Gaza Strip) on the percolation and the surface runoff were investigated. The agricultural land and rangeland decreased equally with the continuous increase in urban areas. Unique linear relationships between the relative change in urban area and the corresponding relative change in surface water and percolation were concluded for different subbasins. The equation '$y = \alpha x$' is the general formula to simulate the surface runoff or percolation response (y) to the urban change (x). Each subbasin has a unique linear relation slope (α), which represents a sensitivity factor of the hydrological components.

Figure 2.10 presents different linear relations for the subbasins having the highest built-up area. Spatial evaluation of the surface runoff and the percolation response to the urban expansion were carried out considering the linear relation slope (α) as Urban-Surface Runoff Index (USI) or Urban-Percolation Index (UPI). The USI reflects the percent change in surface runoff due to a 1% increase in urban area at subbasin level. Similarly, the UPI reflects the percent change in percolation due to a 1% increase in urban area at subbasin level. Figure 2.11 shows the spatial distribution of the USI from 0 to around 1 and exhibits the UPI value (from 0 to -0.41) on the basis of subbasins.

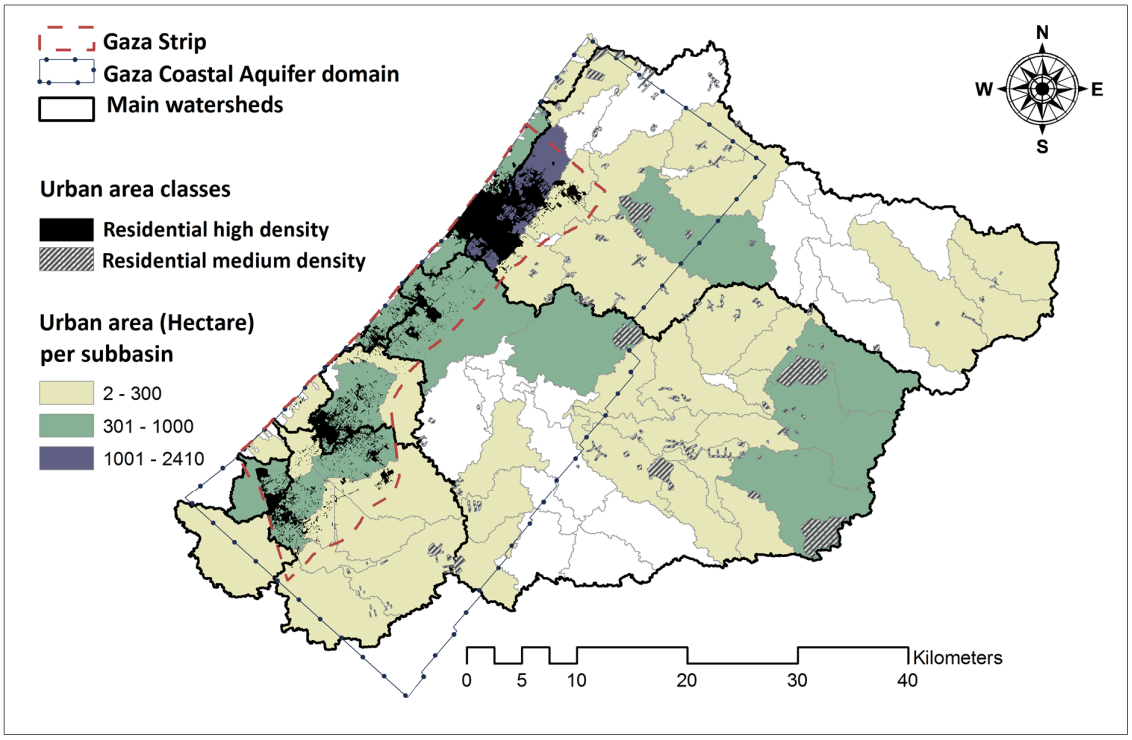

Figure 2.9 Urban area distribution (based on landuse map (Fig. 2.4))

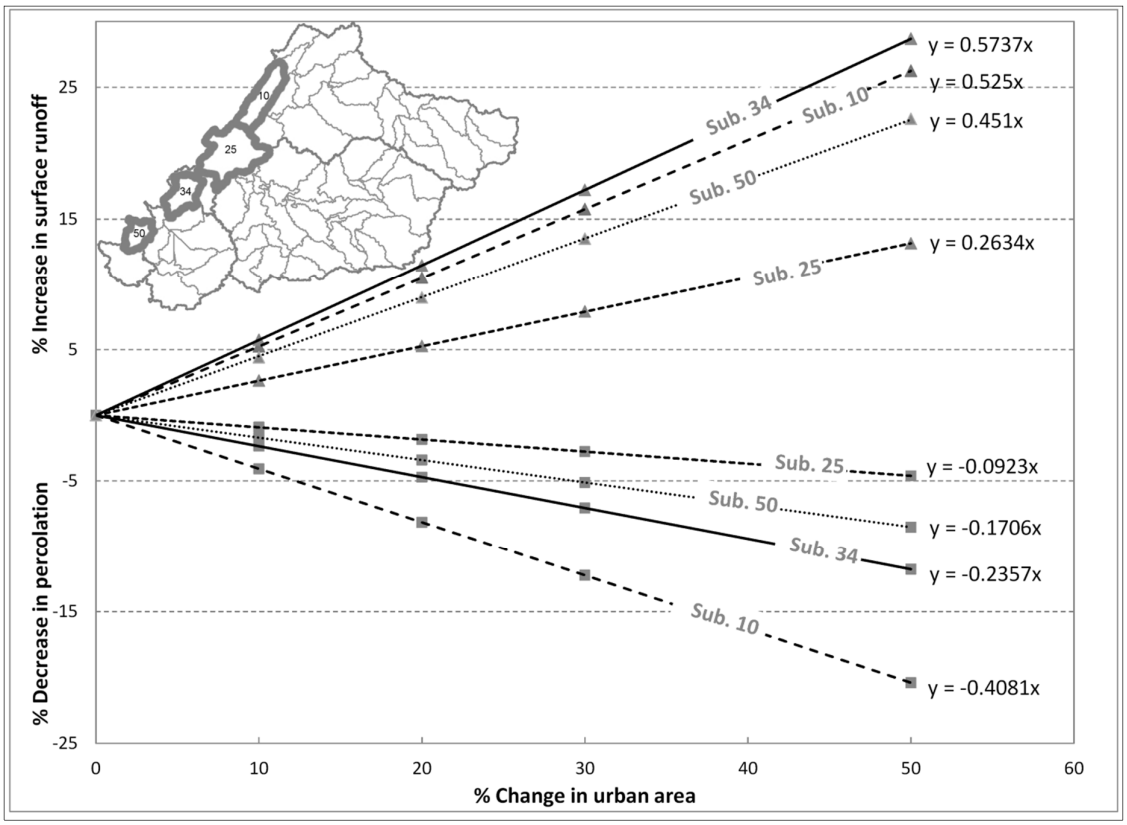

Figure 2.10 Linear relationship between urban area change and percolation / surface runoff

The USI and the UPI give an indication for each subbasin about the reaction of the hydrological system to the urban area change. However, the indexes do not reflect the relative impact between subbasins on the aquifer percolation or on the overall surface runoff. In addition to the hydrological components, variation of the subbasin geometry has an obvious impact on USI and UPI indexes.

The influence on total aquifer percolation and overall surface runoff within the aquifer domain due to urban area change was quantified in a spatial approach. The global Urban-Surface runoff Index (GUSI) and Global Urban-Percolation Index (GUPI) were derived (equations 2.3 and 2.4).

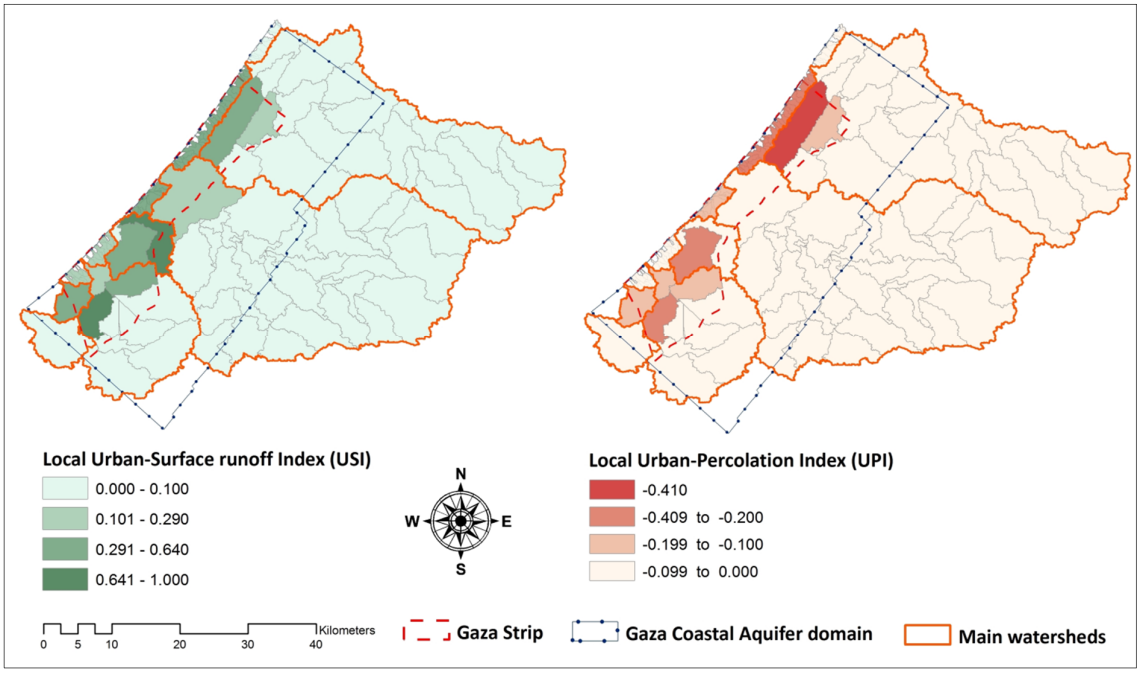

Figure 2.11 Urban-Surface Runoff Index and Urban-Percolation Index

$$\mathrm{GUSI}_i = \mathrm{USI}_i \times \frac{A_i \times S_i}{\sum_i^n A_i \times S_i} \tag{2.3}$$

$$\mathrm{GUPI}_i = \mathrm{UPI}_i \times \frac{A_i \times P_i}{\sum_i^n A_i \times P_i} \tag{2.4}$$

where n is the total number of subbasins shared in the aquifer domain, i is the subbasin number (from 1 to n), A_i is the area of subbasin i, S_i is the surface runoff of subbasin i, and P_i is the percolation of subbasin i.

Figure 2.12 depicts the spatial variability of the percent change in overall surface runoff across the aquifer domain due to urban area expansion by 1% at subbasin level (GUSI). Similarly, it depicts the spatial variability of the percent change in aquifer recharge due to urban area expansion by 1% at subbasin level (GUPI). A larger urban area in a subbasin a higher GUSI and a higher negative GUPI. The large and high density urban area in the northern Gaza Strip is translated into a high GUSI and a high negative GUPI. The previous indexes are valid as long as there is no significant change in the hydrological characteristics of the surrounding areas due to the urban area expansion.

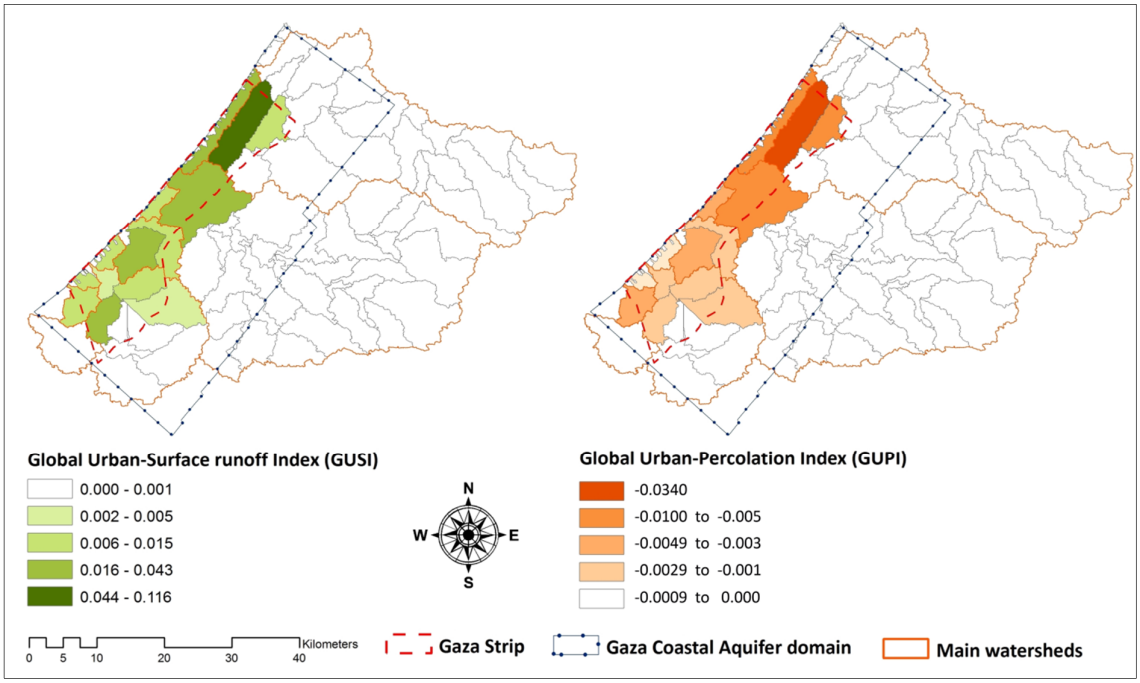

Figure 2.12 Global Urban-Surface Runoff Index and Global Urban-Percolation Index

The Costal Municipalities Water Utility (CMWU, 2010) reported that the Gaza coastal aquifer has two sensitive areas of groundwater depression, i.e. in the north where the groundwater level drops more than 4 m below the mean sea level and in the south where it drops more than 12 m. In this case, the UPI can support the decision maker in the evaluation of different urban change scenarios in the subbasins in the north and south of the Gaza Strip. On the other hand, the GUPI and the GUSI can contribute to the development of spatial sustainability indicators for the Gaza coastal aquifer.

The regional plan for the Gaza Strip (2020) considered the natural resources areas in the planning process of the urban development zone (Ministry of Planning, 2007). Figure 2.13 shows that the southern urban development zone is directed to the east (lower

groundwater quality) and not to the west (higher groundwater quality). By intersecting Figures 2.12 and 2.13, the northern urban development zone has the highest negative GUPI (Fig. 2.12). The urban development zone with high population density will increase the GUSI with increasing negative GUPI, representing a threat to the aquifer sustainability. Decreasing the impervious area in the urban development zone in the north of the Gaza Strip as far as possible is a substantial approach towards a solution. Decreasing the built-up area by introducing taller buildings in the development zone relatively to the existing urban area is recommended. Water-saving schemes like rainwater harvesting and greywater treatment can significantly reduce the pressures of new urban development (Rozos and Makropoulos, 2012). Surface runoff harvesting systems are therefore recommended for the urban development zone, especially in the northern area of the Gaza Strip.

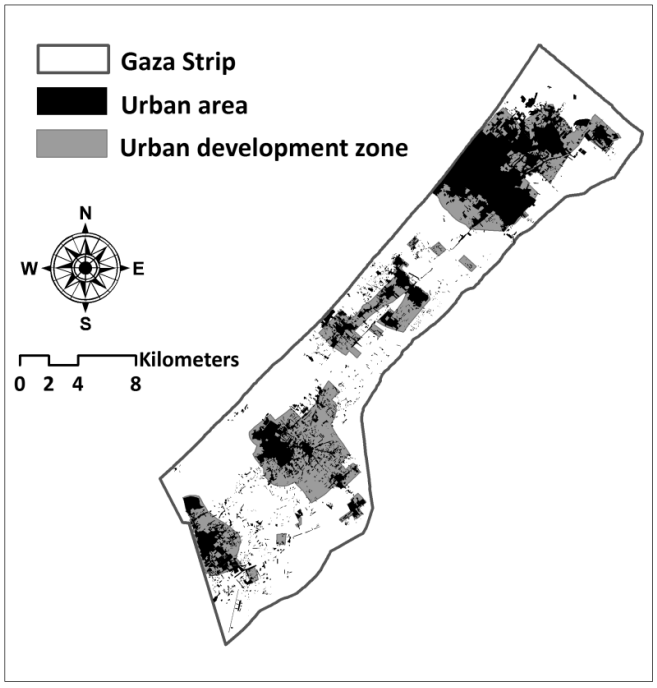

Figure 2.13 Urban development zone (2020) for the Gaza Strip (Ministry of Planning, 2007)

CHAPTER 3

3 Potential impacts of urban area expansion on groundwater level: a spatial-temporal assessment

3.1 Introduction

Where aquifers are over-exploited and where urban expansion has led to uncontrolled land use, deterioration of water quality and decline in exploitable yield are expected. One of the challenges associated with accelerating urban growth is to supply water to urban areas within limited water resources (Srinivasan *et al*., 2013). Mastering this challenge is complicated further by the fact that, in the process of urbanization, soils are often compacted and covered by impervious surfaces resulting in increased runoff and decreased percolation (Carlson *et al*., 2011). Recently, intersections among groundwater, surface water and land use have become hot topics for scientific research (Cho *et al*., 2009; Wang and Hejazi, 2011; Xu *et al*., 2012; Chung *et al*., 2014). A spatial and temporal approach of groundwater simulation in different aquifers was investigated in several studies (Lachaal *et al*., 2012; Benhamiche *et al*., 2014; Liu *et al*., 2014). Moukana and Koike (2008), Chen *et al*. (2010), Sun *et al*. (2011), and Chaudhuri and Ale (2014) assessed and/or simulated the relationship between land use and groundwater level in different regions.

In the Gaza Strip, more than 95% of the domestic and agricultural water supply is groundwater. The current rate of aquifer abstraction is unsustainable, and deterioration of groundwater quality was detected in many parts of the Gaza Strip, mainly caused by saltwater intrusion and nitrate contamination (Qahman and Larabi, 2006). The aquifer is recharged by different components such as rainfall, water and wastewater networks leakage, and agricultural return flow, and from artificial recharge ponds. The recharge quantity is estimated to be on average around 100 to 120 Mm^3 a year, whereas the annual average groundwater withdrawals exceed this amount leading to a deficit in a range between 40 and

60 Mm^3 (PWA, 2013). The Costal Municipalities Water Utility (CMWU, 2010) reported that the Gaza coastal aquifer has two sensitive areas of groundwater depression, i.e., the north and the south area, where the groundwater level elevation drops considerably below the mean sea level. With the impact of rapid urban growth, the Gaza Strip coastal aquifer is at risk of severe depletion in terms of regional water table decline.

Proper development planning is urgently needed to solve these problems and to ensure sustainability of the water environment. Improving the information base and providing appropriate management indicators are the most essential steps to support proper development planning processes. The quantitative evaluation of the impacts by human activities on water resources is in the focus of the present research in hydrology (Chu *et al.*, 2010). Assessment of temporal and spatial patterns of groundwater levels in the Gaza Strip is a prerequisite to formulating realistic actions to meet the accelerated demands in a sustainable way.

Melloul and Collin (2000) proposed an empirical approach toward sustainable management of the Gaza coastal aquifer. Their approach enabled a comprehensive understanding, investigated different hydrological scenarios, and recommended a set of operational activities for the Gaza coastal aquifer. Metcalf & Eddy Inc. (2000) developed a fully 3-dimensional, numerical groundwater model using the flow and transport model DYNCEF for the Gaza coastal aquifer through the Gaza Costal Aquifer Management Program project (CAMP project). This model evaluated the effect of pumping management scenarios on groundwater flow considering seawater intrusion. Moe *et al*. (2001) presented the main steps for simulating the effect of the integrated aquifer management plan that was developed by the CAMP project, which reflects guidelines for water supply and usage until year 2020. Saleh (2007) developed a groundwater flow model for the Gaza coastal aquifer using MODFLOW-2000 to simulate the impact of pumping on saltwater intrusion. Sirhan and Koch (2013) carried out a numerical modeling using visual MODFLOW to evaluate the impact of artificial recharge on the groundwater level to manage the Gaza coastal aquifer. The previous studies estimated the range of rainfall recharge between 25 and 48 Mm^3/y, depending on the methodology used and the base year or period. A surface water modeling with SWAT to quantify the impact of urban area expansion on groundwater recharge and surface runoff was performed in Chapter 2. A spatial distribution of percolation within the Gaza aquifer domain from 2004 to 2010 was developed. These results are used throughout this study, which is an innovative approach as it considers temporal and spatial distribution of

groundwater recharge components, which were not counted through the modeling process as calibration parameters, and provides a more realistic and comprehensive approach during model forecasting.

The objectives of this study are: (1) develop a 3-D groundwater flow model to investigate the groundwater levels within the Gaza coastal aquifer considering the connection to a surface water model as well as a high-precision estimation of other recharge components; (2) assess the long-term trend of groundwater levels and determine the distribution across the Gaza Strip. Figure 3.1 shows the methodological framework used in this study, which comprises three main interfaces, namely tabulated data, GIS interface and visual MODFLOW.

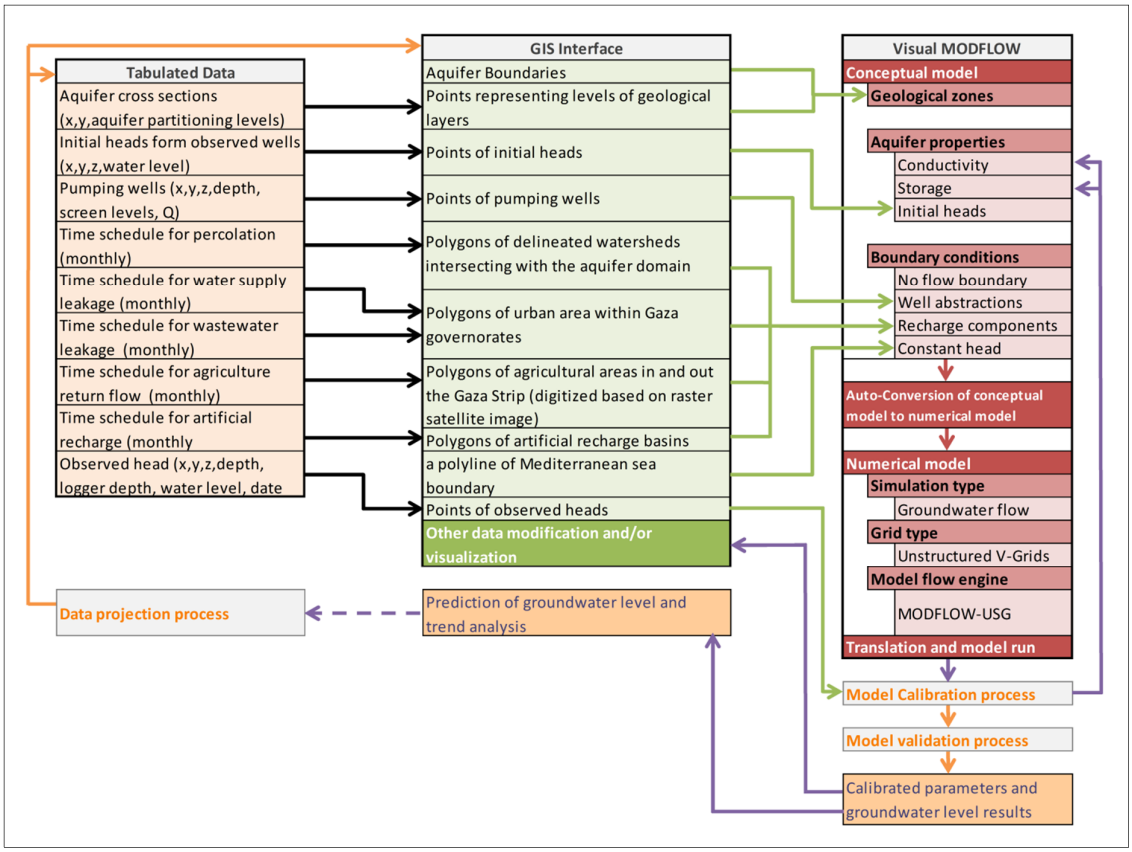

Figure 3.1 Methodological framework

3.2 Study area

Palestine comprises two separate areas, the Gaza Strip and the West Bank. The Gaza Strip (Fig. 1.1) is a narrow strip located on the south-eastern coast of the Mediterranean Sea with a land area covering 365 km^2. The Gaza coastal aquifer is a part of the larger coastal aquifer extending from the Karmel Mountain in the north to the Sinai desert in the south with variable dimensions (Baalousha, 2005). The aquifer is shallow and mainly unconfined with a productive zone forming a narrow strip along the coast, and a groundwater flow from the hinterland towards the sea (UN-ESCWA and BGR, 2013). The Gaza aquifer domain moves beyond the Gaza Strip boundary towards the north (no flow boundary), and towards the east where the water table is close to the aquifer bed (no flow boundary), and towards the south in Egypt, where no data are available and there is no significant flow (assumption: no flow boundary), and finally towards the Mediterranean Sea in the west (fixed head to zero) (Metcalf & Eddy Inc., 2000; HWE, 2010).

3.2.1 Climate

The Gaza Strip has a semi-arid climate with a short and mild rainy season and dry summer (CMWU, 2010). The mean temperature varies from 13 C° in January to 27 C° in June. The average annual precipitation gradually declines away from the coast from the west to the east, and varies from 400 mm/y in the north to 200 mm/y in the south, with a mean value of 320 mm/y (UN-ESCWA and BGR, 2013). The hydrological year usually starts in October or November. The average annual potential evaporation is about 1400 mm/y (PWA, 2010).

3.2.2 Hydrogeology

With a varied total thickness between 100 and 180 m, the Gaza coastal aquifer consists of alluvial deposits with dunes, sand or loess alluvial as a cover. The geological formations of the coastal aquifer are of Pleistocene and Holocene age, and consist of sandstone, dune sand, gravel and conglomerate with a top cover of loess and a marly bottom. Intermediate loamy and clayey intercalations which extend 2–5.5 km inland divide the aquifer into four sub-aquifers, referred to in this study as A, B1, B2 and C (Fig. 3.2). The Pleistocene formation is mostly underlain by the Saqiye Group (impermeable Neogene strata). The upper sub-aquifer (A) is unconfined, whereas some confined parts (sub-aquifer B and C) can be identified near the coast (Dudeen, 2001; UN-ESCWA and BGR, 2013; Metcalf & Eddy Inc., 2000).

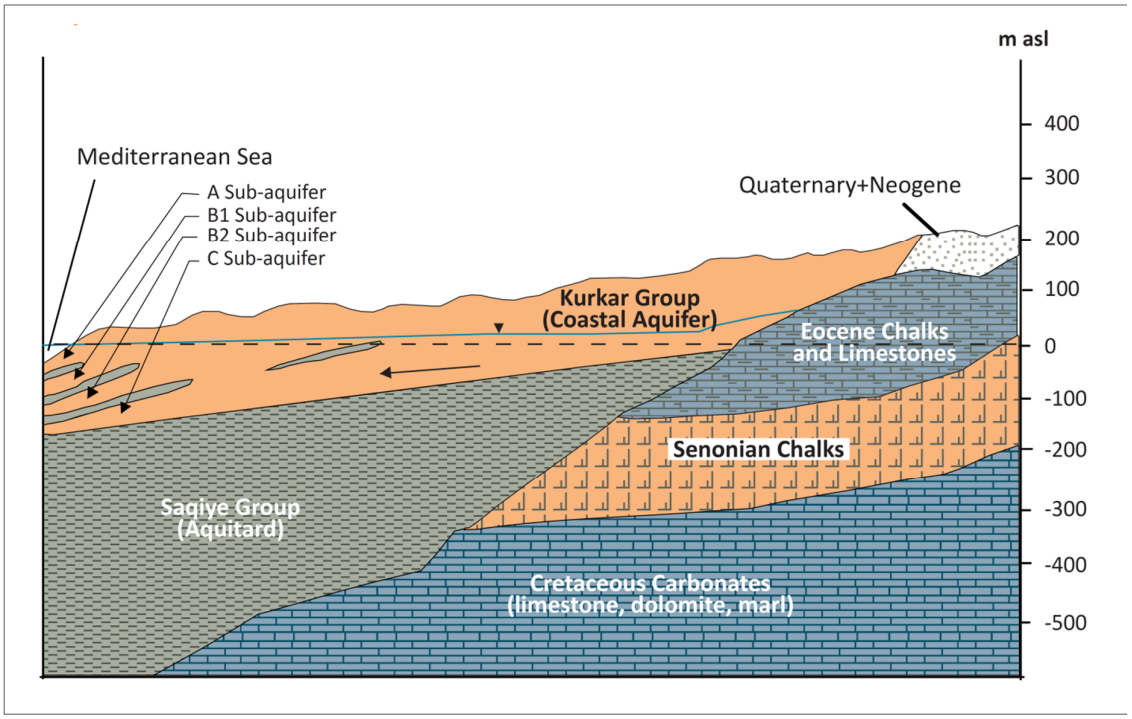

Figure 3.2 Aquifer cross section (UN-ESCWA and BGR, 2013)

3.3 Groundwater recharge and withdrawal

3.3.1 Recharge from rainfall (natural recharge)

The natural groundwater recharge varies annually and seasonally according to rainfall patterns and distribution within the study area and to other recharge components. The estimation of rainfall recharge in previous studies is based on an average recharge value of the aquifer domain or on the concept of the recharge coefficient depending on local soil type only. This study considers a spatial and temporal distribution of percolation within the Gaza aquifer domain derived from a physically based surface water model (SWAT) and documented in Chapter 2 (Fig. 3.3). The water table fluctuation method (WTF), which is one of the most widely used techniques for estimating groundwater recharge over a wide variety of climatic conditions (Obuobie *et al*., 2012), was used to robust the percolation results by the SWAT (Ch.2).

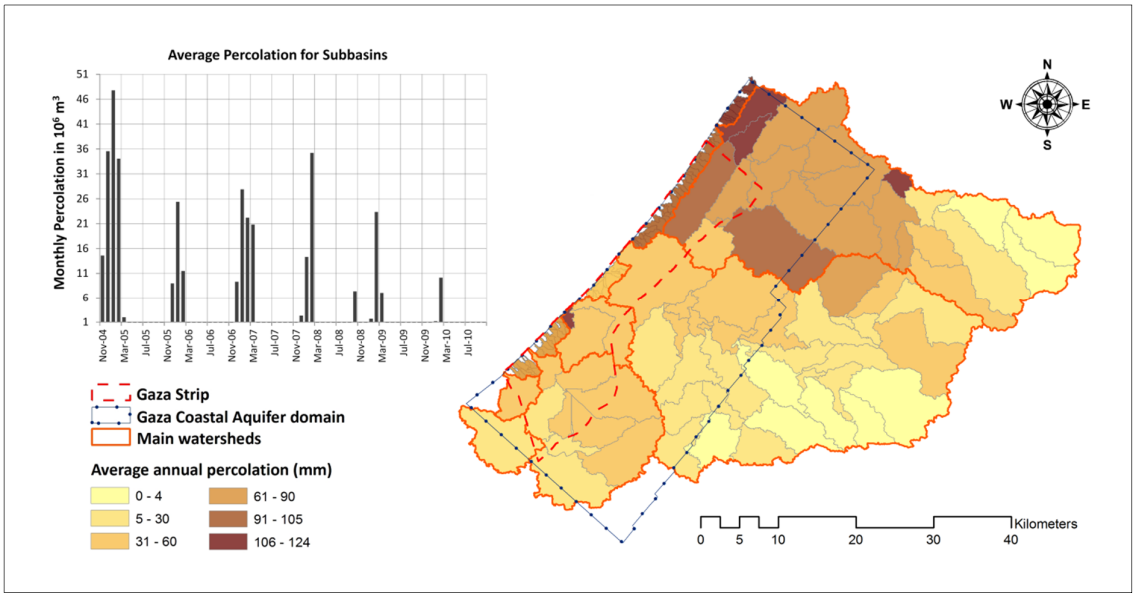

Figure 3.3 Spatially distributed percolation derived from the SWAT model (Ch.2)

The rainfall recharge rate by the WTF method can be expressed as:

$$R = S_y \frac{\Delta h}{\Delta t} \tag{3.1}$$

where R is the groundwater recharge from rainfall (mm/time), S_y is the specific yield (dimensionless), Δh is the water table rise (mm), and Δt is the recharge period. This method is based on inherent assumptions that (1) the change in levels of the water table in shallow unconfined aquifers are only due to recharge and discharge of groundwater, (2) the specific yield of the aquifer is known and constant during the recharge period, and (3) the water table recession curve (pre-recharge) can be extrapolated to determine water table rise (Obuobie *et al.*, 2012). Previous studies obtained a representative specific yield of the Gaza aquifer domain within a range from 0.18 to 0.24. The specific yield of 0.2 was used in this study. The graphical extrapolation method (Delin *et al.*, 2006) was used to estimate Δh. Considering the hydrological year 2004/05 (a wet year), monthly observed heads of 20 monitoring wells distributed through three main subbasins generated from the delineation process of the main watersheds were used (Fig. 3.4). These subbasins cover the northern, middle, and southern parts of the Gaza Strip and have well-distributed observed water wells. Table 3.1 shows the recharge calculation using the WTF method for the three subbasins. In order to achieve a representative estimation of the subbasin recharge, the Thiessen polygon technique (McCuen, 2004) was used to assign a weight at each monitoring well in proportion to the subbasin area,

and then the weighted recharges were calculated. Comparing the tabulated recharges, the results derived from the two methods were convergent, which supports the reliability of the percolation results by the SWAT (Ch.2).

Table 3.1 Recharge by rainfall according to the Water Table Fluctuation method and utilizing data derived by the SWAT (Ch.2)

Subbasin	Water Table Fluctuation method						*R* (mm) (SWAT) (Ch.2)
	Well name	$\Delta h/\Delta t$ (Δt = year(2004/05))	S_y	*R* mm	Assigned weight	Weighted *R* (mm)	
1	A/107	0.90	0.2	180	0.021	3.78	
	A/31	1.24	0.2	247.6	0.097	24.02	
	A/47	1.11	0.2	222.4	0.048	10.68	
	A/64	1.36	0.2	272.4	0.217	59.11	
	A/53	1.27	0.2	254	0.03	7.62	
	CAMP-12	0.27	0.2	53.2	0.029	1.54	
	D/34	0.58	0.2	116.4	0.07	8.15	
	E/116	0.51	0.2	101.92	0.274	27.93	
	R/84	0.25	0.2	49.2	0.121	5.95	
	R/133	0.31	0.2	62	0.091	5.64	
	Total *R* (mm) for subbasin 1					**154.4**	**150.9**
2	T/15	0.55	0.2	110	0.192	21.12	
	T/9	0.12	0.2	24	0.099	2.38	
	L/8	0.64	0.2	128	0.07	8.96	
	T/26	0.58	0.2	115	0.125	14.38	
	CAMP-11	0.74	0.2	148	0.169	25.01	
	L/18	0.81	0.2	162	0.137	22.19	
	M/10	0.37	0.2	74	0.067	4.96	
	L/57	0.08	0.2	16	0.061	0.98	
	J/68	0.50	0.2	100	0.081	8.1	
	Total *R* (mm) for subbasin 2					**108.1**	**99.4**
3	P94	0.46	0.2	92	0.126	11.59	
	L61	0.06	0.2	12	0.139	1.67	
	P61	2.40	0.2	480*	0.104	49.92	
	P68	0.57	0.2	114	0.139	15.85	
	CAMP-9	0.19	0.2	37	0.364	13.47	
	P10	0.01	0.2	2	0.13	0.26	
	Total *R* (mm) for subbasin 3					**92.8**	**103.6**

* This value should be smaller than 480 mm; S_y in this location could be lower than 0.2

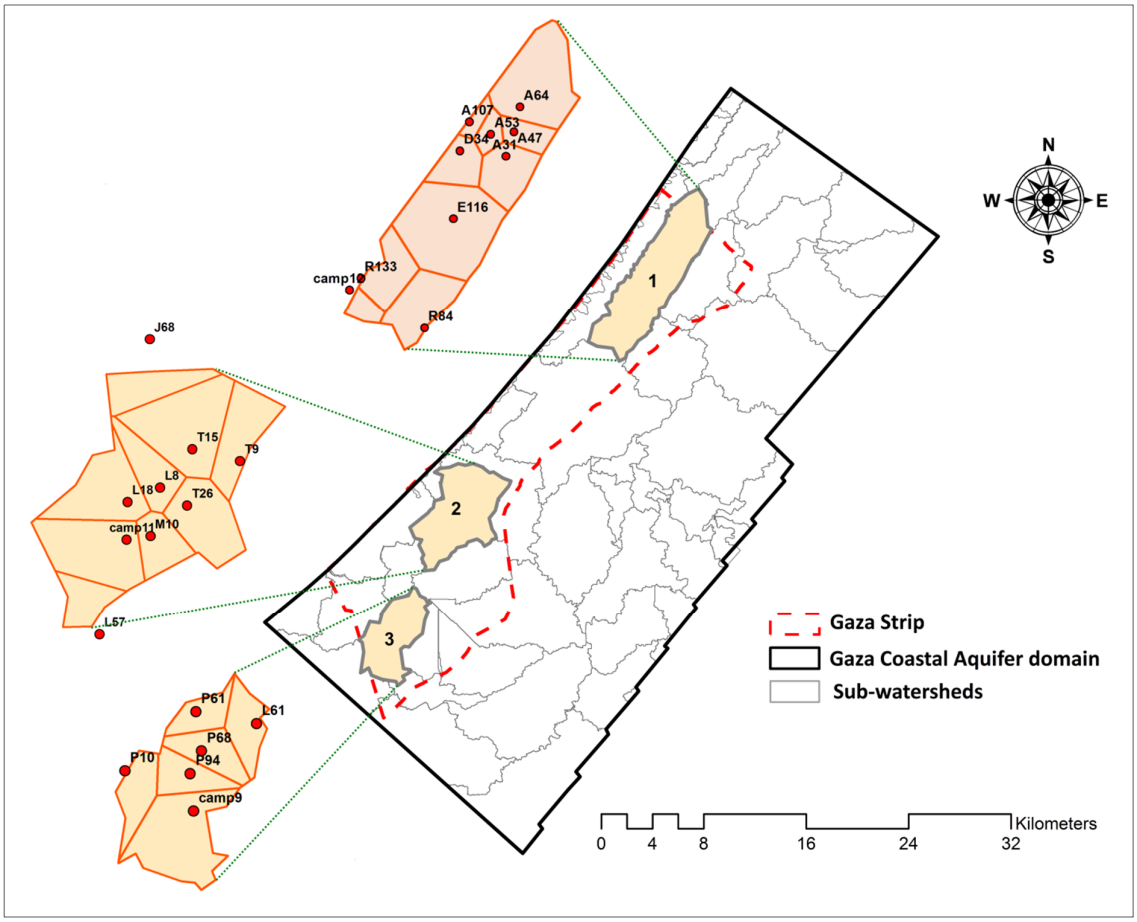

Figure 3.4 Subbasins (Ch.2) used in Water Table Fluctuation method

3.3.2 Recharge from water and wastewater network leakage

Around 98% of the urbanized area of the Gaza Strip is covered by water supply networks (CMWU, 2010). The calculated water supply system efficiency in the Gaza governorate in November 2004 ranged from 0.51 in Khanyounis city (in the southern Gaza Strip) to 0.7 in Gaza city, whereas these values were 0.58 and 0.7, respectively, in November 2009 (PWA, 2013). The overall losses through the water supply system in the Gaza strip are estimated at 45% (35% due to physical losses and 10% due to unregistered connections) (PWA, 2013). For each governorate, the monthly calculated physical losses during 2004–2010 were used to configure water leakage quantities.

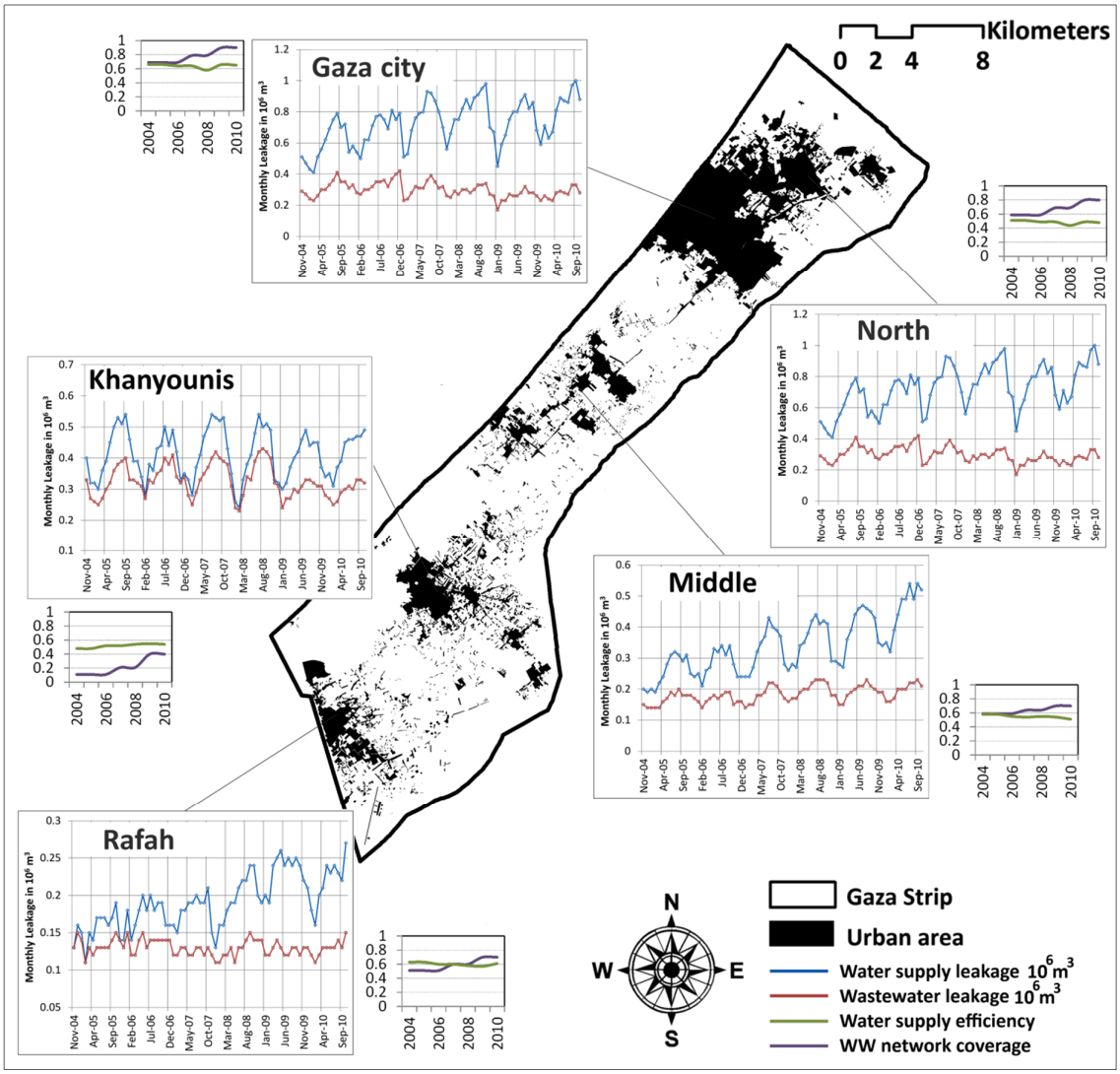

Figure 3.5 Pattern of water and wastewater leakage during simulation period (2004-2010) (developed based on recorded data (CMWU, 2013; PWA, 2013)

Currently, about 75% of the Gaza households are connected to a sewage network (CMWU, 2010). Unconnected households use cesspits releasing wastewater into the aquifer, and flooding on the roads. Sewage network coverage was 0.69 in Gaza city and 0.20 in Khanyounis city in 2005, whereas these values were 0.9 and 0.4, respectively, in 2010 (CMWU, 2013). For each governorate, the monthly coverage rate during 2004–2010 assumed a wastewater network system efficiency of 0.8 (Rabah, 1997). Generated wastewater quantities of around 75% of the consumed water (CMWU, 2013) formed the main elements to calculate wastewater leakage quantities. Figure 3.5 displays the temporal variation of water leakage, wastewater leakage, water supply efficiency, and wastewater network coverage.

3.3.3 Irrigation return flow

Although the Gaza Strip is mostly urbanised, it has a historically active and potentially profitable agricultural sector. The agricultural sector in the Gaza Strip on average consumes around 75–85 Mm^3 of water annually (PWA, 2013), which all comes from the groundwater wells. Irrigated crops are mainly vegetables, citrus, herbs, field crops and varied horticulture. Considering the soil characteristics, the high crop-water demand and water scarcity, drip irrigation and mini-sprinklers are the commonly used irrigation systems (PWA, 2013). Ghabayen and Salha (2013) found that the amount of irrigation return flow is about 22–24 % of the total irrigation water.

Within the aquifer domain, but outside the Gaza region, the Israeli side comprises extensive agricultural cropping areas (CBS, 2013). The Gaza aquifer domain intersects with four natural regions (4 zones), which have different ratios of agricultural crops, namely plantations, vegetables, potatoes, melons and field crops. Goldfarb and Kislev (2009) estimated the proportion of irrigation return flow to total irrigation water of the coastal aquifer outside the Gaza region at 16%.

The spatial monthly estimation of agricultural return flow is based on various factors, namely the monthly pattern of crop water requirements (CEP and FCG, 2010), annual irrigated crops area through governorates (in Gaza region) and zones (outside Gaza region), and estimated overall irrigation returned flow (PWA, 2013) (Fig. 3.6).

3.3.4 Artificial recharge

Artificial recharge is carried out only during years when excess water is available (rainy seasons or wastewater infiltration basin). There are five artificial recharge ponds in the Gaza Strip and another natural infiltration basin outside the Gaza region.

The average recharge of the infiltration lagoons of the Beit Lahia wastewater treatment plant (BLWWT) was estimated at 3.6 Mm^3/y (about 50% of daily effluent from BLWWT to lagoons). Since 2010, the first phase of the North Gaza Emergency Sewage Treatment Project (NGESTP) was established. This project comprises the construction of eight infiltration beds at a new site in response to the severe overloading of the BLWWT (CMWU, 2013). The El-Sheikh Redwan infiltration lake, which is located northwest of Gaza city, has an average infiltration rate of 300 mm/y (Ghabayen *et al*., 2013). The annual recharge of the Alamal infiltration lake located in Khanyounis city can be estimated at 1 Mm^3. The recharge from the wastewater drained to Wadi Gaza amounts to 0.5 Mm^3. The

average annual recharge of the Shiqma storm water bond, outside the Gaza Strip, was estimated at 3.6 Mm^3 (Metcalf & Eddy Inc., 2000).

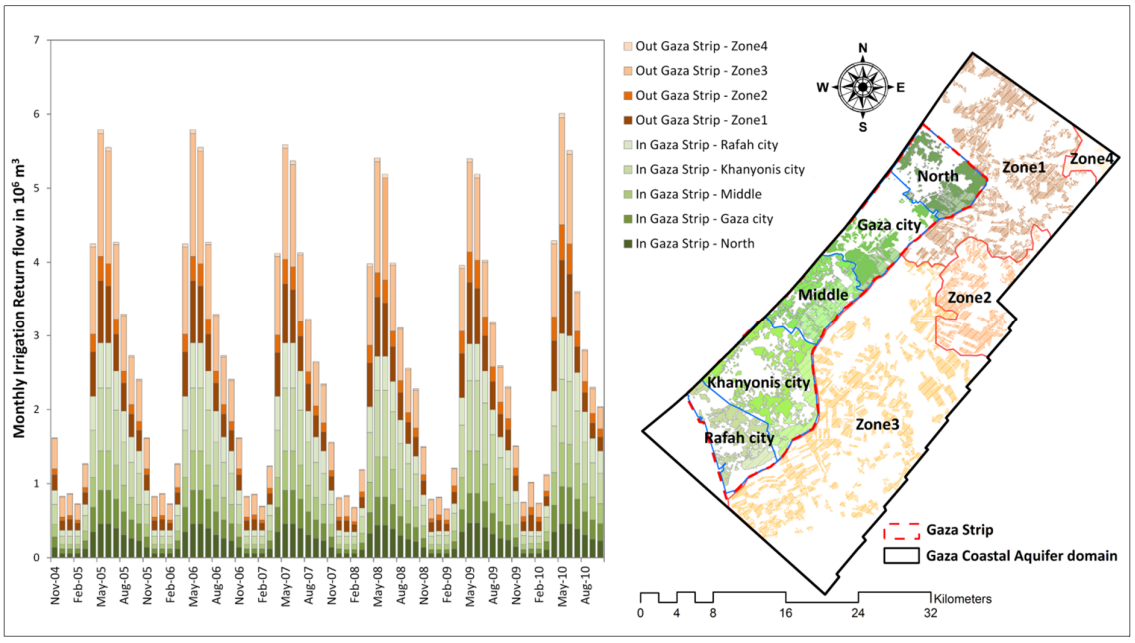

Figure 3.6 Pattern of agricultural return flow during simulation period (2004-2010) (developed based on PWA, 2013; CBS, 2013; CEP and FCG, 2010)

3.3.5 Well abstraction

As a result of the water demand growth, the groundwater abstraction from the Gaza coastal aquifer gained momentum in the early 1930s. Through the period 2004–2010, the annual abstraction ranged between 74 and 80 Mm^3 for agricultural water needs, whereas the annual abstractions by municipal water wells increased from 70 to 88 Mm^3.

More than 4000 water wells are operated in the Gaza Strip to meet both the domestic and agricultural demand (CMWU, 2013) (Fig. A.1). The annual average groundwater abstraction in Israel within the model domain was estimated at around 50 Mm^3 from 90 wells (Metcalf & Eddy Inc., 2000). The measured monthly abstraction rate of 209 municipal water wells within the Gaza region are used in this study. More than 3800 agricultural water wells are considered in this study taking into account the agricultural demand pattern in the estimation of monthly abstraction rates for each well (PWA, 2013).

3.4 Groundwater flow modeling

3.4.1 Flow equation and model used

The 3-D groundwater flow in a porous medium may be expressed as (Bear, 1972):

$$S_s \frac{dh}{dt} - \left[\frac{\partial}{\partial x}\left(K_x \frac{\partial h}{\partial x} \right) + \frac{\partial}{\partial y}\left(K_y \frac{\partial h}{\partial y} \right) + \frac{\partial}{\partial z}\left(K_z \frac{\partial h}{\partial z} \right) \right] = q_s \qquad (3.2)$$

where h is the hydraulic head, S_s is the specific storage, q_s is a sink or source, and K_x, K_y, K_z are hydraulic conductivity in x, y, z directions, respectively.

The MODFLOW model was chosen for simulating the 3-D, constant density, groundwater flow regime based on Darcy's law and the mass conservation concept developed by McDonald and Harbaugh (1988) and Harbaugh *et al*. (2000). MODFLOW numerically solves the groundwater flow equation (equation 3.2) by using a finite-difference method.

The Gaza aquifer domain comprises a high density of wells concentrated within the Gaza region, which represents a challenge for model discretization in terms of cell size and run time where accurate results are to be obtained.

This study applied MODFLOW-USG, which is a new version of MODFLOW that uses unstructured grids. By enabling the use of different polygon shapes, the unstructured grid enhances the MODFLOW simulation to appropriately discretize an aquifer domain. Taking into account the same level of simulation accuracy, MODFLOW-USG is faster than the conventional version of MODFLOW (MODFLOW-2005). MODFLOW-USG and MODFLOW-2005 functionally have similar components (Panday *et al*., 2013).

The Visual MODFLOW software provides both GIS-based conceptual modeling and numerical modeling in an integrated environment, and allows generation of multiple numerical models with minimum effort.

3.4.2 Conceptual model

Four sub-aquifers, referred to as A, B1, B2 and C, were conceptualized considering the intermediate loamy and clayey layers (aquitards) (Fig. 3.7).

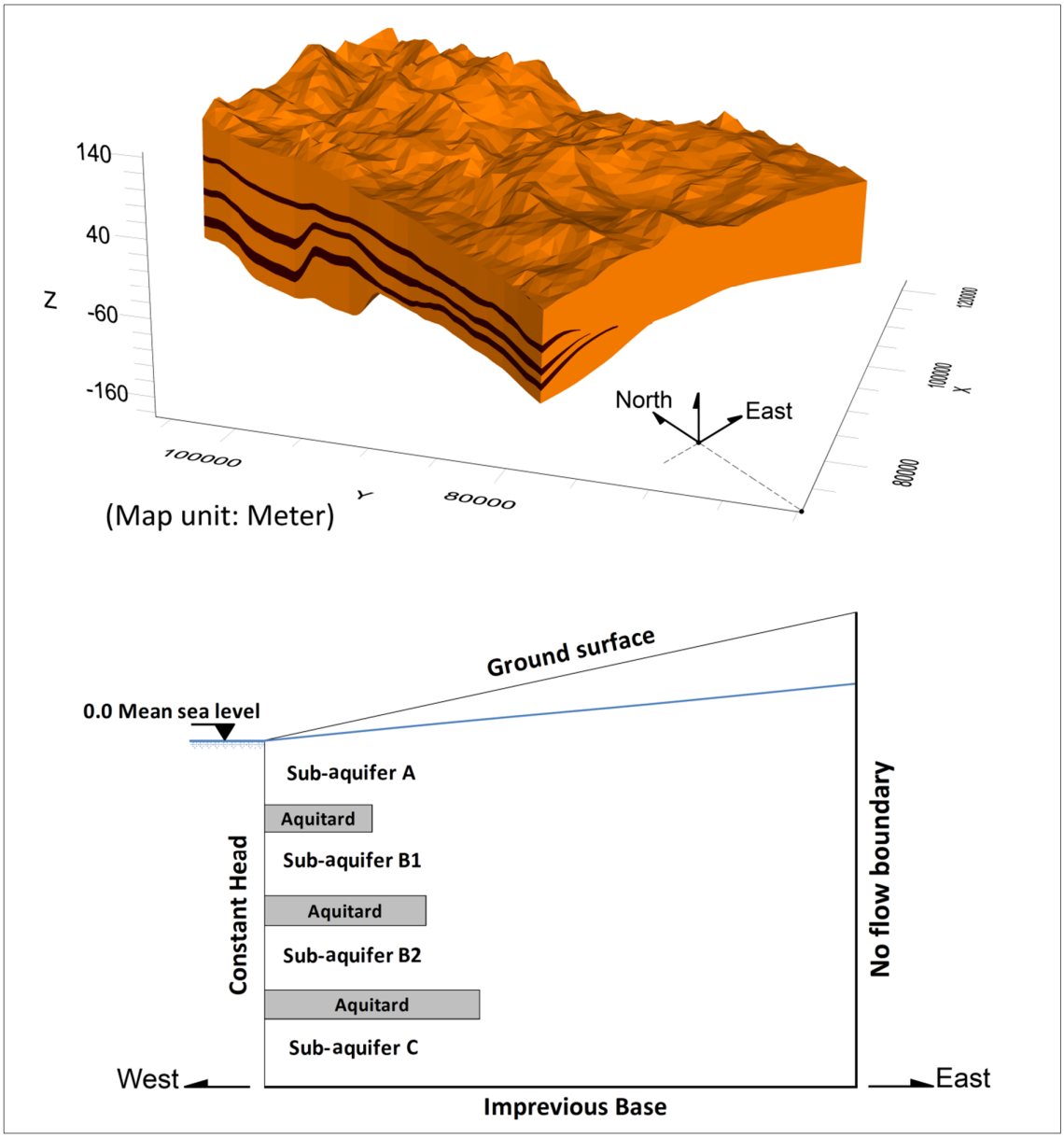

Figure 3.7 Conceptual model

Initial conditions and aquifer parameters

The initial flow head was drawn in November 2004 based on 138 observed water wells distributed through the model domain. The estimation of the hydraulic conductivity, specific storage and porosity of the Gaza coastal aquifer system is based on pumping tests, which were carried out for different municipal wells as part of the CAMP project (PWA, 2013) and previous studies (Table 3.2).

Table 3.2 Aquifer parameters (previous studies and initial estimation)

Parameter	Pumping tests by CAMP project (PWA, 2013)	Calibrated values in previous studies				Initial estimation in this study	
		Metcalf & Eddy Inc., 2000		Sirhan and Koch, 2013			
		aquifers	aquitards	aquifers	aquitards	aquifers	aquitards
Hydraulic conductivity (K_x, K_y, or $10K_z$) (m/d)	20–80	30	0.2	34	0.2	30	0.2
Specific yield (S_y)	0.15–0.30	0.24	0.10	0.18	0.05	0.21	0.05
Specific storage (S_s) (m^{-1})	10^{-4}–10^{-5}	10^{-4}	10^{-5}	10^{-4}	10^{-5}	10^{-4}	10^{-5}
Effective porosity		0.25	0.30	0.25	0.30	0.25	0.30
Total porosity		0.30	0.45	0.30	0.45	0.30	0.45

Boundary conditions

In the simulation zone, the east, north and south were considered as confining boundaries (no flow boundaries); the west boundary was considered as a constant head boundary. The lower interface was generalized as an impervious boundary. Water exchanges occur at the top interface, which is in contact with the atmosphere. Monthly records for percolation, water and wastewater leakage, irrigation-return flow, artificial recharge and well abstraction (see section 3.3) were used as boundary conditions for the simulation period from 1 November 2004 to 31 October 2010.

3.4.3 Numerical model

Discretization

The Gaza coastal aquifer domain was discretized as Voronoi cells using a built-in mesh generator called "Triangle" in MODFLOW-USG. The Voronoi grid (cells) is a way of dividing space into a number of regions considering a set of points specified beforehand. For each point, there is a corresponding region consisting of all points closer to it than to any other (Siegkas *et al*., 2014).

The model domain was divided into 18546 active cells, which represent the total area of 1232 km^2 (Fig. 3.8). The cell size varied through the model domain; localized refinement was concentrated around wells and boundaries. As the average vertical cross section was dissected into seven layers, the simulation zone is dissected into (129822) active cells. The

area of Voronoi cells ranges between 0.9 m^2 (around 1 m^2) and 1035079.0 m^2 (around 1 km^2) with an average of 66747.4 m^2.

As the total simulation period is 6 years from November 2004 to October 2010 based primarily on monthly pumping and recharge data, the stress period of the model is 72 months. Figure 3.9 shows the compatibility of the boundary conditions with the discretized grids.

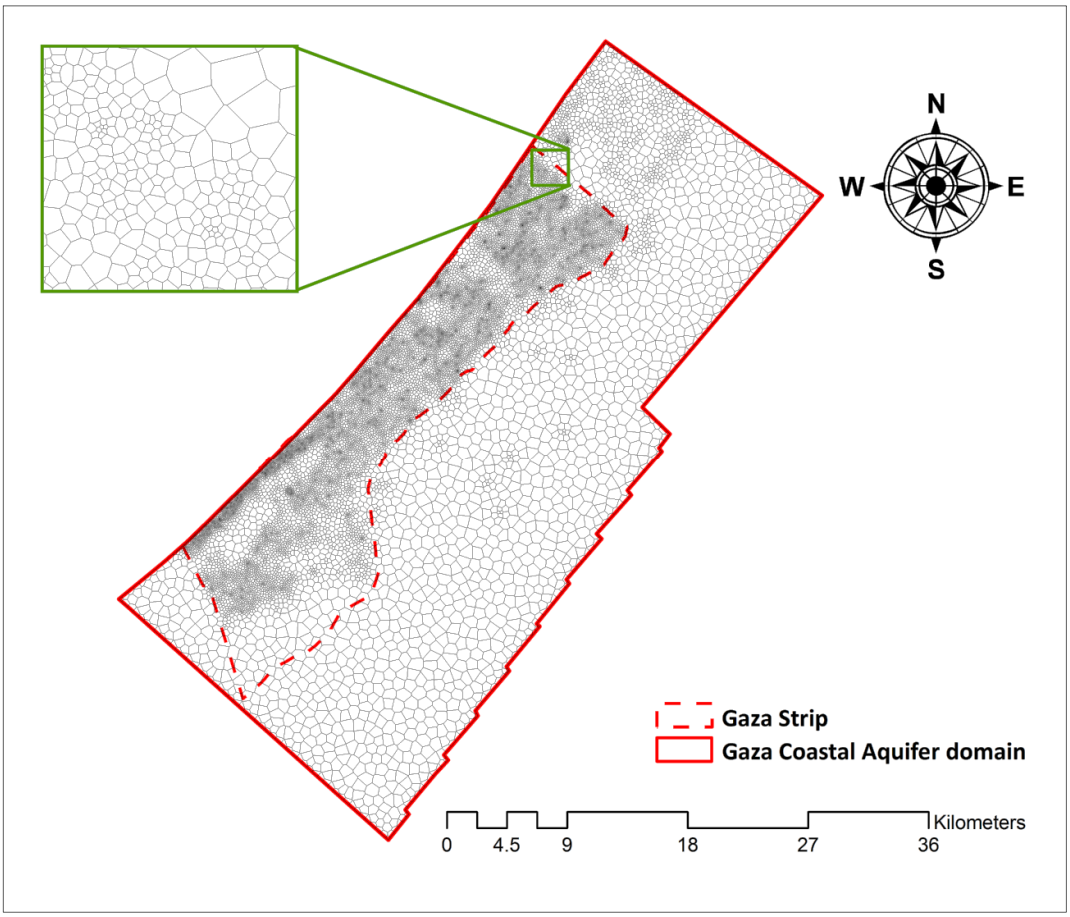

Figure 3.8 Numerical unstructured grid (Voronoi cells)

3.4.4 Model calibration and validation

A calibration aims to obtain an optimal fit between the calculated and measured data, and is an important measure for modeling reliability (Lachaal *et al.*, 2012). The model was calibrated through the periods from November 2004 to October 2007 and from November 2009 to October 2010. The calibration period consists of relatively wet, normal, and dry hydrological years. To ensure that the calibrated model properly assessed all the variables and conditions that could have affected the model results, model validation was performed from November 2007 to October 2009.

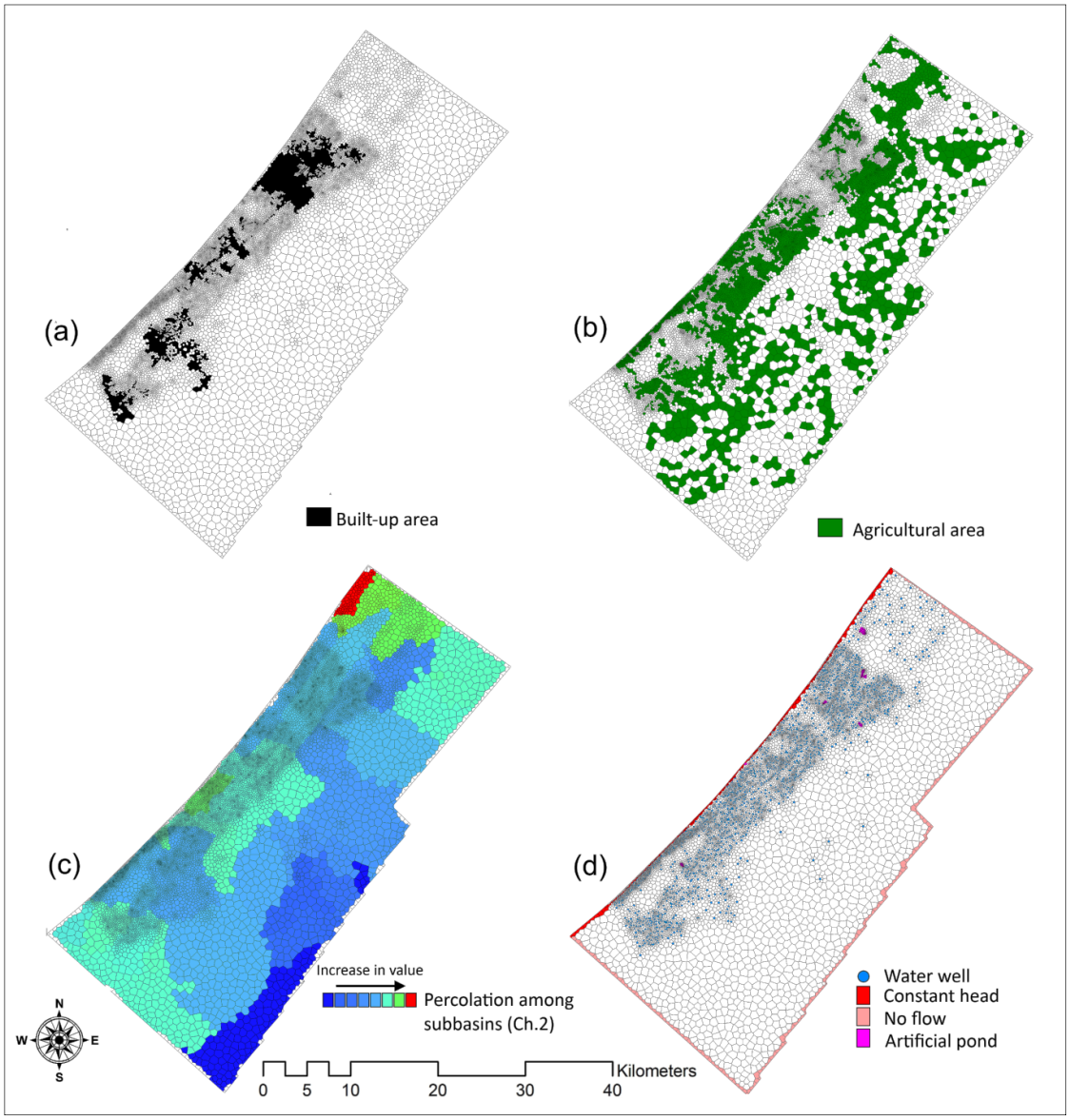

Figure 3.9 Compatibility of boundary conditions with discretized grid: (a) grid with water and wastewater leakage, (b) grid with aquiculture return flow, (c) grid with rainfall recharge (total percolation in a specific month), and (d) grid with pumping wells, artificial recharge basins, constant head (west boundaries), and no flow boundaries (north, east and south boundaries)

In this study, the calibration approach is based on transient calibration considering: (1) field-measured initial heads distributed through the model domain, (2) no calibration for boundary conditions, specific recharge and abstraction through the simulation period, and (3) initial estimation of specific yield, specific storage and porosity parameters derived from measured values and/or calibrated values from previous studies. Using the field-measured head values as initial conditions requires a final evaluation of the early time steps in terms of

detected offset between simulated and observed heads representing the lack of correspondence between model hydraulic inputs and parameters and the initial head values as explained by Franke *et al*. (1987). In this case, it is necessary to select a steady-state head generated by a calibrated model as the initial heads. The transient model calibration was carried out by simulating groundwater head changes in response to changes in a spatial hydraulic conductivity considering observed data of groundwater levels (97 observed wells). After obtaining an acceptable matching between observed and simulated head, specific yield and porosity were adjusted several times within a range of ±20% of the initial values through several computer runs to refine the previous calibration.

3.4.5 Results

During the calibration period, model efficiency measures for the monthly simulation R^2 (coefficient of determination) and E (Nash-Sutcliffe efficiency) are 0.934 (Fig. 3.10) and 0.936, respectively, which indicate a very good fit between measured and simulated head. The summary of calibration and validation statistics are tabulated in Table 3.3. Figure 3.11 spatially exhibits the calibrated hydraulic conductivity (K_x), while Table 3 shows the other calibrated parameters. A residual mean of -0.0284 as well as an absolute residual mean of 0.293 for the early time steps (first two months of the stress period) ensures that the initial head data (field-measured data) and the model hydraulic inputs and parameters are consistent.

Table 3.3 Summary of calibration and validation statistics

Calibration results (monthly base)		
	Observed	Simulated
Average groundwater heads (m*)	-1.15	-1.22
Standard deviation of groundwater heads (m)	2.56	2.45
Average of the highest 25% heads (m)	0.97	1.21
Average of the lowest 25% heads (m)	-4.50	-4.60
Residual mean (m)	-0.072	
Absolute residual mean (m)	0.503	
Residual mean for the early 2 months (m)	-0.028	
Absolute residual mean for the early 2 months (m)	0.293	
Efficiency measures	Coefficient of Determination, R^2	Nash-Sutcliffe efficiency, E
	0.934	0.936
Validation results (monthly base)		
Residual mean (m)	0.033	
Absolute residual mean (m)	0.539	
	Coefficient of Determination, R^2	Nash-Sutcliffe efficiency, E
Efficiency measures	0.925	0.926

* All heads datum are mean sea level

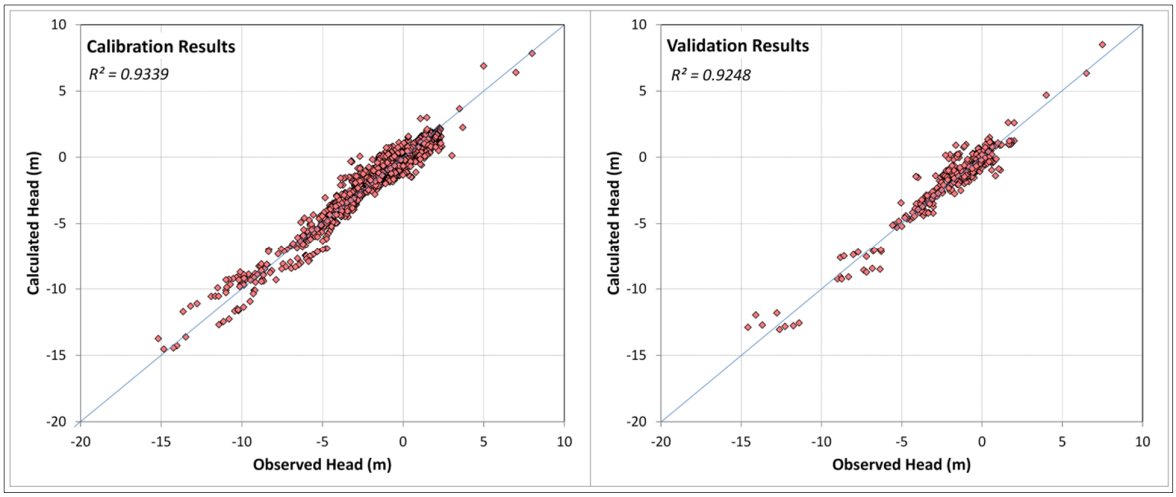

Figure 3.10 Calibration and validation results

During the validation period, it was found that the model has good predictive capability with R^2 and E values of 0.925 (Fig. 3.10) and 0.926, respectively. Through the calibration process, hydraulic conductivity reflects the most sensitive parameter of the aquifer properties.

The comparison of simulated and observed head at five representative observation wells (Fig. 3.12) distributed through the Gaza Strip (north, middle and south) indicates a substantial agreement during the calibration and validation processes.

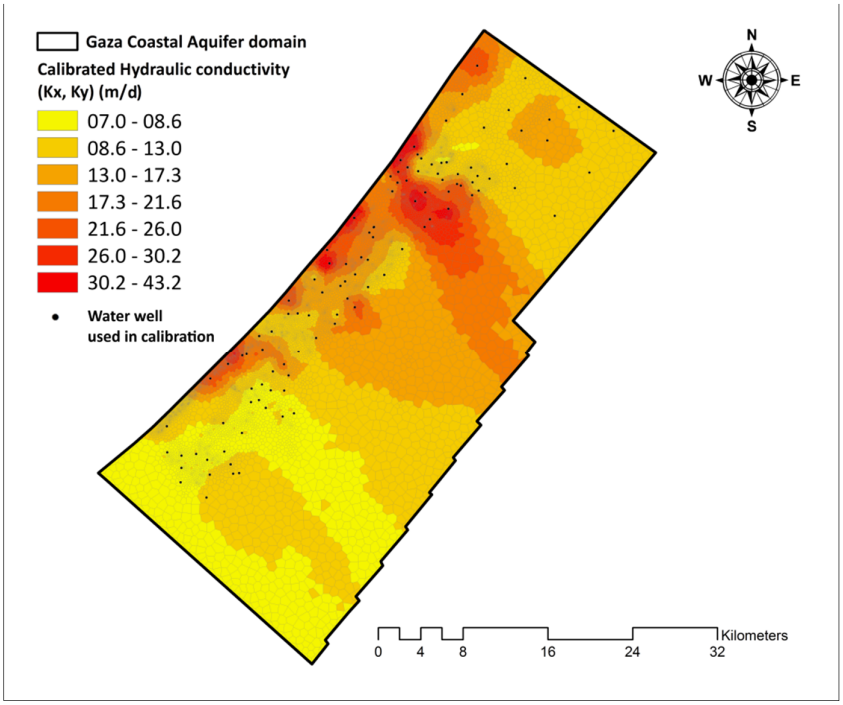

Figure 3.11 Calibrated hydraulic conductivity

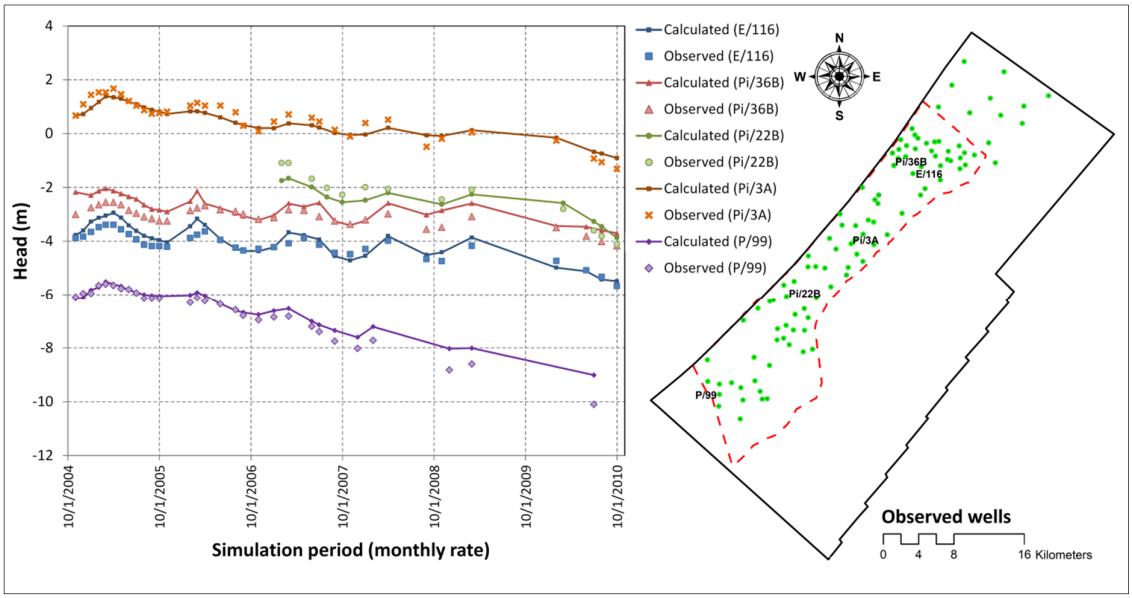

Figure 3.12 Comparison of simulated and observed heads

After obtaining the calibrated parameters, the model was run to map the simulated groundwater level (Fig. 3.13) and to investigate the annual groundwater balance from 2005 to 2010 (Fig. 3.14). Aquifer net replenishment (by subtracting wells abstraction from total recharge) reduced from 50 Mm^3 in 2004/05 (wet year) to -86 Mm^3 in 2009/10 (dry year), whereas seawater intrusion increased from 24 Mm^3 to 47 Mm^3, respectively, for the same hydrological years.

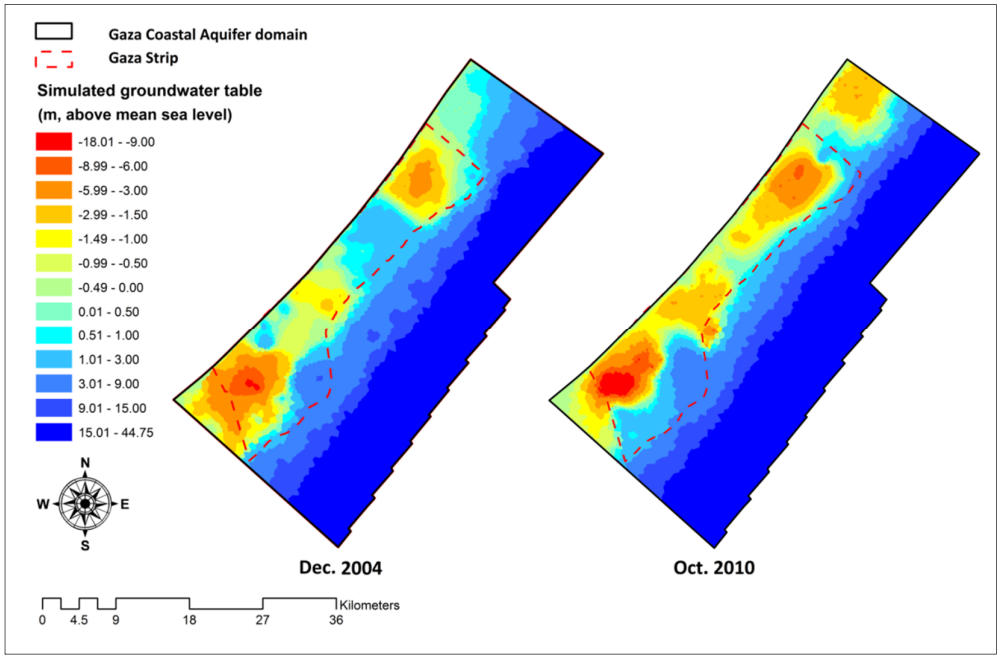

Figure 3.13 Simulated groundwater levels (2004 and 2010)

3.5 Groundwater level trend and urban expansion

3.5.1 Urbanization analysis and projection

Urbanization is a major source of additional pressure on the environment and the resources in terms of quantity and quality (Rozos and Makropoulos, 2012). The main driver of urban groundwater use is accelerating rates of urbanization. In 2013, the estimated total population in the Gaza Strip was 1.70 million (PCBS, 2013). The land area covers 365 km^2, making the Gaza Strip one of the most densely populated areas in the world (ca. 4660 inhabitants/km^2). The population growth rate in the Gaza Strip was determined by PCBs (2013) to be 3.3%. Based on an aerial image of the Gaza Strip in 2007, the built-up area was digitized and estimated at 72.32 km^2 (around 20% of the total area). The Israeli colonies in the study area have low to moderate residential density and are located outside the boundary of the Gaza Strip away from the most deteriorated area in terms of groundwater level decline. Therefore, the relatively small scattered urban areas outside the Gaza region are not included in the urbanization analysis. Population forecasting is based on the average between two methods, namely the arithmetic mean method and the geometric method (UN, 1956).

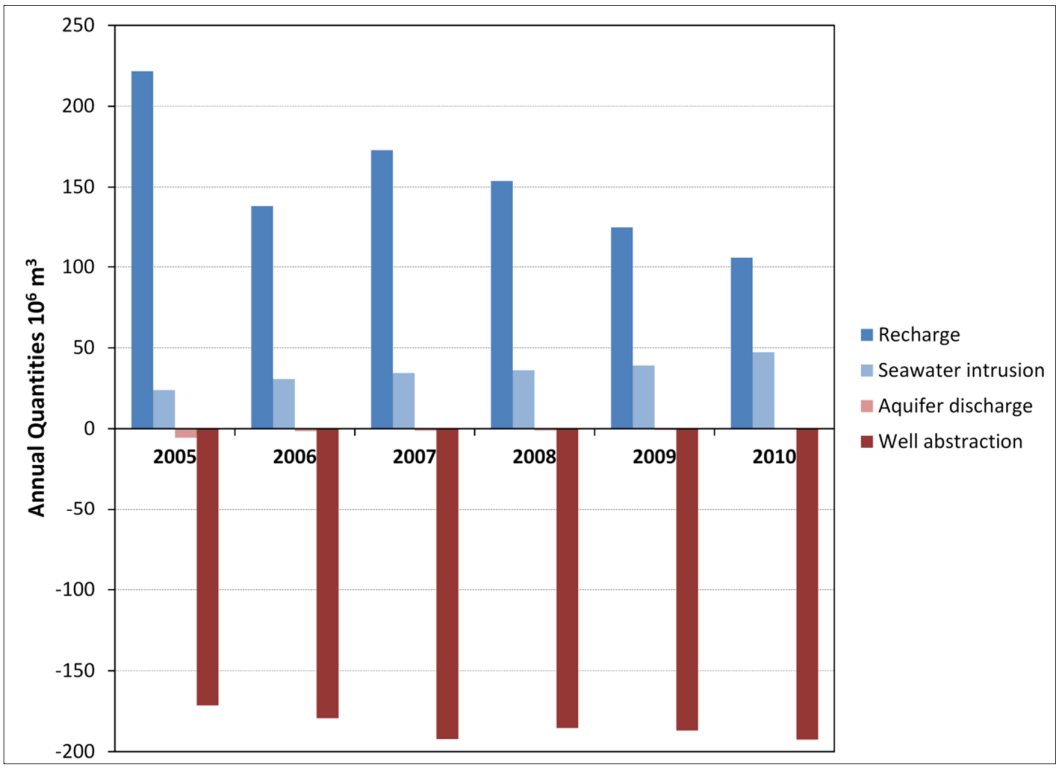

Figure 3.14 Water balance components

The linear prediction of the built-up area (km^2) was performed considering historical data (2001–2005 (Isaac *et al*., 2006), 2007). The data in Table 3.4 show that the population is expected to grow by 53% from 2013 to 2030 within an expected expansion in the built-up area by 36%. Due to the political conflict in the region, construction materials were not allowed to enter the Gaza Strip, which delayed the natural expansion of the built-up area from 2007 to 2010, whereas this delay was compensated in 2011 and 2012 in an accelerated way. This stage was not considered in the built-up area projection.

Table 3.4 Population, built-up area and water demand projections

Year of estimation	Population [a] Million	Built-up area [b] (km^2)	Water demand [c] (Mm^3)	Water supply [d] (Mm^3)	New well consumption [e] (Mm^3)	No. of new wells
2011	1.636	79.44	59.7	91.9	1.84	3
2012	1.668	81.28	60.9	93.7	3.68	5
2013	1.701 [f]	83.12	62.1	95.5	5.53	7
2014	1.746	84.96	63.7	98.0	8.02	9
2015	1.791	86.8	65.4	100.6	10.56	12
2016	1.837	88.64	67.1	103.2	13.15	15
2017	1.884	90.48	68.8	105.8	15.80	18
2018	1.932	92.32	70.5	108.5	18.50	21
2019	1.981	94.16	72.3	111.3	21.26	24
2020	2.032	96	74.2	114.1	24.09	27
2021	2.083	97.84	76.0	117.0	26.97	30
2022	2.136	99.68	78.0	119.9	29.92	33
2023	2.189	101.52	79.9	122.9	32.94	36
2024	2.244	103.36	81.9	126.0	36.02	40
2025	2.300	105.2	84.0	129.2	39.18	43
2026	2.358	107.04	86.1	132.4	42.41	47
2027	2.417	108.88	88.2	135.7	45.71	50
2028	2.477	110.72	90.4	139.1	49.09	54
2029	2.539	112.56	92.7	142.6	52.56	58
2030	2.602	114.4	95.0	146.1	56.10	61

a) The population was estimated as the average results by two methods, namely arithmetic mean method ($P_f=P_o+r.\Delta t$) and geometric method ($P_f=P_o(1+r)^{\Delta t}$). Where P_f is the targeted or final population, P_o is the initial population, r is the population growth rate (r = 0.033 for the Gaza Strip) and Δt is the time period.

b) The built-up area was estimated based on a linear projection of historical data (built-up area of 61.2, 62.9, 64.7, 66.5 and 72.3 km^2 for years 2001, 2002, 2003, 2004 and 2007, respectively).

c) The water demand was based on per capita daily consumption of 100 L/d (the current average consumption is around this value).

d) The average efficiency of the water supply network (65%) in 2010 was used to estimate the water supply amounts from the water demand.

e) The additional supplied water amounts relatively to 2010 were assumed to be covered by new wells with a pumping rate of 105 m^3/h for each (PWA, 2013; Metcalf & Eddy Inc., 2000).

f) Accounted population by PCBs (2013).

3.5.2 Projection of model boundary conditions

Estimating the future impacts of population growth as well as built-up area on hydrogeological boundary conditions is an essential step towards refined prediction of groundwater flow regimes. The spatial average recharge by rainfall in the simulation period (2004–2010) was used as an annual recharge during the model prediction period (2010–2030) considering an annual reduction due to built-up area expansion developed in Chapter 2, who quantified the relationship between built-up area and percolation at a subbasin level. The Urban-Percolation Index (UPI) was developed, which reflects the percent of change in percolation due to 1% increase in urban area at subbasin level (Fig. 3.15). In light of the above, the annual increase in built-up area in the urbanized subbasins was quantified, and the corresponding recharge reduction was estimated. The relationship between the projected urban expansion areas and urban development zones of the regional plan of the Gaza Strip (2020) was considered to match the planned situation.

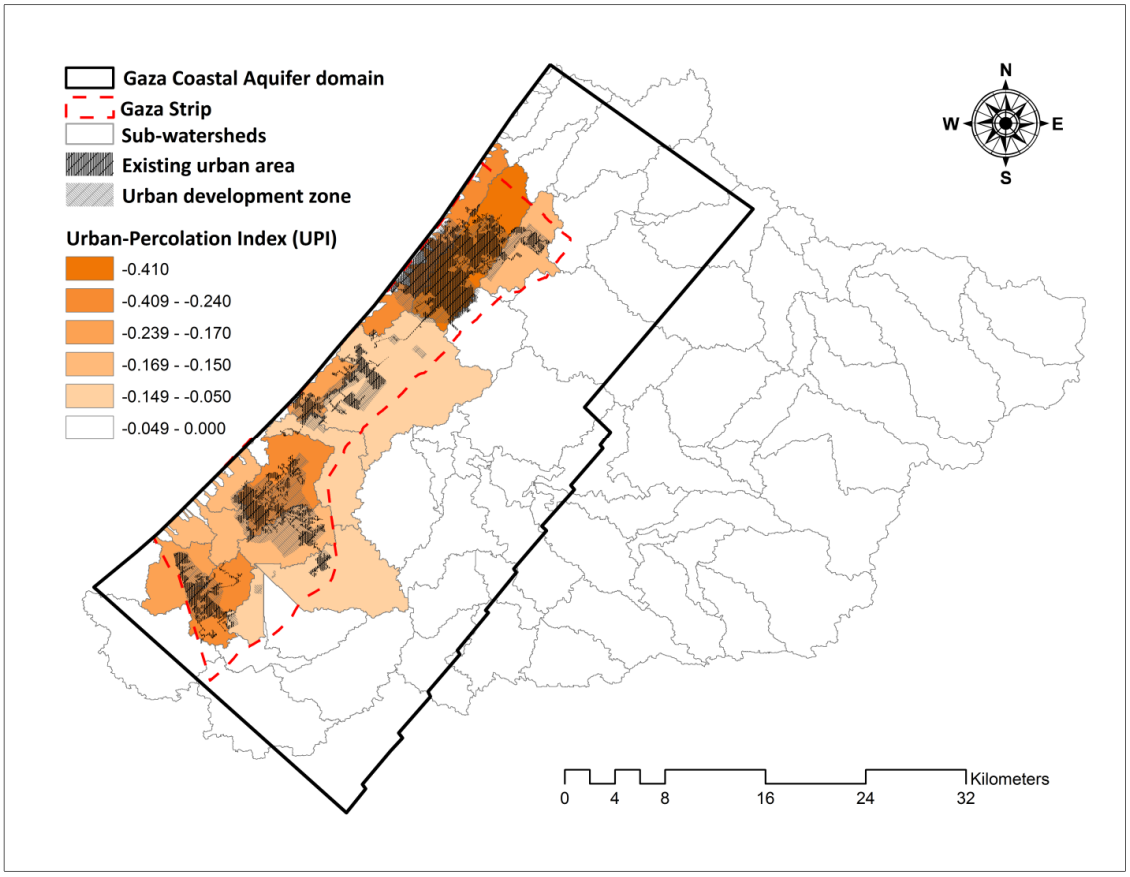

Figure 3.15 Urban-Percolation Index (Ch.2) and its intersection with the existing urban area and planed urban development zone

Increasing water demand due to population growth was projected for 2010–2030 considering the current per capita consumption (around 100 l/d) (Table 3.4), and the related water and wastewater leakage was estimated. Taking into account the maximum pumping rate of water wells (105 m^3/h) recommended by PWA (2013), the increasing demand was assumed to be met by new municipal wells (not increasing the current abstraction rate) taking into account urban development zones (Fig. 3.15). No change in irrigation return flow or artificial recharge was considered throughout the prediction period.

3.5.3 Prediction of groundwater level

Based on the calibrated parameters, the MODFLOW model was run at a monthly base over the prediction period 2010–2030. The projected boundary conditions were considered, and the simulated groundwater levels during October 2010 used as initial heads to start the transient simulation. Figure 3.16 depicts the spatial distribution of simulated groundwater levels of the years 2020 and 2030. Boxplots for the years 2010, 2020 and 2030 show the long-term behavior of the groundwater levels.

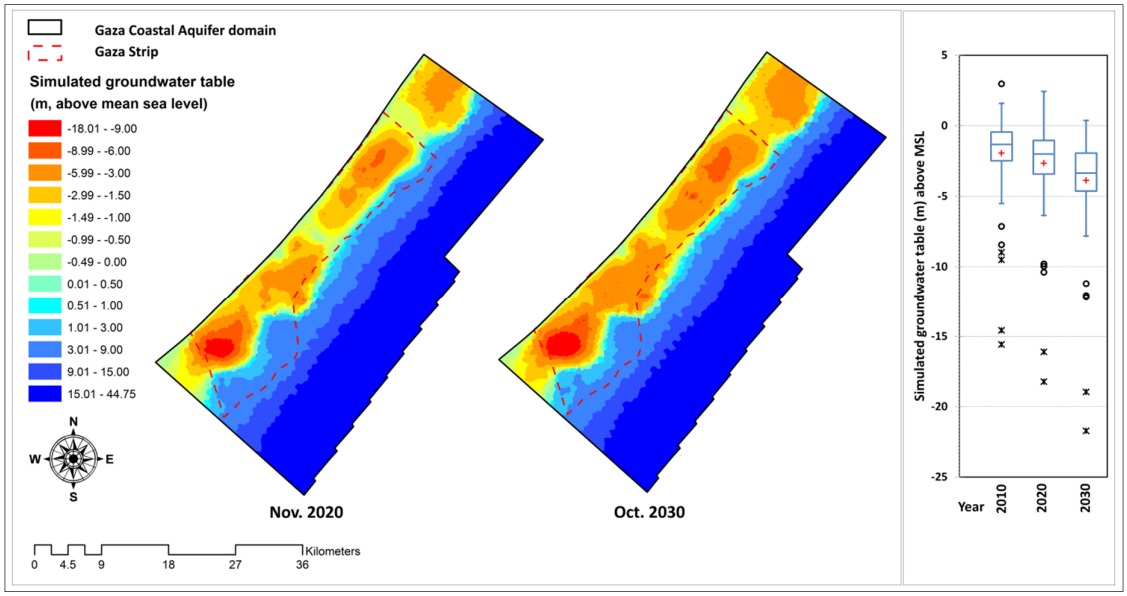

Figure 3.16 Simulated groundwater levels (2020 and 2030) and boxplot results (2010, 2020 and 2030)

Long-term (2004–2030) trends in groundwater levels are visualized in Figure 3.17. Using the linear regression method, the trend line slope of the average groundwater levels was -0.1024 (each year, the average groundwater level decreases by 10 cm) (Fig. 3.17 (b)). Positive slopes indicate increases in groundwater level, while negative slopes indicate

declines. The trend line of the average lowest 25% of the groundwater levels reveals a steeper slope than the average highest 25% of the groundwater levels and the average groundwater levels. Long-term trend line slopes of groundwater levels for the observed wells in the Gaza Strip boundaries (88 wells) were calculated, and their spatial distribution is presented in Figure 3.17 (c) as a groundwater-level trend index.

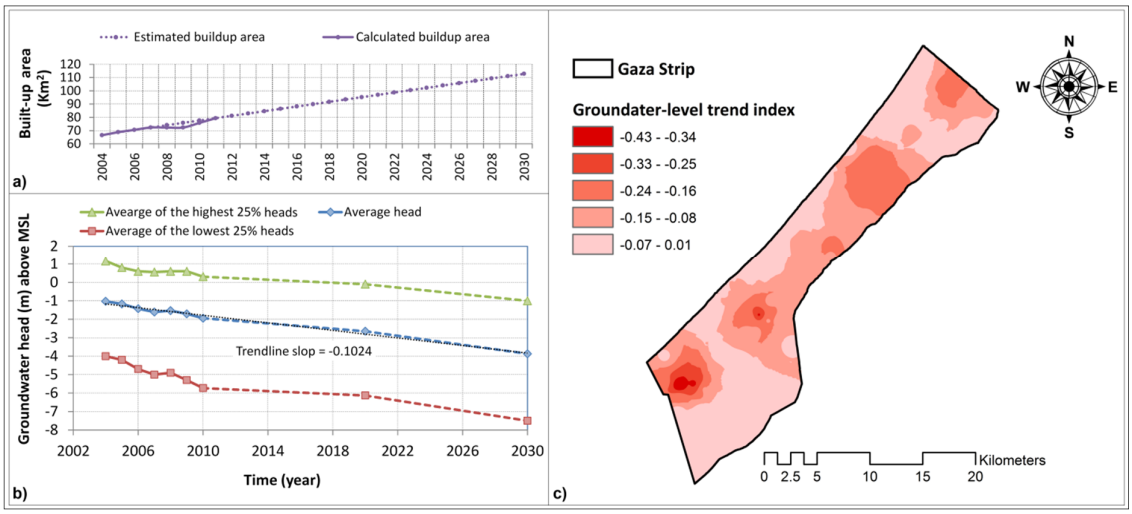

Figure 3.17 Groundwater level trend analysis: (a) annual estimated built-up area, (b) long-term (2004-2030) estimation of groundwater head, and (c) spatial distribution of long-term trend of groundwater levels

3.5.4 Interrelation between groundwater level and built-up area

Figures 3.16 and 3.17 show that the average groundwater level obviously declines across the Gaza aquifer domain during the simulation period (2004–2030). Figure 3.17 (a) shows an estimated linear increase in built-up area within the Gaza Strip at a rate of 1.84 km^2/y. The corresponding average groundwater level decline rate is 0.1024 m/y. Increasing built-up area can be considered as an indicator for the impacts of urban expansion relating to water supply quantities, water and wastewater leakage and rainfall recharge. When increasing the built-up area by 1 km^2, the average groundwater level decline could be estimated at 0.056 m without considering any new urban management scenario or a potential climate change. Referring to Figure 3.15 and 3.17 (c), it should be noted that urban areas in the Gaza Strip intersect with the highest negative values of the groundwater-level trend index. The groundwater level was estimated to decline by 0.43 m/y in sensitive locations (Fig. 3.17 (c)), where an increase in built-up area by 1 km^2 reflects an estimated decline in groundwater level by 0.23 m.

CHAPTER 4

4 Integrated hydrologic modeling as a key for sustainable urban water resources planning

4.1 Introduction

Urban water in cities worldwide is facing many challenges, including accelerating population growth and inadequate infrastructure. Understanding urban water sustainability and enhancing the process of decision making to achieve sustainable development planning are pressing needs of the 21st century (Childers *et al*., 2014). Increasing demands for clean water, combined with changing land-use practices, population growth, aging infrastructure, and climate change pose significant threats to the sustainability of the water resources. The recent approach of sustainability science seeks to address the symbiosis between human activity and water environment (Rapport, 2007). Sustainability needs to be quantified in order to evaluate the progress made in achieving sustainability over time and space (Pandey *et al*., 2011). Sustainable urban water concepts have been discussed and developed in a variety of ways over a number of decades (Marlow *et al*., 2013).

Groundwater is the world's most extracted raw material. Depletion of water levels in aquifers, deterioration of groundwater quality, and salinity intrusion in coastal aquifers caused by urbanization processes, industrial discharge and agricultural intensification are becoming major concerns across the globe (Pandey *et al*., 2011; Wu and Tan, 2012; Barron *et al*., 2013; Chaudhuri and Ale, 2014). Urbanization processes generally impact on groundwater through a tendency to increase contaminant loads and recharge rates as a result of water and wastewater network leakage in parallel with increasing surface runoff and decreasing percolation. The groundwater-urbanization relation is dynamic and mostly not linear (Tuinhof *et al*., 2011). Measures to 'repair' the associated problems are time

consuming and often more costly than trying to avoid or reduce the problems by management paying attention to sustainability.

In light of the above, urban groundwater sustainability moves us toward non-conventional water resources using what we have learned about the urban water system to effectively make the water environment more sustainable.

The groundwater aquifer is considered as the only water supply source for all kinds of human usage in the Gaza Strip (domestic, agricultural and industrial). The current rate of aquifer abstraction is unsustainable, and deterioration of the groundwater quality was documented in many parts of the Gaza Strip, mainly caused by saltwater intrusion and nitrate contamination (CMWU, 2010). In 2014, the estimated total population in the Gaza Strip was 1.76 million (PCBS, 2015). The land area covers 365 km^2, making it one of the most densely populated areas in the world (ca. 4820 inhabitants/km^2). The current status quo of the water resources in the Gaza Strip hampers the transition toward sustainability. Significant changes in the urban water management as well as in the water resources system are urgently required.

Metcalf & Eddy Inc. (2000) developed a fully 3-dimensional, numerical groundwater model using the flow and transport model DYNCEF for the Gaza coastal aquifer in the Gaza Coastal Aquifer Management Program project (CAMP project). This model evaluated the effect of pumping management scenarios on groundwater flow considering seawater intrusion. Moe *et al*. (2001) presented the main steps for simulating the effect of the integrated aquifer management plan that was developed by the CAMP project, which reflects guidelines for water supply and usage until year 2020. Mogheir *et al*. (2005) evaluated the monitoring cycle in the Gaza Strip using the entropy theory. The approach involved a gathering of data needs for groundwater resource management and planning through a questionnaire. Almasri and Ghabayen (2008) analyzed nitrate concentrations in the Gaza coastal aquifer for different land-use classes. Aish (2010) investigated the feasibility of a proposed discharge of treated wastewater in the Gaza Strip to the aquifer. Analytical and numerical models for calculating the groundwater mounding were applied. Baalousha (2010) presented a new approach for groundwater contamination risk mapping based on hydrogeological setting, land use, contamination load, and groundwater modeling. He used a spatial analyst tool within a geographical information system (GIS) to interpolate and manipulate data to develop GIS maps of vulnerability, land use, and contamination impact. The above studies focused on the evaluation of the current situation of the water environment

of the Gaza Strip region and mainly considered specific questions or single components of the hydrological system. These studies did not consider the urban water system in the research context as a paradigm clearing synergies between the human decisions and biophysical processes toward sustainable use of water resources. Figure 4.1 conceptualizes the relationship between water resources (water inputs) and the urban water system in the Gaza Strip, which comprises urban water budget (vertical and horizontal components), urban hydro-ecosystem function, climate function, and urban hydro-ecosystem structure. Not only does this conceptual approach integrate the human and ecological structures and functions as figured by Childers *et al*. (2014), it also reflects synergies and symbiosis between water resources, human decisions, and biophysical processes on a macro-scale level (the Gaza coastal aquifer domain). Human decisions related to water management and water use are critical components of an urban water system. The groundwater as well as the non-conventional water resources (desalinated water, treated wastewater, and harvested stormwater) has mutual impacts on the urban hydro-ecosystem functions. Horizontal urban water components are dominated by: (1) surface runoff, which follows the geomorphological and topographic template of the landscape and can be regulated by human management decisions and could influence the quantities of the harvested stormwater (mainly by water retention structures), and (2) water supply and drainage, which are fully regulated by human management decisions and influence the quantities of the treated wastewater as a non-conventional water resource. Vertical urban water components include evapotranspiration, groundwater recharge components (rainfall percolation, water and wastewater leakage, irrigation return flow, and artificial recharge) and abstracted water from wells, which are a function of both ecological processes and human decisions and strongly influence groundwater replenishment and quality. The urban hydro-ecosystem structure spatially controls the effects of the climate function and the urban hydro-ecosystem functions on the urban water budget components. To overcome the sustainability challenges related to the Gaza coastal aquifer, the non-conventional water resources have to be considered in the water resources management agenda.

Through integrated hydrologic modeling, the main hydrological processes can be fully coupled, and their relationships with the urban water system features defined and quantified. Shu *et al*. (2012) applied the integrated hydrological model MIKE SHE to a part of the North China Plain to examine the dynamics of the hydrological system, and to assess water management options to restore depleted groundwater resources. Du *et al*. (2012)

developed and used an integrated modeling system, coupling a distributed hydrologic and a dynamic land-use change model, to examine effects of urbanization on annual runoff and flood events of the Qinhuai River watershed in Jiangsu Province, China. Barron *et al*. (2013) investigated the impact of urbanization on the water balance of a catchment dominated by surface water and groundwater interactions by using a process-based coupled surface water and groundwater model called MODHMS. Rassam *et al*. (2013) used the Upper Namoi numerical groundwater model to demonstrate the importance of incorporating surface water and groundwater interactions into river management models, and demonstrated the advantages of incorporating groundwater processes in the Namoi River model. Hassan *et al*. (2014) applied the transient, integrated hydrologic model GSFLOW (Groundwater and Surface water FLOW) to evaluate the surface-groundwater interactions in a semi-arid catchment in Spain characterized by shallow water table conditions, relatively low storage, dense drainage networks and frequent, high intensity rainfall.

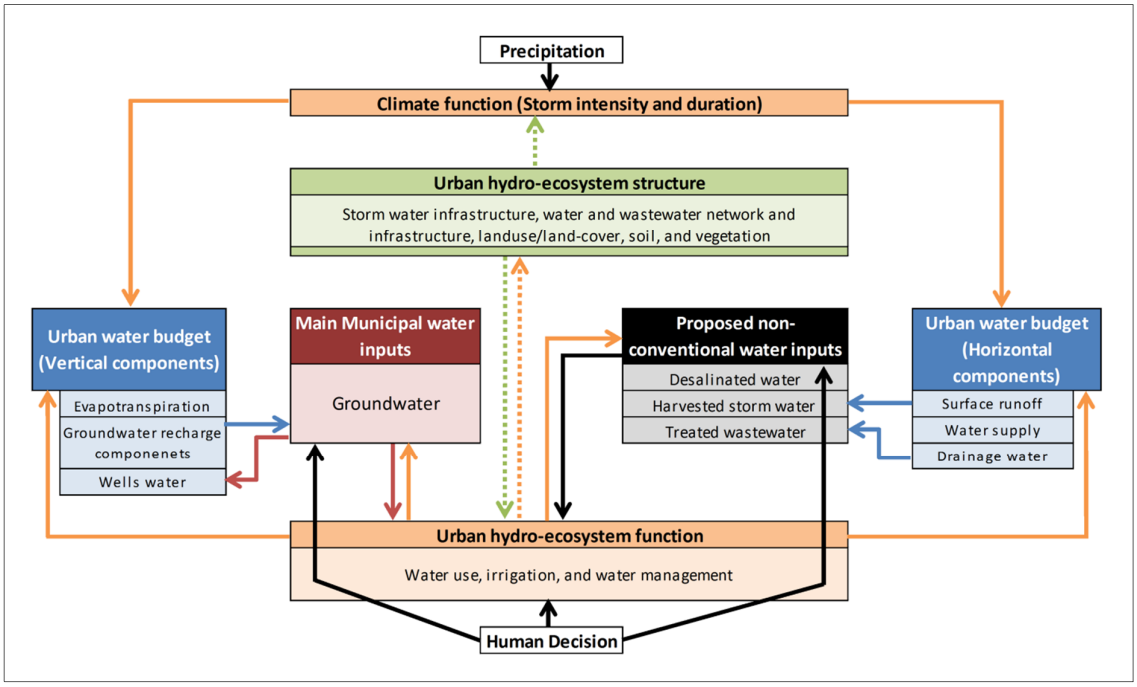

Figure 4.1 Urban water system of the Gaza Strip

Taking into account integrated hydrologic modeling, the main goal of this study is to quantify the spatial trade-offs and synergies between the urban water system components of the Gaza Strip considering the potential for use of non-conventional water resources in addition to or in order to replace groundwater use and, as a consequence, support a sustainable water environment. The specific objectives include: (1) provide a complete view

of the urban water budget components (vertical and horizontal) based on a comprehensive approach including the connection to a surface water model (Soil and Water Assessment Tool (SWAT)); (2) develop a 3-D groundwater flow and transport model to investigate groundwater levels, nitrate concentration, and chloride concentration within the Gaza coastal aquifer; (3) investigate the groundwater quality deterioration cycle concerning the urban water system; (4) develop sustainability measures to quantify the effectiveness trend of non-conventional water resources scenarios, namely desalination, stormwater harvesting and treated wastewater reuse as well as an infrastructure performance scenario aiming at sustainable groundwater management.

4.2 Study area

Palestine belongs to the sub-tropical zone. On the coast (Gaza Strip) and in the highlands (West Bank), the climate is of Mediterranean type with a long hot and dry summer, and short cool and rainy winter (Dudeen, 2001). The Gaza Strip (Fig. 1.1) is a narrow coastal strip located on the south-eastern coast of the Mediterranean Sea with a land area amounting to 365 km^2. Gaza has a sub-aquifer, which is part of the larger coastal aquifer extending from the Karmel Mountain in the north to the Sinai desert in the south with a variable width and depth (Baalousha, 2008).

The study area forms a transitional zone between the sub-humid coastal zone in the north, the semi-arid loess plains of the northern Negev Desert in the east and the arid Sinai Desert of Egypt in the south (Isaac *et al.*, 2006). The mean temperature varies from 12–14 C° in January to 26–28 C° in June. Precipitation levels also gradually decline away from the coast. The Gaza Strip receives 200–400 mm/y, with a mean value of 320 mm/y (UN-ESCWA and BGR, 2013). The hydrological year usually starts in October or November. The average annual potential evaporation is about 1400 mm/y (PWA, 2010).

The coastal aquifer thickness varies between 60 and 140 m. It is comparatively shallow, renewable and mainly unconfined. The basin's productive zone forms a narrow strip along the coast, with groundwater generally flowing from the hinterland towards the sea (UN-ESCWA and BGR, 2013). The aquifer domain boundary extends beyond the political boundaries of the Gaza Strip towards the north (no flow boundary), and towards the east where the coastal aquifer pinches out the surface (no flow boundary), and towards the south in Egypt, where no data are available and there is no significant flow (assumption: no flow boundary), and finally towards the Mediterranean Sea in the west (fixed head to zero)

(Metcalf & Eddy Inc., 2000; HWE, 2010). The aquifer formations are of Pleistocene and Holocene age, consisting of clastic series such as sandstone, dune sand, gravel and conglomerate with some top cover of loess and a marly bottom. Intermediate loamy and clayey intercalations in the aquifer belong to the marine Kurkar A (a type of calcareous sandstone) and continental Kurkar B. They extend 2–5 km inland and divide the aquifer into four sub-aquifers, referred to in this study as A, B1, B2 and C (Fig. 4.2). The Pleistocene formation is mostly underlain by impermeable Neogene strata (Saqiye Group). Near the coast, where intercalations with clay lenses occur, the upper sub-aquifer (A) is unconfined, whereas at deeper levels some confined parts (B and C) can be identified (Dudeen, 2001; UN-ESCWA and BGR, 2013).

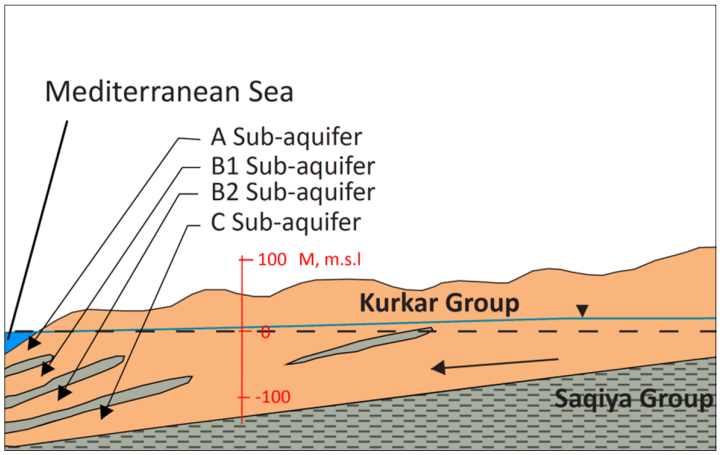

Figure 4.2 Sub-aquifers and aquitard (UN-ESCWA and BGR, 2013)

4.3 Urban water budget components

This study considers the spatial and temporal distribution of water budget components of the Gaza aquifer domain based on a physically based surface water model (SWAT) (Ch.2). They calibrated and validated a surface water modeling using data from 2004 to 2010 with SWAT to quantify the impact of urban area expansion on groundwater recharge and surface runoff. Figure 4.3 shows the average annual surface runoff (horizontal water budget component) and the average annual percolation (vertical water budget component). Other horizontal urban water budget components, namely water supply and drainage, were estimated based on recorded data (PWA, 2013) taking spatio-temporal variability into account.

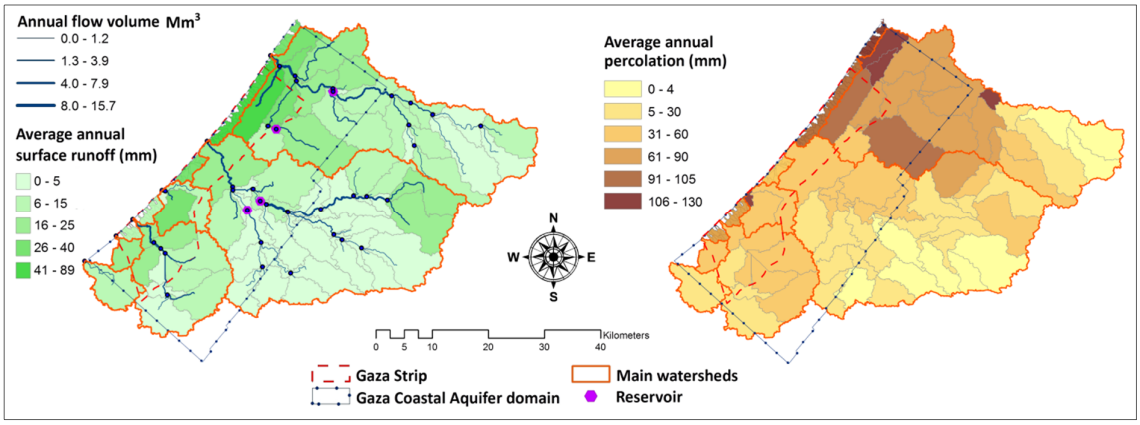

Figure 4.3 Surface runoff and percolation derived from a surface water model (Ch.2)

Water and wastewater network leakage, irrigation return flow, and artificial recharge are significant components in the vertical urban water budget. The Gaza Strip population is supplied by around 90 Mm^3 of water annually (CMWU, 2010). For each governorate in the Gaza Strip, the monthly calculated physical losses during 2004–2010 were used to configure water leakage quantities. The main elements to calculate wastewater leakage quantities are (1) spatial coverage of the sewage network, (2) household cesspits, (3) wastewater network system efficiency, and (4) generated wastewater quantities of around 75% of the consumed water (CMWU, 2010). The agricultural sector in the Gaza Strip on average consumes around 75–85 Mm^3 of water annually (PWA, 2013). The spatial monthly estimation of agricultural return flow is based on various factors (Ch.3), namely the monthly pattern of crop water requirements (CEP and FCG, 2010), annual irrigated crop area through governorates (in Gaza region) and zones (outside Gaza region), and estimated overall annual irrigation returned flow (PWA, 2013).

There are five artificial recharge ponds in the Gaza Strip and another natural infiltration basin outside the Gaza region. The average annual recharge of these ponds ranges between 0.5 Mm^3 and 3.6 Mm^3. More than 4000 water wells are operated in the Gaza Strip to meet both the domestic and agricultural demand (CMWU, 2010). The annual average groundwater abstraction in the Israeli side within the model domain was estimated at around 50 Mm^3 from 90 wells (Metcalf & Eddy Inc., 2000). The measured monthly abstraction rate of 209 municipal water wells within the Gaza region are used in this study. More than 3800 agricultural water wells are considered in this study in the estimation of monthly abstraction rates for each well taking into account the agricultural demand pattern (PWA, 2013). Figure 4.4 shows the urban and agricultural areas within the model domain.

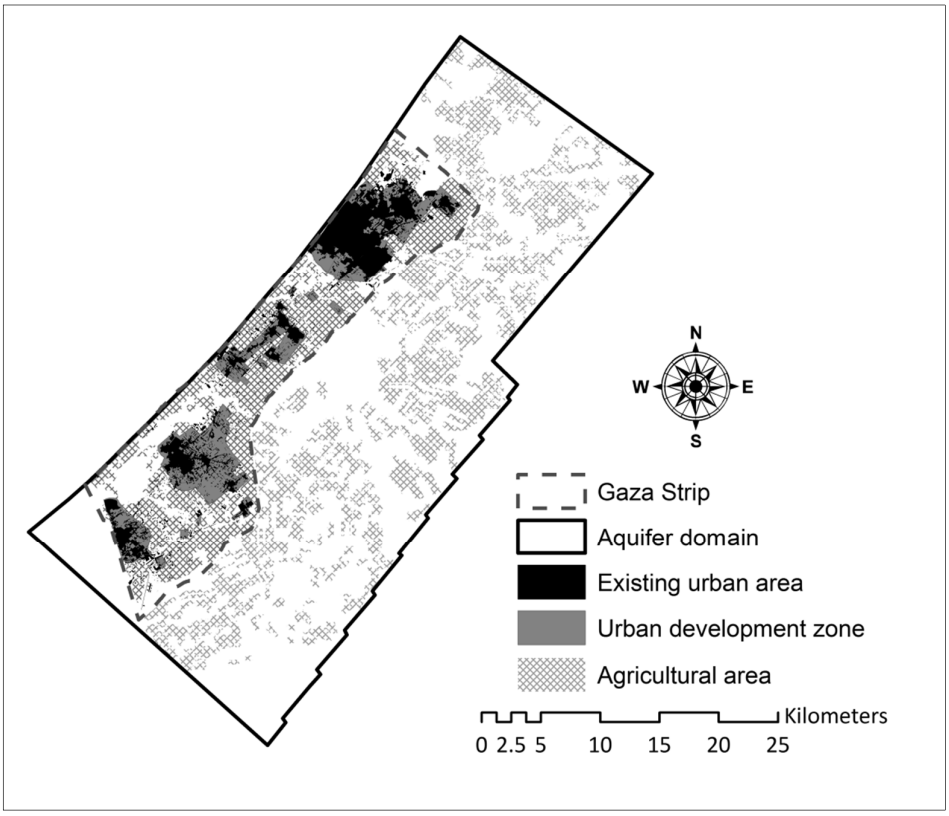

Figure 4.4 Urban and agricultural area in the model domain

4.4 Groundwater quality

In addition to over-pumping of the Gaza coastal aquifer, a severe deterioration of the water quality was documented (CMWU, 2013). Salinity caused by seawater intrusion has increased over time. In many areas of the Gaza Strip, the total dissolved solids have exceeded 1000 mg/l and even 3000 mg/l in some areas (Al-Khatib *et al*., 2009). Chloride (a seawater intrusion indicator) and nitrate (a human activities indicator) are the main indicators for the groundwater quality in the Gaza coastal aquifer. The aquifer has an average nitrate level over 150 mg/l, whereas the World Health Organization (WHO, 2008) recommends a nitrate (NO_3) concentration less than 50 mg/l in drinking water. High positive correlation was observed between the NO_3 concentrations (higher than 80 mg/l) in the groundwater of the Gaza Strip and the occurrence of methemoglobinemia in babies younger than six months of age (Shomar *et al*., 2008). More than 90% of the groundwater has chloride (Cl) concentrations higher than 250 mg/l (recommended by WHO (2008)). The over-pumping rate from water wells is the main reason for seawater intrusion into the Gaza aquifer, which increases the Cl rate dramatically. The Cl concentrations vary among the groundwater recharge components as

well as among the Gaza strip governorates. Municipal water and wastewater show Cl values between 200 and 800 mg/l, whereas the Cl in the irrigation water ranges between 300 and 1000 mg/l. The Cl concentration in the precipitation was estimated at 15 mg/l (Turkeltauub, 2011). Table 4.1 presents the Cl concentrations in the recharge components that were used in the modeling process.

Table 4.1 Cl concentrations used in the modeling process

Gaza governorate	Average Cl concentrations in water and wastewater (mg/l) [a]	Average Cl concentrations in irrigation water (mg/l) [b]
North	210.0	297.0
Gaza	790.0	725.0
Middle	755.0	1014.0
Khanyounis	713.0	871.0
Rafah	407.0	680.0
Outside the Gaza Strip		250 [c]

(a) Based on the average Cl concentrations among municipal wells (2004-2010) (PWA, 2013).
(b) Based on the average Cl concentrations among agricultural wells (2004-2010) (PWA, 2013).
(c) Assumed by the researcher

Due to the high permeability of most of the Gaza soil profiles, the Gaza coastal aquifer is extremely susceptible to surface-derived contamination related to human activities (Shomar *et al*., 2008). Wastewater leakage as a point source of contamination and the agricultural activities as nonpoint sources of contamination are responsible for the increasing rate of NO_3 levels in the Gaza coastal aquifer (Baaloush, 2008). NO_3 is a compound predominantly found in the groundwater, and easily reaches the aquifer from the soil especially under geological conditions such as those in the Gaza coastal aquifer.

The general nitrogen balance (soil and vadose zone) can be formulized by $N_{in} - N_{out} = \Delta N_{st}$, where N_{in} is the nitrogen input to the system, N_{out} is the nitrogen losses excluding leaching, and ΔN_{st} is the nitrogen storage in the system that is potentially leachable to the aquifer in the long term. Figure 4.5 conceptualizes the main processes that govern NO_3 occurrences in groundwater.

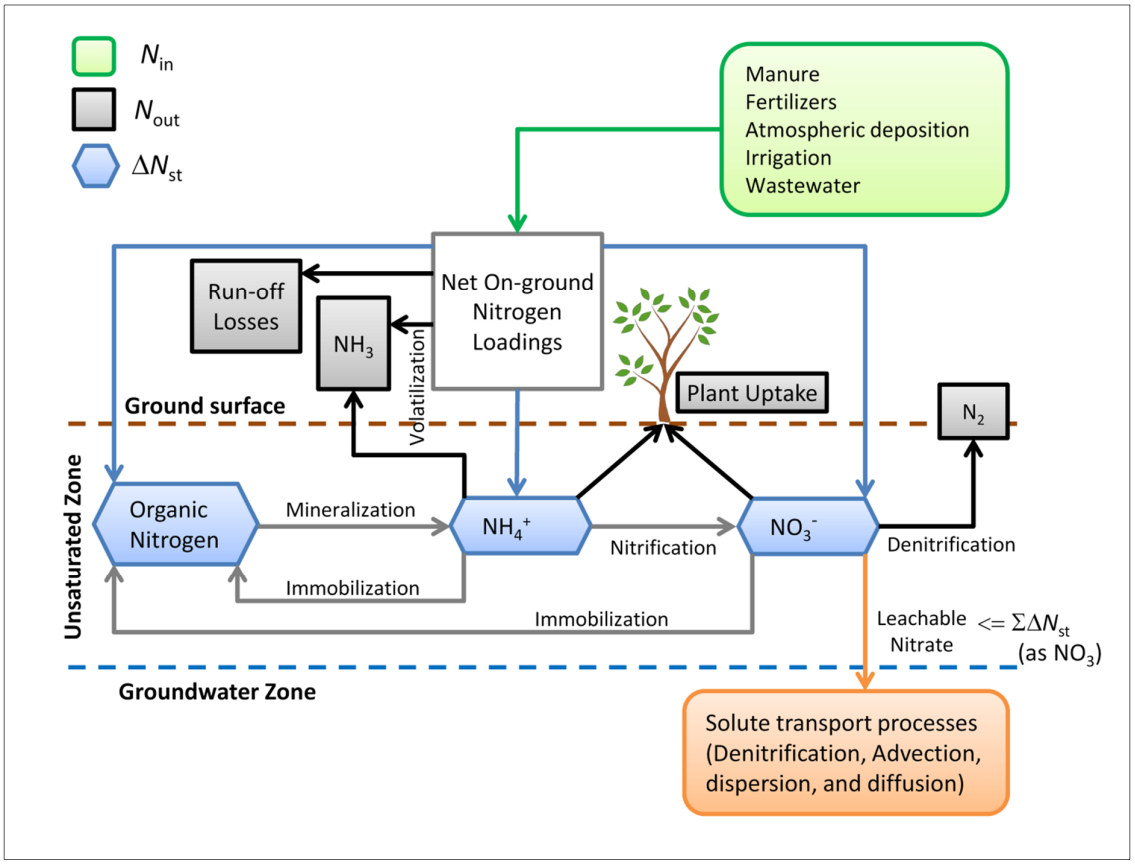

Figure 4.5 The main processes that govern NO_3 occurrences in groundwater (developed based on Almasri and Kaluarachchi, 2007)

When conducting macro-scale analysis and modeling, it is important to understand the main processes that could govern NO_3 occurrences in groundwater in order to account for the transient and spatially variable NO_3 leaching to groundwater (Almasri and Kaluarachchi, 2007). Almahallawi (2005) estimated the nitrogen balance considering the main sources of nitrogen (N_{in}) in the Gaza Strip, namely wastewater leakage and septic tanks, manure and chemical fertilizers, water supply leakage, solid waste, and precipitation. Plant uptake, denitrification from all nitrogen sources, and ammonia volatilization from fertilizers and manure were accounted for as losses (N_{out}) from the nitrogen input by Almahallawi (2005). In this study, the potentially leachable nitrogen load (= ΔN_{st} as NO_3) that can reach the groundwater (as mg/l) was loaded to the recharge components as shown in Table 4.2.

Table 4.2 NO_3 concentrations used in the modeling process

Gaza Strip governorate	Average leachable total nitrogen concentrations in wastewater network leakage (sewered and un-sewered areas) (mg/l) [a]	Average NO_3 concentrations in water supply pipes leakage (mg/l) [b]	Average leachable total nitrogen concentration from agricultural area loaded to irrigation quantity (mg/l) [c]
North	160.4	85.6	222.0
Gaza	120.9	78.4	227.8
Middle	130.1	80.0	242.5
Khanyounis	263.0	89.6	336.4
Rafah	168.1	110.4	329.2
Outside the Gaza Strip			280.0 [d]

(a) Based on coverage of wastewater network, total nitrogen in sewage system, total nitrogen in cesspits (un-sewered areas), and assumed 20% denitrification due to surface activities (Almahallawi, 2005).
(b) Average NO_3 concentration in municipal wells (2004-2010) (PWA, 2013).
(c) Considers (1) nitrogen load from chemical fertilizers, manure and irrigation water; (2) nitrogen losses due to plant uptake, ammonia volatilization, and denitrification (Almahallawi, 2005).
(d) Based on average value of Gaza Strip governorates.

4.5 Groundwater flow and transport modeling

4.5.1 Governing equation

The modular three-dimensional finite-difference groundwater flow model (MODFLOW) was used for simulating a 3-D, constant density, groundwater flow equation and contaminant transport equation. The 3-D groundwater flow in a porous medium is mentioned in Chapter 3 (equation 3.2). The equation that describes the transport of contaminants of species k in a three-dimensional transient groundwater flow system can be written as follows (Zheng and Wang, 1999; Almasri and Kaluarachchi, 2007):

$$\frac{\partial(\theta C^k)}{\partial t} = \frac{\partial}{\partial x_i}\left(\theta D_{ij}\frac{\partial C^k}{\partial x_i}\right) - \frac{\partial}{\partial x_i}(\theta v_i C^k) + q_s C_s^k - \rho_b \frac{\partial C_{so}{}^k}{\partial t} - \lambda_1 \theta C^k - \lambda_2 \rho_b C_{so}{}^k \qquad (4.1)$$

where C^k is the dissolved concentration of species k (mg/l), θ is the aquifer porosity, t is time, D_{ij} is the dispersion coefficient (m^2/day), v_i is the linear pore water velocity (m/day), q_s is the flow rate per unit volume of aquifer (source of sink) (day^{-1}), C_s^k is the concentration of the source or sink for species k (mg/l), ρ_b is the bulk density of the aquifer (kg/m^3), $C_{so}{}^k$ is the concentration of species k sorbed on the aquifer particles (mg/g), λ_1 is the first-order recation rate for the dissolved phase (day^{-1}), and λ_2 is the first-order recation rate for the sorbed phase (day^{-1}).

4.5.2 Model used

Since the main objective of this is study based on a macro-scale modeling framework with high resolutions, the following model and engines were chosen. The visual MODFLOW model was used for simulating a 3-D, constant density, groundwater flow regime and contaminant transport based on two engines namely, MODFLOW-2005 and the modular three-dimensional multispecies transport model (MT3DMS). MODFLOW-2005 was used to simulate the groundwater flow system; this is the most recent release of the MODFLOW model (MODFLOW-USG mentioned in CH.3 is not fully developed to deal with transport modeling tasks). It simulates steady and nonsteady flow in an irregularly shaped flow system in which aquifer layers can be confined, unconfined, or a combination of confined and unconfined (Harbaugh, 2005). The MT3DMS engine was used for NO_3 and Cl transport simulation. It is a 3-D multispecies contaminant transport model with a modular structure to permit simulation of solute transport processes independently or jointly. The engine interfaces directly with the visual MODFLOW for the flow solution, and supports all the hydrologic and discretization features of MODFLOW (Zheng, 2009).

4.5.3 Conceptual model

As shown in Figure 4.6, the conceptual model comprises four sub-aquifers, referred to as A, B1, B2 and C, taking into account the intermediate loamy and clayey layers as aquitards.

Initial conditions and aquifer parameters

The initial flow head is based on previous work in Chapter 3, and drawn in November 2004 based on 138 observed water wells distributed through the model domain. The hydraulic conductivity, specific storage and porosity of the Gaza coastal aquifer system is based on the calibrated groundwater flow model (Ch.3). The initial flow concentrations of NO_3 and Cl were drawn in November 2004 based on 96 and 114 observed water wells, respectively, distributed through the model domain. The longitudinal, horizontal, and vertical transverse dispersivity was estimated at 10 m, 1 m, and 0.1 m, respectively.

Boundary conditions

Within the aquifer domain, the east, north and south were conceptualized as no-flow boundaries; the west boundary was conceptualized as a constant head boundary. The lower interface was considered as an impervious boundary. Water exchanges and contaminants

transport occur at the top interface. Monthly records of recharge quantity and quality (NO_3 and Cl concentrations) for rainfall percolation, water and wastewater leakage, irrigation-return flow, artificial recharge and well abstraction were used as boundary conditions for the simulation period from 1 November 2004 to 31 October 2010.

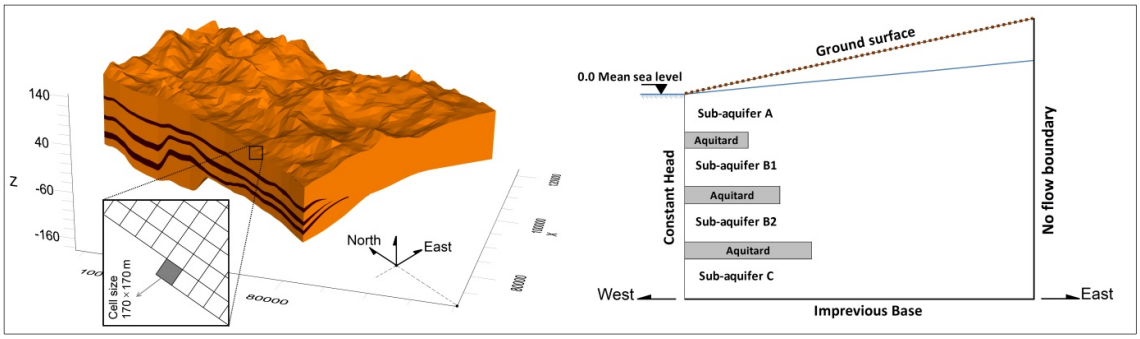

Figure 4.6 Conceptual model and numerical cells

4.5.4 Numerical model

Discretization

The Gaza coastal aquifer domain was discretized into square cells (170 m × 170 m). The model domain was divided into 42689 active cells, which represent the total area of 1232 km^2. As the average vertical cross section was dissected into seven layers, the simulation zone is dissected into 298823 active cells.

The simulation period was 6 years (monthly based) from November 2004 to October 2010, and the stress period of the model 72 months. Denitrification was considered as the only chemical reaction that may affect NO_3 concentrations in the aquifer without any possibility for sorption. Neither chemical reaction nor contaminant sorption was considered regarding Cl.

4.5.5 Model calibration and validation

This study is based on a previous calibrated and validated groundwater flow model which represents the base to set up the contaminant transport simulation. The dispersivity components seem to be non-sensitive. The simulated Cl concentrations were validated (without need for calibration) through the simulation period. The simulated NO_3 concentrations were calibrated through the periods from November 2004 to October 2007 and from November 2009 to October 2010, and validated from November 2007 to October 2009. The calibration of the transient NO_3 transport model was carried out by simulating NO_3

concentration changes in response to changes in the first-order denitrification rate considering observed data of NO_3 concentrations (142 observed wells, 622 records). As the model simulation is a baseline for the next step (model forecasting using difference management scenarios), the NO_3 balance components were not considered in the calibration process.

4.6 Model forecasting and planning scenarios

In this study, different scenarios were investigated at a macro-scale level with high resolution. Model forecasting is based on the population projection (2010-2030) and the linear prediction of the built-up area (km^2) that were developed in Chapter 3. Increasing water demand due to population growth is based on the current per capita consumption (around 100 l/d), and the related water and wastewater leakage was estimated. The increasing demand was assumed to be met by new municipal wells (not increasing the current abstraction rate per well) taking into account urban development zones. No change in irrigation return flow or artificial recharge was assumed throughout the prediction period. The average rainfall recharge in the simulation period (2004–2010) was used as an annual recharge during the model prediction period (2010–2030) considering annual reductions due to built-up area expansion developed in Chapter 2. The MODFLOW model was run at a monthly base over the prediction period 2010–2030 to derive a baseline scenario (S0) to compare the effectiveness of other scenarios toward sustainability.

The scenarios represent the current institutional trend toward sound water resources management. Several scientific as well as governmental and non-governmental reports and studies were discussed with the stakeholders to elaborate realistic scenarios that consider different sustainable development aspects (social, economic, and environmental aspects). The main stakeholders are the Palestinian Water Authority (PWA), Coastal Municipalities Water Utility (CMWU), Ministry of Agriculture, and Ministry of Planning. The stakeholder interviews focused on the recent planning agenda of using non-conventional water resources, available data, and current and future infrastructure projects related to water and wastewater sector. Three main scenarios of water resources planning, namely desalination, stormwater harvesting, and treated wastewater reuse as well as an infrastructure performance scenario are addressed in the following.

4.6.1 Desalination scenario (S1)

As more than 90% of the population of the Gaza Strip depends on desalinated water for

drinking purposes (purchased from desalinated water vendors or directly from small-scale private brackish water desalination plants), large-scale desalination of seawater could be a sustainable solution to face the accelerating water demand. This study examines a proposed desalination scenario considering the expected reduction of the abstracted water from wells as well as the expected reduction of NO_3 and Cl concentrations in the water and wastewater leakage; the scenario considers desalinated water quantities of 13 Mm^3 in 2015 to 72 Mm^3 in 2030 (PWA, 2011). These quantities varied within the Gaza governorates; they were estimated at 23% and 100% in the north and south governorates, respectively, in 2030. Figure 4.7 shows the estimated quantities of the desalinated water (PWA, 2011) and the corresponding ranges of Cl and NO_3 concentrations in the water supply.

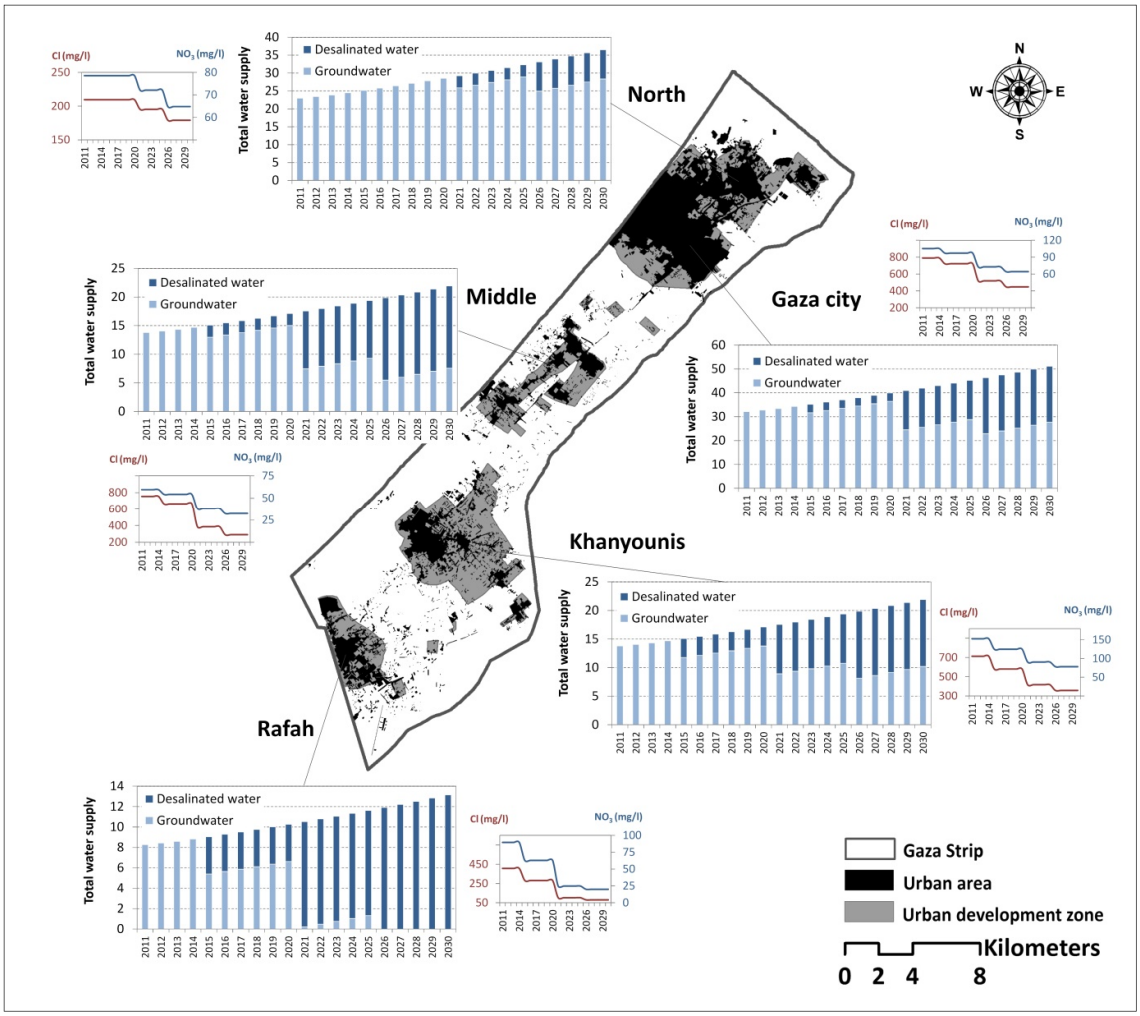

Figure 4.7 Desalination quantities in water supply and the corresponding chloride and nitrate concentrations in water supply

4.6.2 Stormwater harvesting scenario (S2)

The average annual surface runoff within the Gaza region was estimated at 12% of the average annual precipitation (Ch.2), which is directed mostly to the sea or to small infiltration basins. Although most of the covered soils have moderate to high infiltration capacity, no sufficient system exists to harvest and return the stormwater to the groundwater on a large scale. In a realistic scenario, this study investigated the effectiveness of harvesting stormwater by roofs and returning it to the aquifer. An intersection between the existing built-up area as well as the development urban zone with the high infiltration capacity soils was developed and used by the model to build a temporal-spatial approach of stormwater harvesting. The generated theme was intersected again with the subbasins developed in Chapter 2 to determine the monthly rainfall for the generated zones. The roof area was estimated at 60% of the impervious area, which represents 60% of the total urban area (Ministry of Planning, 2013). The percentage of roof area in the existing urban area that could collect the stormwater and infiltrate it into the soil was predicted at 20% of the total roof area in 2015 and 60% in 2030, whereas 100% of the area in the development urban zone was considered based on the expected growth of the built-up area.

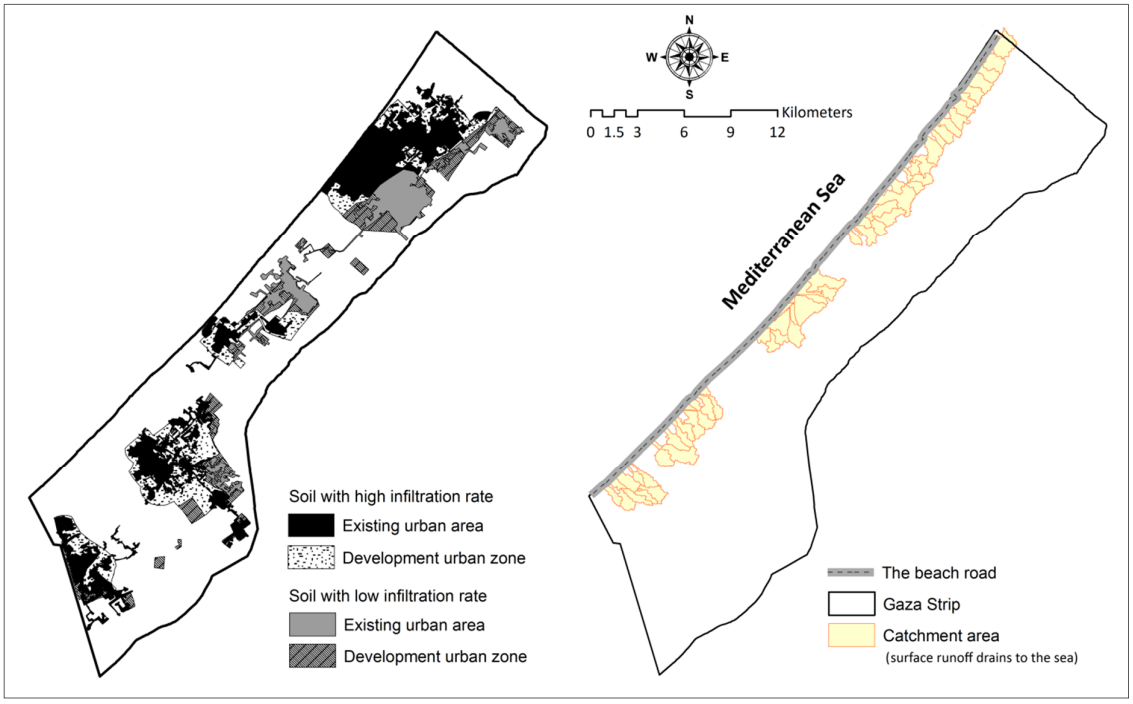

Figure 4.8 Targeted urban area by the harvested stormwater scenario

The surface runoff that drains to the sea from small catchment areas near the beach was accounted for in this scenario (around 3 Mm^3/y); in the simulation process, this water was allowed to infiltrate through the beach road into the underlying soil using an infiltration system that allows rainfall to infiltrate into the ground. Street soakaway pits or dry wells were investigated as a potential stormwater harvesting system at street level by ADA & PWA (2011). 50% of the surface runoff from those small catchment areas was considered to be collected by the stormwater harvesting system through the street near the beach from 2015 to 2020, whereas this ratio was increased to 80% from 2020 to 2030. Figure 4.8 illustrates the urban area targeted by the stormwater harvesting scenario (S2).

4.6.3 Wastewater reuse scenario (S3)

Currently, the agriculture sector in the Gaza strip consumes around 50% of the abstracted water from the Gaza coastal aquifer. At the same time, the wastewater quantity equals more than 30% of the total consumed water from the groundwater. Wastewater reuse in agriculture is a possible strategy for addressing water scarcity in the face of accelerating demand, but the quality of the treated wastewater effluent could hinder strategies towards sustainable groundwater management. This study examines the possibility of reuse treated wastewater on a large scale, and considers the future planning of sufficient wastewater treatment from three wastewater treatment plants with a high quality effluent with less than 20 mg/l total nitrogen. The planned wastewater reuse system (PWA, 2011) is based on the construction of infiltration basins near the treatment plants to store the treated effluent and allow its infiltration into the aquifer in parallel with the construction of recovery wells to extract and reuse most of the infiltrated water in the agricultural sector.

The percentage of the cultivated area to the proposed zone was estimated at 50% to 90% through the simulation period (2010−2030). The treated wastewater (TWW) quantities that could be generated from the wastewater treatment plants were predicted for the same period. The quantities needed for irrigation were estimated based on the crop types and the area of the proposed zones. This study assumes that the cropping pattern, which is citrus 30%, olives 25%, fruit trees 15%, alfalfa 10%, grains 10% and vegetables 10%, consumes 1000 mm/y (CEP and FCG, 2010). The Cl concentration in the TWW ranges from 200-800 mg/l based on the location of the treatment plant. The total nitrogen in the TWW was considered at 20 mg/l, and ranges from 17 to 24 mg/l in the agricultural water wells in the Gaza Strip governorates. Total nitrogen, potentially leachable to the aquifer, was assumed at

85% of the average leachable total nitrogen of the Gaza strip (230 mg/l) taking into account the cropping pattern of this scenario, which has a lower percentage of vegetables than other agricultural areas (from 30% to 10%); this reflects a lower amount of chemical fertilizers or manure. The same irrigation efficiency was considered in this scenario (around 23% of the TWW reused for irrigation will be lost to the groundwater). Figure 4.9 exhibits the area targeted by this scenario with the estimated TWW amounts.

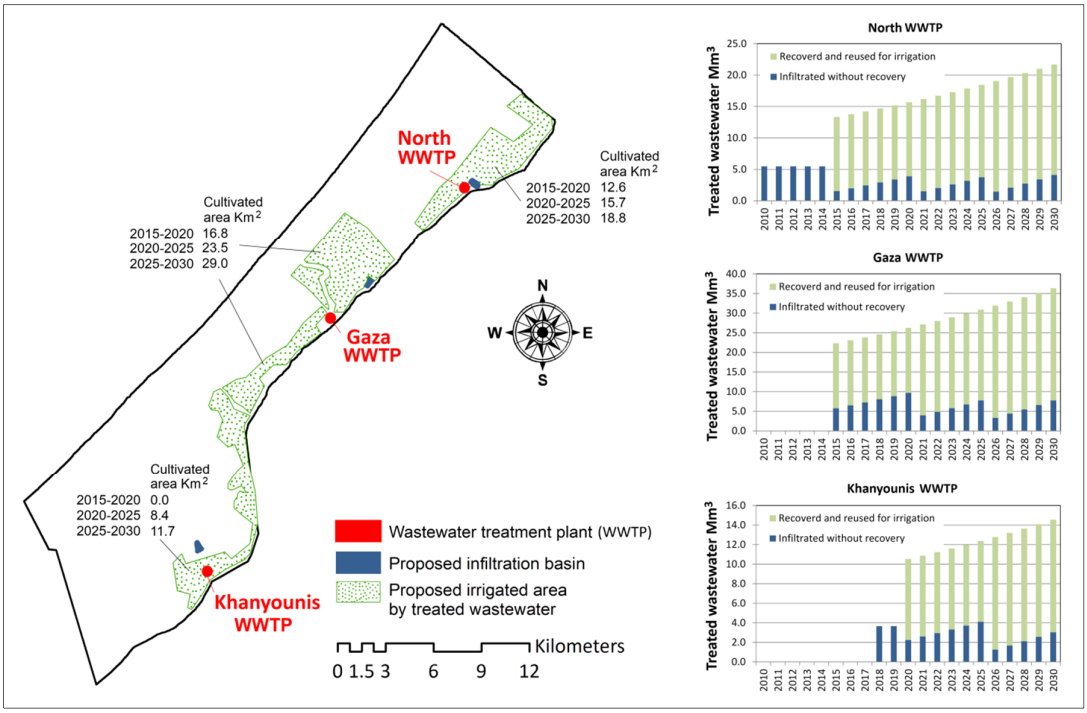

Figure 4.9 Treated wastewater reuse scenario

4.6.4 Infrastructure performance scenario (S4)

Urban water infrastructure is a major driver for sustainable urban water management. The classification of a sanitary, non-sanitary and sustainable city by Childers *et al*. (2014) is related to the performance of the available infrastructure in the city. Around 98% of the urbanized area of the Gaza Strip is covered by water supply networks with an efficiency of 65%, whereas about 75% of the Gaza households are connected to a sewage network with an efficiency of 80% (CMWU, 2010). Improving the efficiency and enhancing coverage of water and wastewater networks might be a sustainable solution. This study investigated an infrastructure scenario by reducing water and wastewater leakage quantities by 30% that influenced groundwater recharge components as well as water supply quantities, which were reduced by 13%.

4.7 Deterioration and sustainability measures

4.7.1 Groundwater quality deterioration cycle

The groundwater quality deterioration cycle of the Gaza Strip was defined and quantified in this study to provide measures for groundwater improvement considering the baseline scenario (S0) and the targeted scenarios (S1, S2, and S3). Figure 4.10 (a−d) demonstrates the importance of human decisions in urban water system dynamics. It shows the interaction between urban water system function, urban and agricultural area and the Gaza coastal aquifer, and reflects an obvious quality deterioration cycle that hampers the development towards sustainable groundwater management.

Slowing down the groundwater quality deterioration cycle is a first step toward sustainable groundwater management. This cycle comprises three dimensions. Regarding the forecasted year of 2030 in the baseline scenario, abstracting 146 Mm^3 from the Gaza aquifer to meet the municipal water demand and then returning 49 Mm^3 (water supply leakage) and 34 Mm^3 (wastewater network leakage) represents the first dimension of the deterioration cycle, as the returned wastewater carries 120–270 mg/l total nitrogen. The second dimension is related to the agricultural return flow to the aquifer; 75 Mm^3 was consumed for irrigation whereas 23% of the irrigation quantities returned to the aquifer were loaded by high total nitrogen (250−350 mg/l leachable nitrogen). Through the first and second dimensions of the deterioration cycle, the returned water to the aquifer has moderate to high quality regarding the Cl concentrations. The third dimension is related to the over-pumping rate from the aquifer and the corresponding seawater intrusion (Cl > 5000 mg/l).

It was assumed that high quality recharge has Cl concentrations below 600 mg/l and total nitrogen concentrations below 16 mg/l (70 mg/l as nitrate (NO_3)), whereas low quality recharge has Cl concentrations above 600 mg/l and total nitrogen concentrations above 16 mg/l, Cl concentrations above 1200 mg/l or total nitrogen concentrations above 32 mg/l. Moderate quality recharge has Cl concentrations and total nitrogen concentrations between low and high quality recharge. The above values (600 mg/l for Cl and 16 mg/l for NO_3-N) are recommended by the Palestinian standards as limits of permitted Cl and NO_3 concentrations in the drinking water (PWA, 2013).

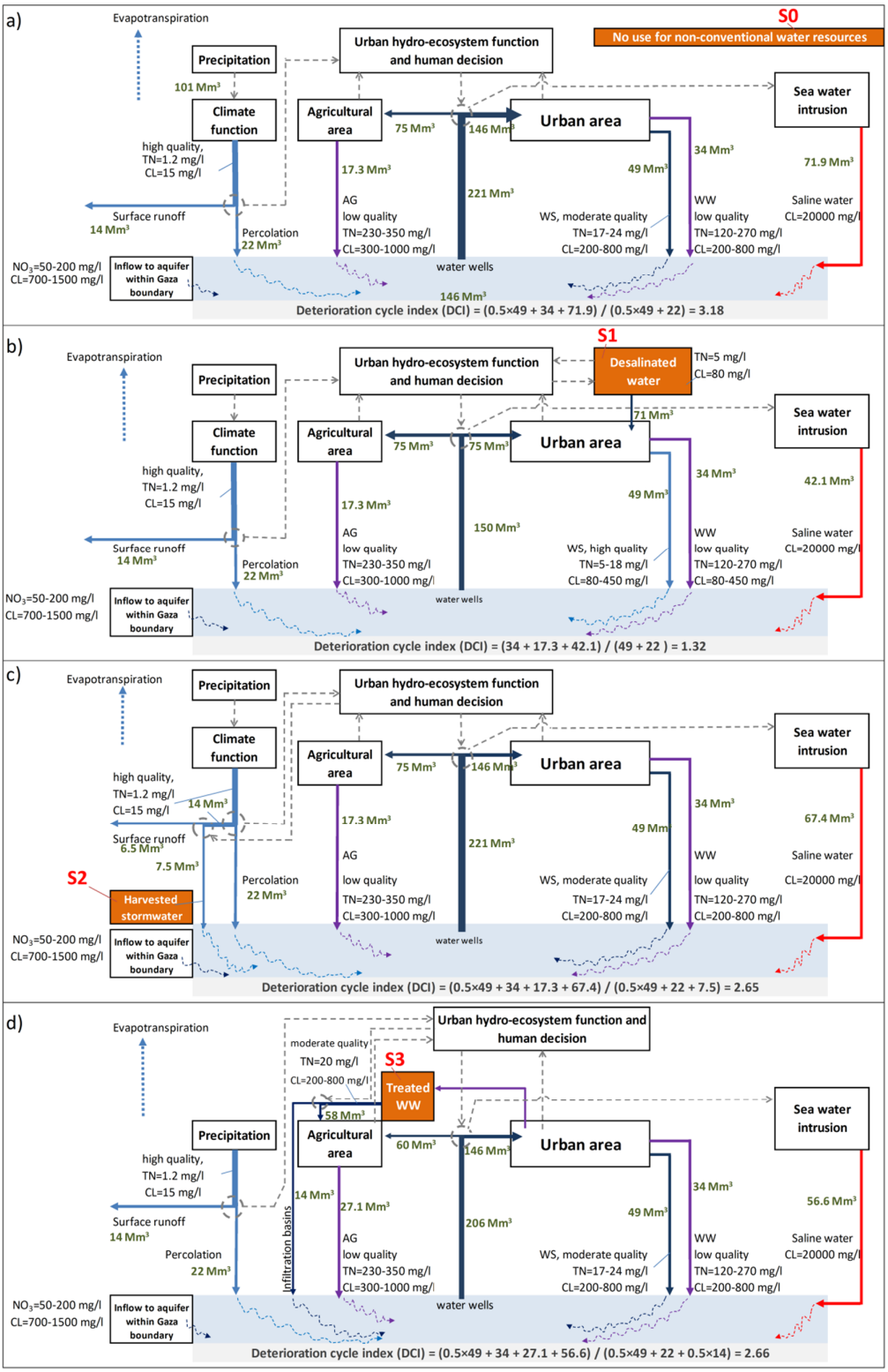

a) Urban water system interactions considering groundwater (GW) as the only water resource (WS = water supply leakage, WW = wastewater network leakage, AG = agriculture return flow). **b)** Urban water system interactions considering desalinated water beside GW. **c)** Urban water system interactions considering harvested stormwater beside GW. **d)** Urban water system interactions considering treated waste water beside GW. Sea water intrusion quantities are derived from the model forecasting results.

Figure 4.10 Urban water system dynamic and groundwater quality deterioration cycle

Figure 4.10 (a-d) depicts the baseline scenario (S0) as well as the targeted scenarios (S1, S2, and S3) in terms of groundwater quality deterioration cycle. The deterioration cycle index was estimated in equation 4.2.

$$\mathrm{DCI} = \frac{V_{low}}{V_{high}} \tag{4.2}$$

where DCI is the deterioration cycle index, V_{low} is the amounts (Mm^3) of low quality recharge components predicted for year 2030, and V_{high} is the amounts (Mm^3) of high quality recharge components predicted for year 2030. Moderate quality recharge was considered as 50% high quality recharge and 50% low quality recharge in the calculation of the DCI.

4.7.2 Groundwater sustainability measures

The groundwater quality deterioration index is represented as an indicator to assess scenario effectiveness of slowing down the deterioration cycle and directing towards a sustainable groundwater situation.

With respect to the current unsustainable groundwater use in the Gaza Strip, this study quantifies the improvement in groundwater quantity and quality among different scenarios using non-conventional water resources aiming toward sustainable groundwater conditions. The improvement index for groundwater level (IIL) was calculated based on the groundwater level difference between the targeted scenario (S1, S2, or S3) and the baseline scenario (S0) (ranging from 0 to >10 m).

The improvement index for groundwater quality (IIQ) was derived based on three ranking steps according to the NO_3 and Cl concentrations. Equation (4.3) ranks the NO_3 and Cl concentrations for each scenario from -1 to 1, while equation (4.4) recodes it to be from 0 to 1.

Equation (4.5) merges the second NO_3 and Cl ranks within one new rank considering probability concepts. As the second ranking value ranges from 0 to 1, it was assumed as a probability value, i.e. the higher value, the higher chance for quality deterioration. Under this assumption, the second ranking value of NO_3 is the probability of event A, while the second ranking value of Cl is the probability of event B. Considering that events A and B are independent, the third rank represents the probability of occurrence of A or B (Kerns, 2010).

$$x_{1(NO_3 \text{ or } Cl)} = \frac{C_x - C_o}{C_x + C_o} \tag{4.3}$$

$$x_{2(NO_3 \text{ or } Cl)} = \frac{x_{1(NO_3 \text{ or } Cl)} + 1}{2} \tag{4.4}$$

$$x_{3(merged)} = P(A \text{ or } B) = P(A) + P(B) - P(A \,\&\, B) = x_{2(No_3)} + x_{2(Cl)} - (x_{2(No_3)} \times x_{2(Cl)}) \tag{4.5}$$

where C_x is the NO_3 or Cl concentration (mg/l) under the targeted scenario (S1, S2, or S3), C_o is the NO_3 or Cl concentration (mg/l) under the baseline scenario (S0), $x_{1(NO3 \text{ or } Cl)}$ is the first ranking value regarding NO_3 or Cl concentrations, $x_{2(NO3 \text{ or } Cl)}$ is the second ranking value, and $x_{3(merged)}$ is the third ranking value.

When $x_{1(NO3)}$ and $x_{1(Cl)}$ are zero (no difference in the NO_3 or Cl concentrations between S0 and (S1, S2, or S3)), $x_{2(NO3)}$ and $x_{2(Cl)}$ will equal 0.5, which means $x_{3(merged)}$ will equal 0.75 (0.5 + 0.5 – 0.5×0.5). The improvement index for the groundwater quality (IIQ) was based on $x_{3(merged)}$ which was categorized into 6 categories (based on the record distribution), namely IIQ = 3 ($x_{3(merged)} < 0.500$), IIQ = 2 ($0.500 < x_{3(merged)} < 0.675$), IIQ = 1 ($0.675 < x_{3(merged)} < 0.725$), IIQ = 0 ($0.725 < x_{3(merged)} < 0.775$), IIQ = -1 ($0.775 < x_{3(merged)} < 0.875$), and IIQ = -2 ($0.875 < x_{3(merged)} < 1.000$).

(IIQ = 0) represents a non-considerable change regarding the groundwater quality influenced by the targeted scenarios. The positive sign means an improvement in the groundwater quality, whereas the negative sign reflects the opposite situation.

4.8 Results and Analysis

4.8.1 Simulation results

During the simulation period of the NO_3 transport model, the model efficiency measure for the monthly simulation R^2 (coefficient of determination) is 0.81 in the calibration and 0.78 in the validation (Fig. 4.11), which indicates a good fit between measured and simulated NO_3 concentrations. It was found that the model had good predictive capability of Cl concentrations with R^2 of 0.91 during the simulation period.

Table 4.3 shows the summary of the calibration and validation statistics. The calibrated first-order denitrification rate (λ_1) is 2×10^{-4} day^{-1}, which represents a low denitrification rate in comparison with other similar studies (e.g. 8.25×10^{-3} day^{-1} by Almasri

and Kaluarachchi (2007) in Whatcom County in USA). The model was run to map the simulated NO_3 and Cl concentrations (Fig. 4.12).

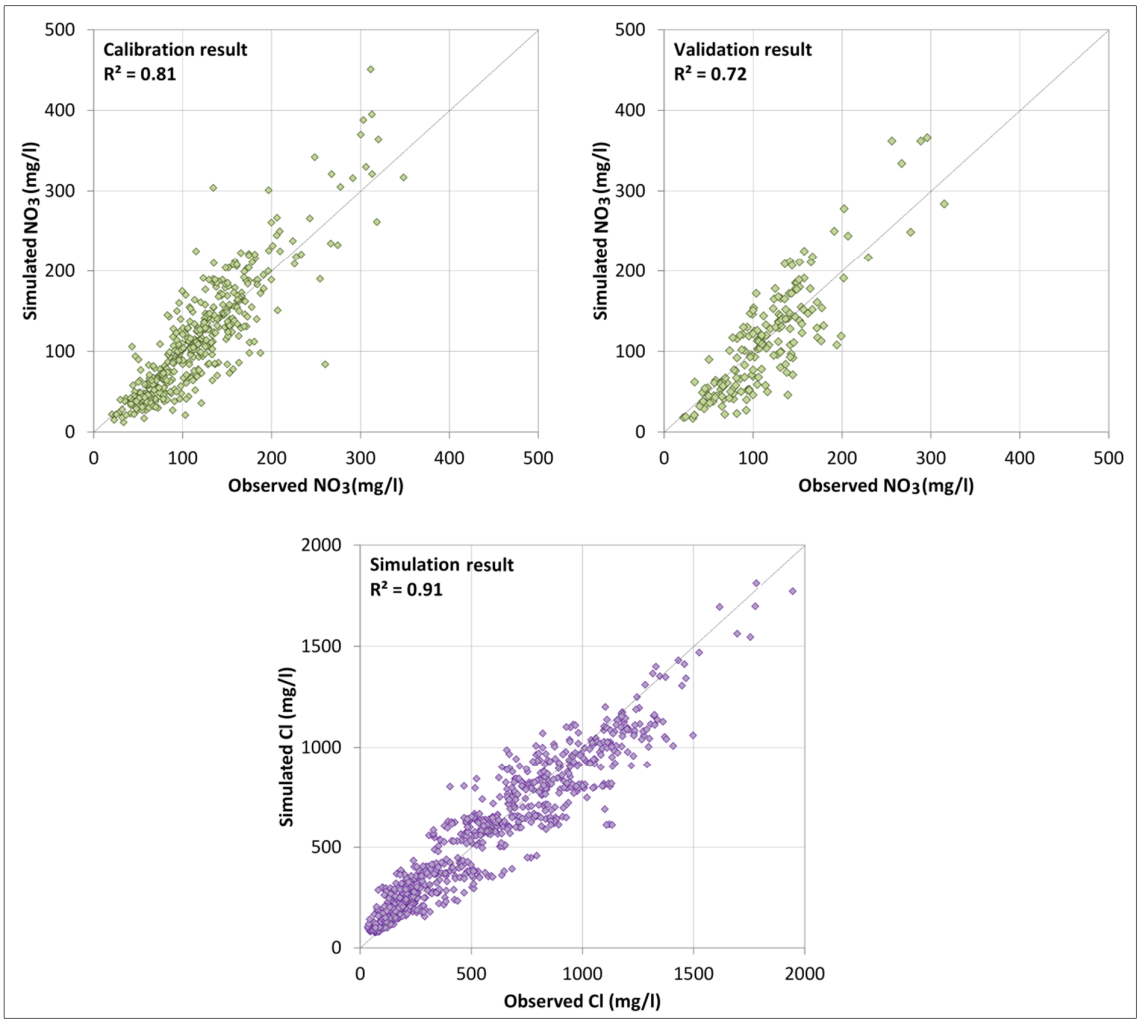

Figure 4.11 Comparison of simulated and observed nitrate and chloride concentrations

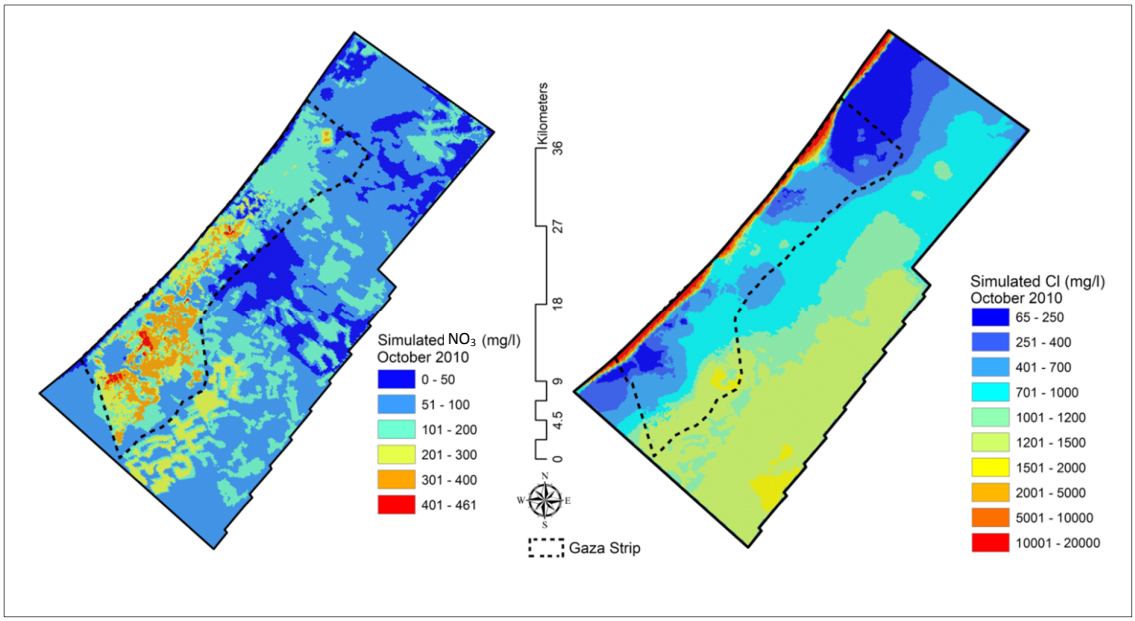

Figure 4.12 Simulated nitrate and chloride concentrations (2010)

Table 4.3 Summary of calibration and validation statistics

NO_3 concentrations		
Calibration results (monthly base)		
	Observed	Simulated
Average (mg/l)	115.60	116.48
Slandered deviation (mg/l)	71.51	59.53
Average of the highest 25% heads (mg/l)	47.40	55.20
Average of the lowest 25% heads (mg/l)	202.30	188.54
Residual mean (mg/l)	0.89	
Absolute residual mean (mg/l)	24.65	
Coefficient of determination, R^2	0.81	
Validation results (monthly base)		
Residual mean (mg/l)	1.41	
Absolute residual mean (mg/l)	27.49	
Coefficient of determination, R^2	0.72	
Cl concentrations		
Simulation results (monthly base)		
	Observed	Simulated
Average (mg/l)	522.91	520.88
Slandered deviation (mg/l)	386.8	341.3
Average of the highest 25% heads (mg/l)	110.92	128.85
Average of the lowest 25% heads (mg/l)	1065.32	998.50
Residual mean (mg/l)	2.10	
Absolute residual mean (mg/l)	89.73	
Coefficient of determination, R^2	0.91	

4.8.2 Forecasting and scenario results

The results confirm the expected deterioration of the groundwater quality from 2010 to 2030 considering the baseline scenario (S0) combined with a marked decline in the groundwater level. Figures 4.13 and 4.14 depict the spatial distribution of simulated NO_3 and Cl concentrations of the years 2010, 2020 and 2030.

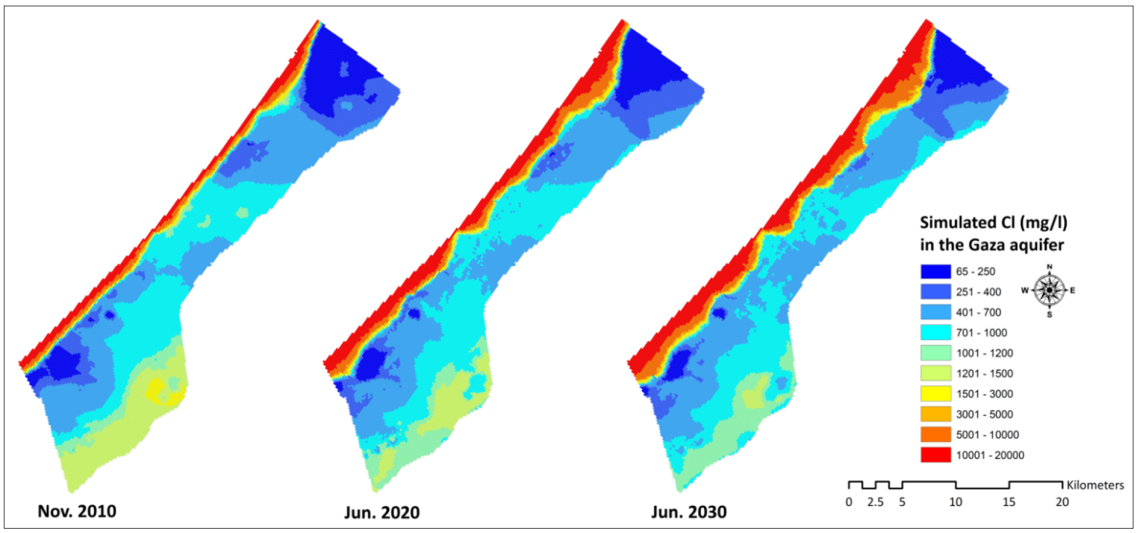

Figure 4.13 Simulated Cl concentrations of years 2010, 2020 and 2030 (baseline scenario S0)

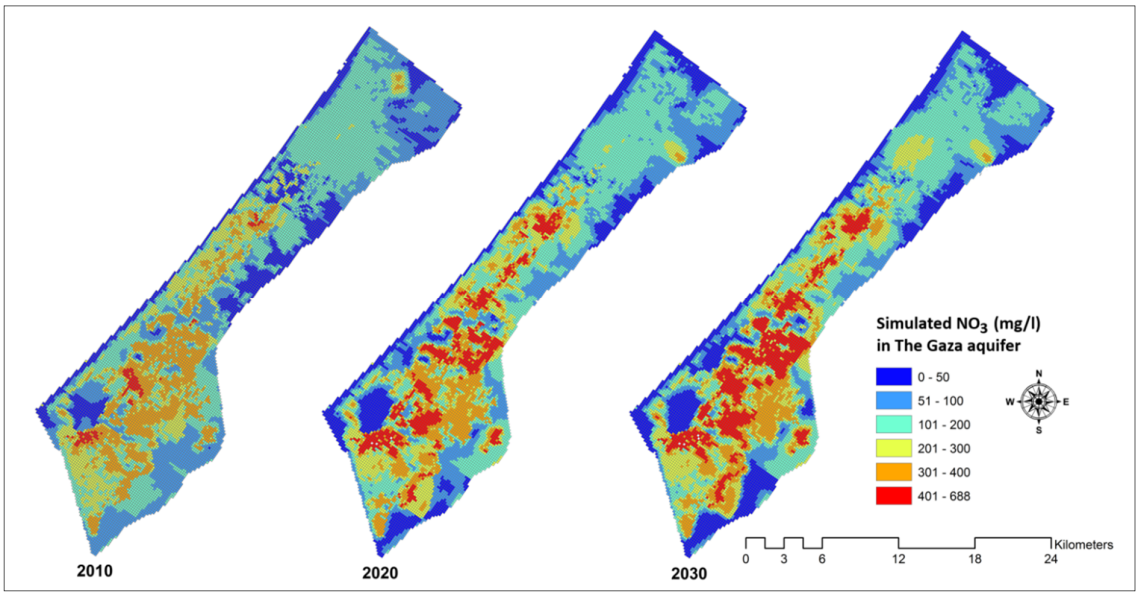

Figure 4.14 Simulated NO_3 concentrations of years 2010, 2020 and 2030 (baseline scenario S0)

The seawater intrusion band (Cl concentration > 5000 mg/l) increases dramatically near the shore. The Cl concentrations increase in general, whereas they slightly reduce in

limited areas in the south of the Gaza Strip by recharge quantities having lower Cl concentrations than groundwater beneath these areas. The NO_3 concentrations increase in some locations up to 600 mg/l.

Figures 4.15 to 4.17 illustrate the variation of groundwater heads, NO_3 concentrations, and Cl concentrations in scenarios S1, S2, and S3 and the baseline scenario (S0) within the Gaza Strip boundaries in year 2030. The results for year 2020 are presented in Figure A.2 to A.4.

Regarding the groundwater level in 2030, the desalination scenario (S1), which represents a kind of relaxation in the groundwater withdrawal quantity in the over-exploited urban areas, reflects an obvious improvement in the groundwater level, not only on average but also in the most deteriorated areas compared to the baseline scenario. The stormwater harvesting scenario (S2) shows a slight improvement in the groundwater level, whereas the TWW reuse scenario (S3) shows a marked improvement. The groundwater level reflects a relative departure under the TWW reuse scenario (S3) in specific areas around the proposed infiltration basins. In Figure 4.15, the box plots characterize the head values (2030) using minimum, quartiles, maximum and outliers. The mean values are presented in the box plots graph. Compared with the baseline scenario (S0), the desalination scenario (S1) represents a departure in the statistical characteristics, which is marked in the difference between the lower outliers of the baseline and the S1. The TWW reuse scenario (S3) maintains the lower outliers in the baseline with a significant push of the mean and maximum values as well as the box plot quartiles.

Compared with the baseline scenario (S0), changes in groundwater quality are visible in the desalination scenario (S1); the seawater intrusion strip (high salinity band, > 5000 mg/l) retreated, and the Cl concentrations were improved in general, whereas no significant change in the NO_3 concentrations was detected except a slight reduction in some peak values. The stormwater harvesting scenario (S2) shows a slight improvement in the groundwater quality (NO_3 and Cl concentrations). The TWW reuse scenario (S3) shows a positive impact regarding the Cl and a negative impact regarding the NO_3 concentrations in specific locations; the salinity strip obviously moves back under the hydraulic head difference due to the increasing groundwater levels beneath the infiltration basins.

The scenario increases the NO_3 concentrations in the eastern side of the Gaza Strip in comparison with the baseline, which is related to the cropping pattern change. The TWW reuse scenario requires a higher amount of fertilizers or manure than the current rainfed

agricultural pattern, and represents a more intensive agriculture than the existing pattern. Regarding the box plots in Figure 4.16, the upper outliers in S1 reflect the potential of this scenario to retreat the high salinity strip near the shore. The lower quartiles in Figure 4.16 which vary from 450 mg/l in S1 to 600 mg/l in S3 reflect the potential of S1 to improve the Cl concentrations in groundwater having low to moderate level of Cl (acceptable for water use). The value of the lower quartile in S3 was higher than that in S0 (Fig. 4.17), which is related to the possible impacts of the reused TWW on groundwater that has a high to moderate quality regarding NO_3 concentrations.

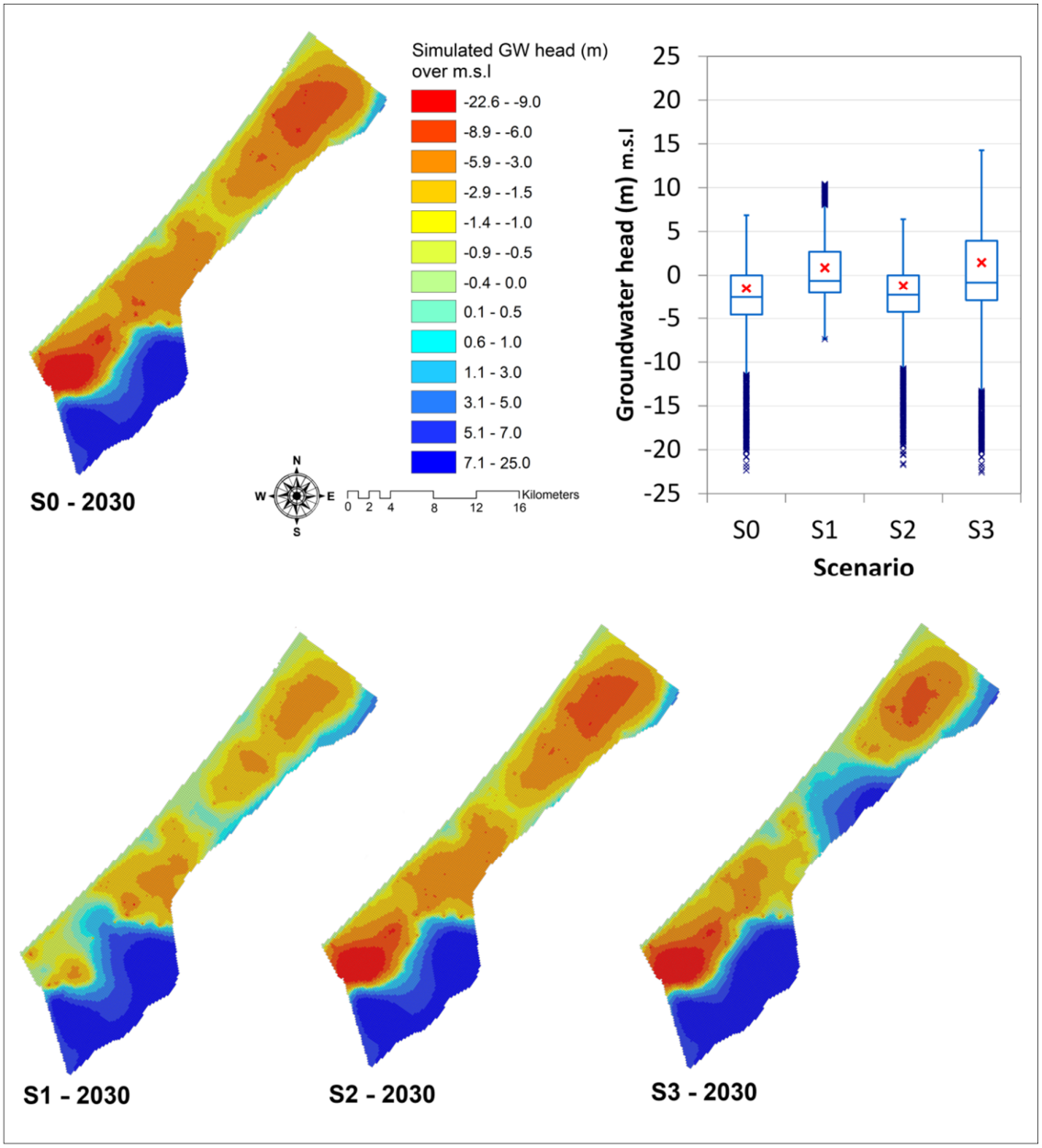

Figure 4.15 Simulated groundwater head in 2030 among scenarios

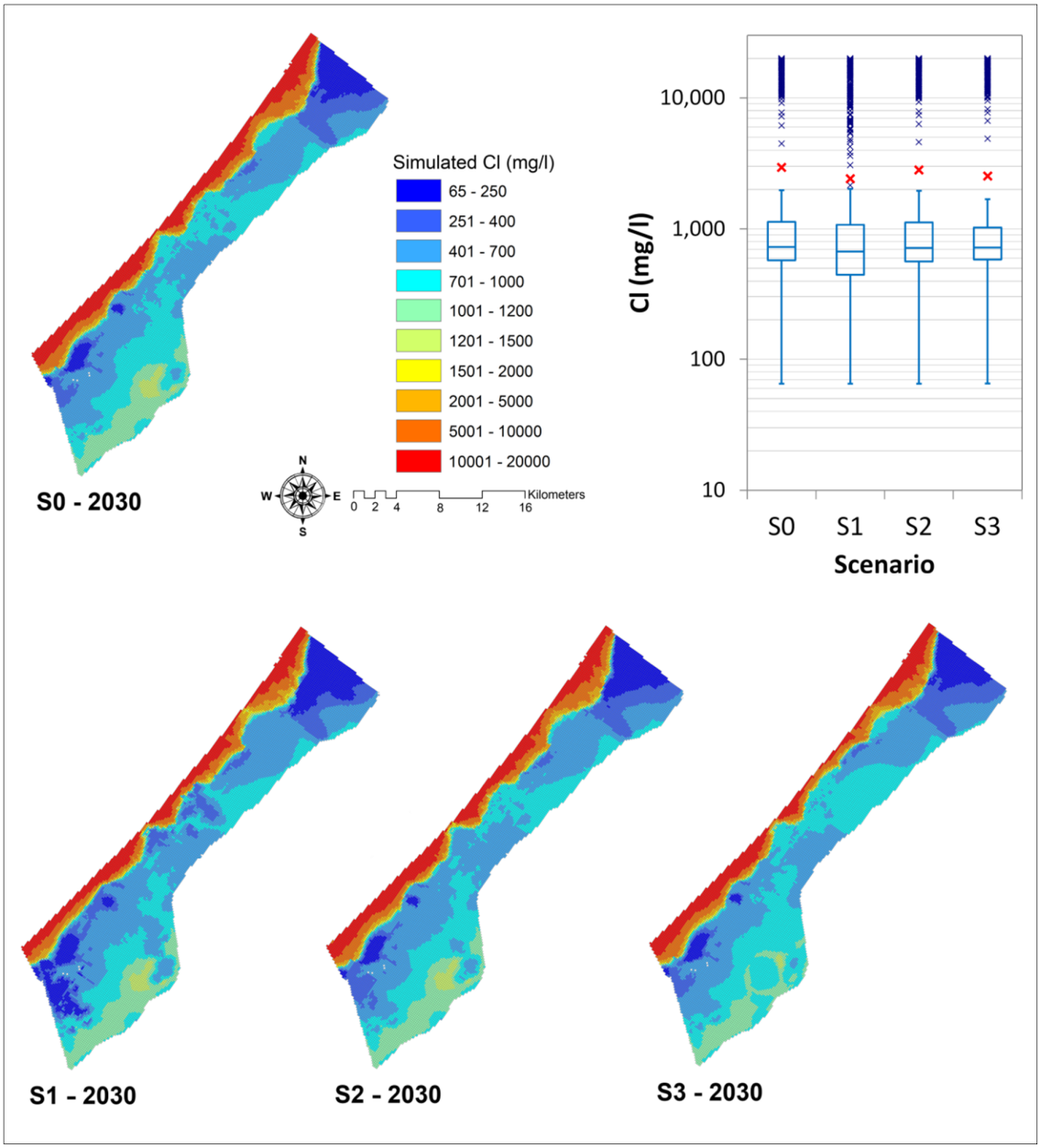

Figure 4.16 Simulated chloride concentrations in 2030 among scenarios

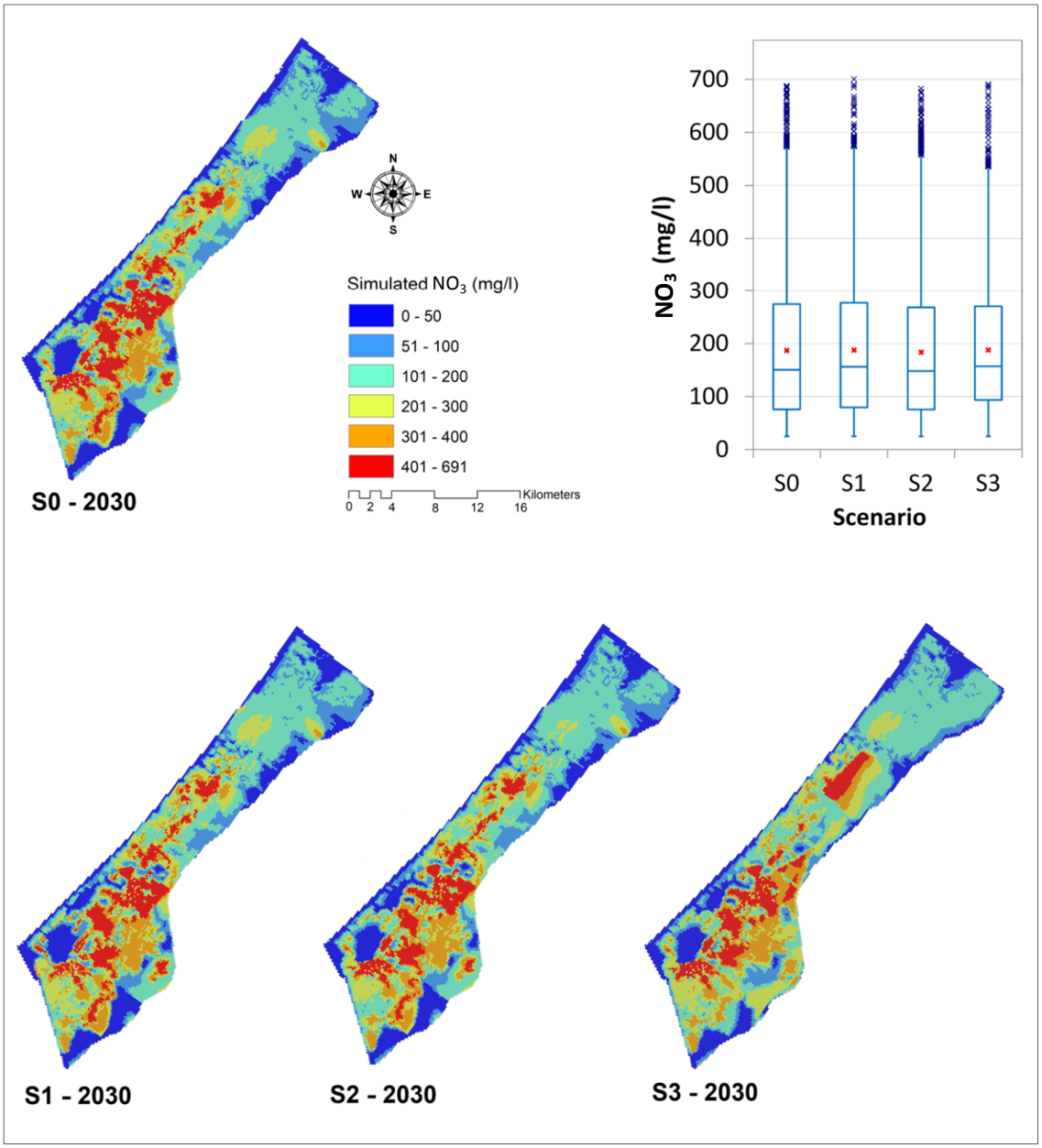

Figure 4.17 Simulated nitrate concentrations in 2030 among scenarios

4.8.3 Deterioration and sustainability measures

The desalination scenario (S1) (Fig. 4.10 b) has the highest potential of reducing the DCI, which was 1.32 compared with 3.18 of the baseline scenario (S0). Concerning the model results, enhancing the water supply by 71 Mm^3 of desalinated water (in 2030) improves the quality of water supply leakage and reduces the pumping water as well as the corresponding intrusive seawater; S1 slows down the first and third dimensions of the deterioration cycle. The stormwater harvesting scenario (S2) (Fig. 4.10 c) provides new high quality recharge to replenish the aquifer, and has a DCI of 2.65. While the TWW scenario (S3) (Fig. 4.10 d) adds 58 Mm^3 of TWW of moderate quality to the aquifer (for irrigation and artificial infiltration), which slows down the first and third dimensions of the deterioration cycle, the second dimension of the deterioration cycle is accelerated by increasing irrigation returned flow of low quality reflecting a DCI of 2.66.

Figures 4.18 and 4.19 show two improvement indexes for groundwater quantity (level) and quality (IIL and IIQ). The desalination scenario (S1) has the highest average IIQ value (0.5) among the scenarios. Although the other scenarios (S2 and S3) have close averages (0.1, 0.05, respectively), they have a different distribution of the IIQ values; S3 has a wider range of positive and negative values than S2, which generally has low positive values.

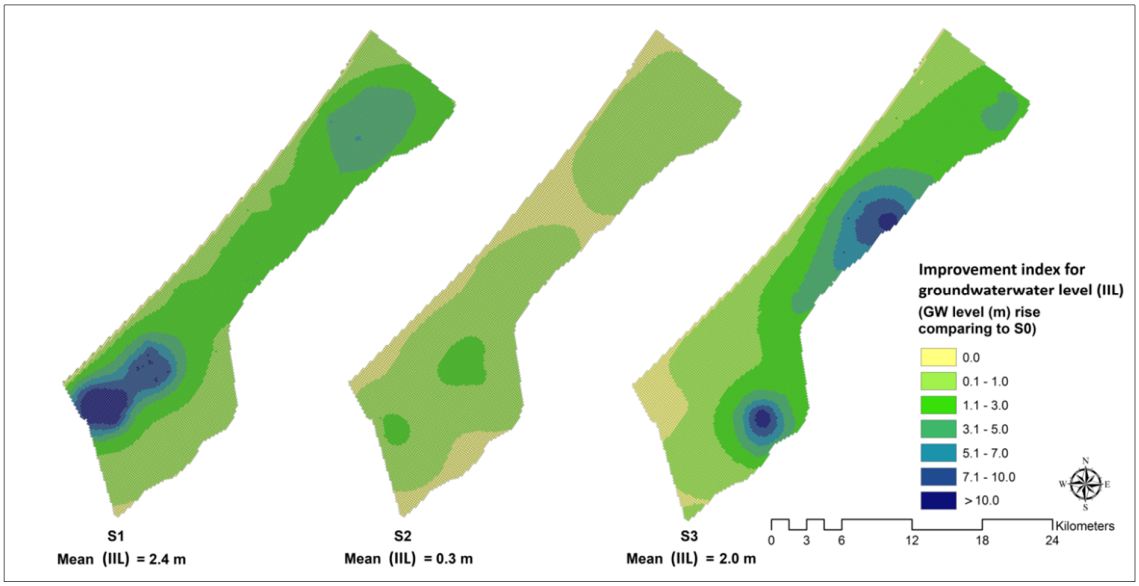

Figure 4.18 Improvement index for groundwater level

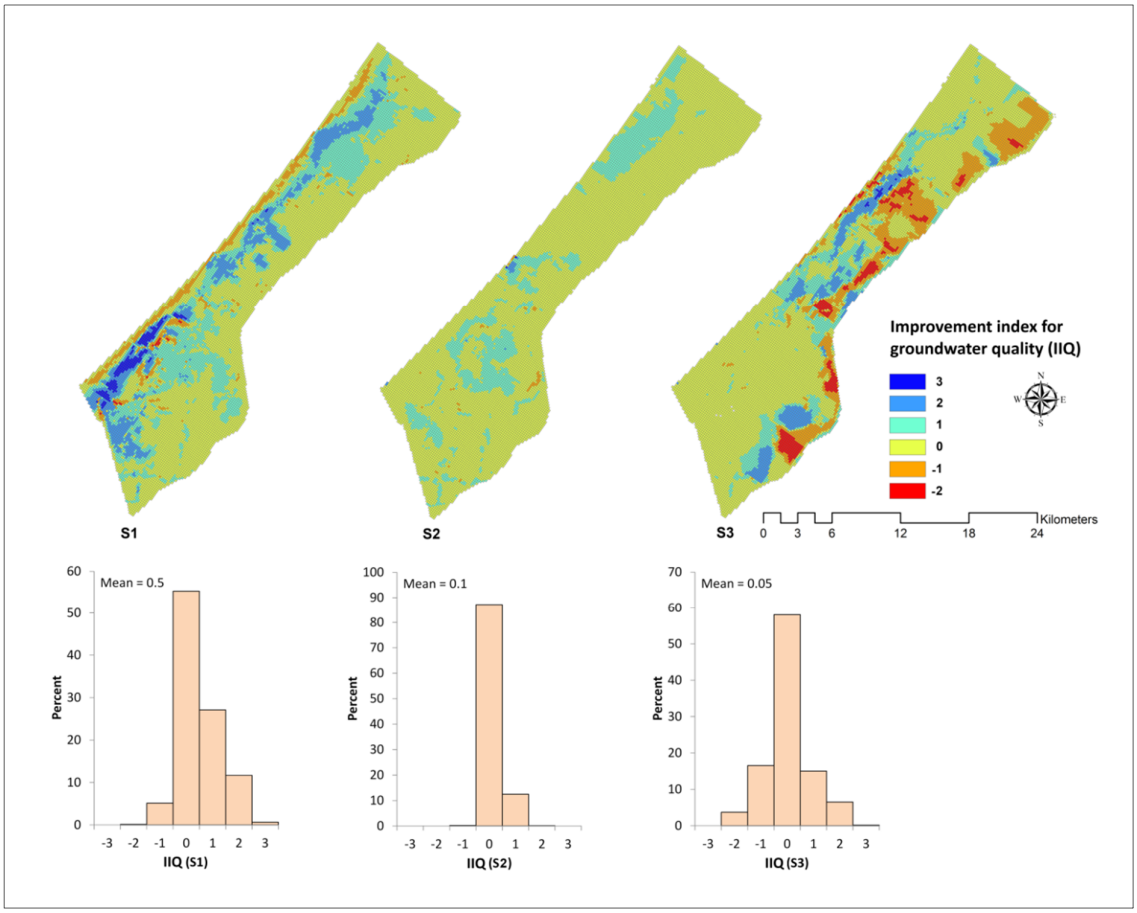

Figure 4.19 Improvement index for groundwater quality

The negative IIQ values in few locations near the shore in S1 and S3 are related to the retreating seawater and its replacement by the groundwater. Even though this groundwater is less saline, it features higher NO_3 concentrations. This finding emerged from the sustainability ranking steps due to the influence of relatively large changes in NO_3 concentrations that produced negative IIQ values.

The highest IIL and IIQ values in the desalination scenario (S1) were in the south with the most strongly deteriorated groundwater and the lowest rainfall quantity. As illustrated in Figure 4.15 to 4.17, the north can be considered as a strategic storage area of relatively moderate to high quality groundwater, thus more desalinated water could be a prospect to prevent seawater intrusion in that area.

As the stormwater harvesting scenario (S2) reflects a modest improvement in the groundwater quality and quantity, a balance between the benefits (indicators IIL and IIQ) and the expected cost is recommended in this study. The low effectiveness of the stormwater

harvested by the beach street is marked, and is related to the direct interaction with the saline strip.

TWW reuse is a controversial scenario in the decision-making agenda. This study, which investigated this scenario (S3) using a spatial and temporal approach, promotes its feasibility in terms of groundwater quantity enhancement, but it raises the possibility of quality deterioration. As the expected deterioration source was related to the irrigation area by the TWW (negative IIQ) while the area beneath the infiltration basins has relatively positive IIQ values, it is recommended to increase the ratio of the infiltrated TWW to the TWW reused for irrigation. A potential sensitivity of this scenario to the wastewater effluent quality can be deduced from the results; the TWW reuse properties should be within the national guidelines, otherwise a dramatic deterioration can be expected. Improving irrigation efficiency and optimizing fertilizers in the area targeted by the scenario could achieve a more sustainable groundwater quality.

Since the infiltrated TWW in S3 reflects a high potential to limit seawater intrusion, the use of combined infiltration basins for TWW and harvested stormwater from catchments inside or/and outside the Gaza Strip boundary could achieve both higher IIL and IIQ. These infiltration basins should be larger than the existing ones. The possibility to harvest large amounts of stormwater in specific years has to be considered in the decision-making agenda.

4.8.4 Infrastructure performance and groundwater sustainability

Figure 4.20 exhibits the simulated changes in groundwater levels and the relative simulated changes in Cl and NO_3 concentrations of the infrastructure scenario compared with the baseline scenario (S0). It can be deduced that the Gaza Strip comprises two main areas related to the response of the groundwater level to water and wastewater leakage and pumping water. In the first area, the groundwater level is more sensitive to the reduction in water and wastewater leakage than the reduction in pumping rate. The opposite applies to the second area.

Based on the infrastructure scenario and compared with the baseline (S0), the groundwater level reduced up to 2.5 m in locations in the first area whereas it increased up to 2 m in the second area. The seawater intrusion strip expanded by the infrastructure scenario in some locations and retracted in others. Figure 4.20 depicts the relative changes in Cl concentrations from -17% (area highly sensitive to changes in pumping rate) to higher than 50% (area highly sensitive to changes in water and wastewater leakage). A marked

improvement regarding NO_3 concentration related to the reduction in the wastewater leakage quantities in the infrastructure scenario was detected.

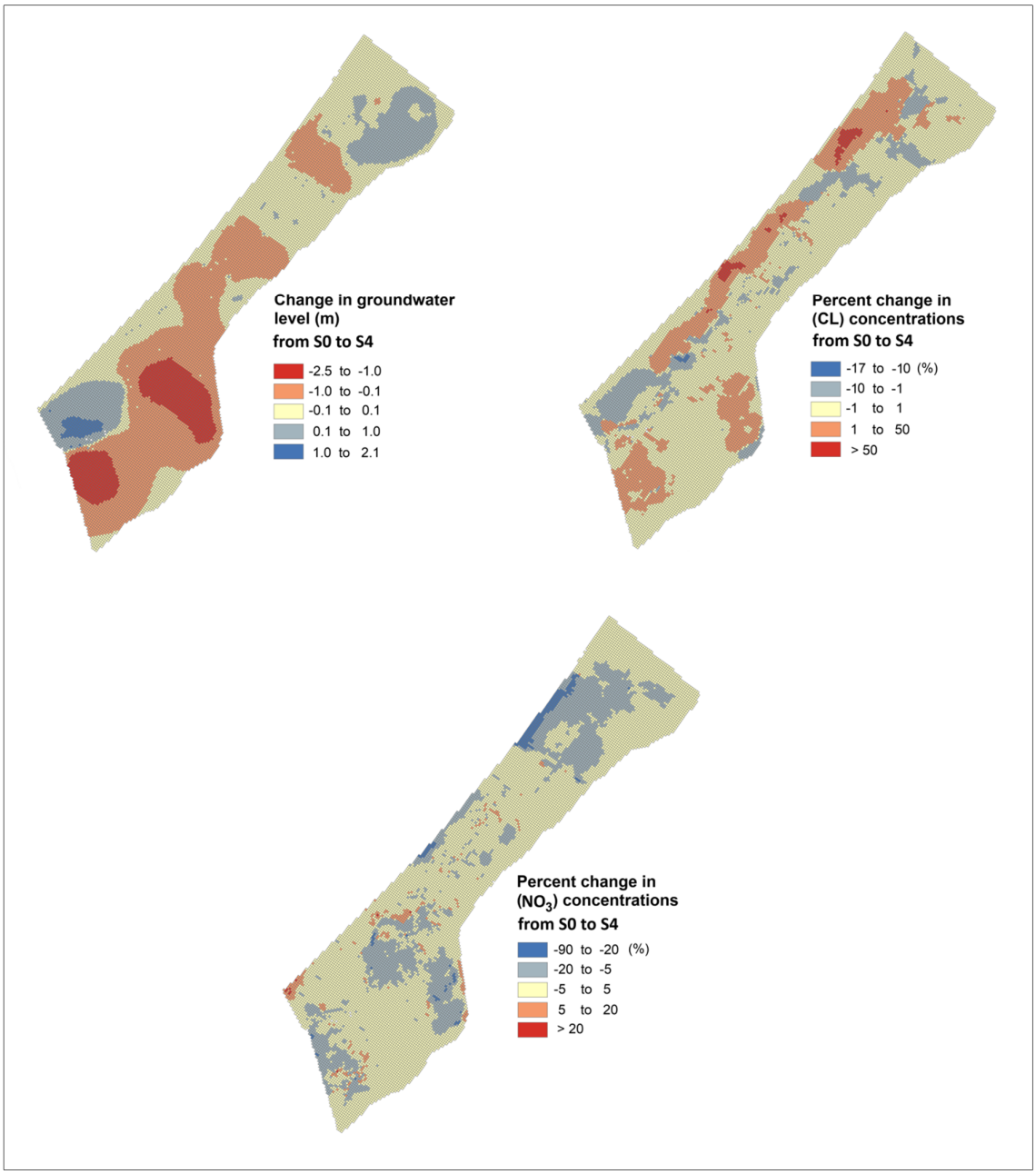

Figure 4.20 Infrastructure scenario (S4) and expected changes in groundwater level and relative changes in Cl and NO_3 concentrations

CHAPTER 5

5 Summary and conclusions

5.1 First part: Quantifying the impact of urban area expansion on groundwater recharge and surface runoff

This part quantifies the impact of urban area expansion on the coastal aquifer recharge and surface runoff of the semi-arid watersheds intersecting with the Gaza Strip. The results show that the SWAT model could simulate water budget components adequately within these complex watersheds. Based on a semi-automated approach of calibration and sensitivity analysis using SWAT-CUP software, the most sensitive parameters are available water capacity of the soil layer, depth from soil surface to bottom of layer, soil evaporation compensation factor, and initial SCS curve number for moisture condition II. Therefore, as the soil package of the SWAT parameters has the most sensitive parameters, this package can be defined as the most sensitive. The simulations reveal a considerable spatial variability of the water budget components throughout the study area. The simulated percolation, surface runoff and evapotranspiration represent on average 22.4%, 11.7%, and 65.0%, respectively, of the rainfall quantities within the Gaza Strip boundary, whereas these values are 17.9%, 6.5%, and 74.5%, respectively, considering the aquifer domain boundary. The average annual surface runoff varies from 0 mm in the south-east to 89 mm in the north-west. The maximum average annual percolation (124 mm) takes place in the northern part of the study area. The average annual evapotranspiration ranges widely from 132 to 265 mm. The maximum average annual flow-volume was 15.7 Mm^3 in the largest northern watershed whereas it decreased sharply in the southern main watersheds to around 4 Mm^3. Based on SWAT, the relationship between the relative change in urban area and the corresponding relative change in surface runoff or percolation can be estimated to be nearly linear. The Urban-Surface runoff Index (USI) which reflects the percent of change in surface runoff due to a 1% increase in urban area at subbasin level ranges from 0 to around 1, while the Urban-

Percolation Index (UPI) which represents the percent of change in percolation due to a 1% increase ranges from 0 to -0.41. To identify the relative impact between subbasins, the Global Urban-Surface runoff Index (GUSI) and Global Urban-Percolation Index (GUPI) were derived to quantify the influence on the total aquifer percolation and the overall surface runoff due to (high density) urban area change. USI and UPI can support the decision makers in the micro-level evaluation of different urban change scenarios in the subbasins. For instance, the UPI can be used to evaluate the influence of urban area change on the sensitive areas of groundwater depression related to specific subbasins. Whereas GUSI and GUPI are macro-level factors, they can be of significant importance for framing a sustainable planning for the water resources in the Gaza Strip. Based on GUPI and GUSI, decreasing the impervious areas and developing surface runoff harvesting systems in the urban development zone of the Gaza Strip are important options for aquifer sustainability, especially in the northern area.

5.2 Second part: potential impacts of urban area expansion on groundwater level: a spatial-temporal assessment

A 3-D groundwater flow model was developed in this part of the study, using MODFLOW-USG, to investigate the groundwater levels within the Gaza coastal aquifer considering the connection to a surface water model as well as a detailed estimation of other recharge components. Model inputs in terms of geological and hydrogeological data and model outputs were exhibited in a spatial approach. The high density of wells concentrated within the Gaza region in the model domain represents a typical example of using unstructured grids (Voronoi cells) to reduce run time within an accepted accuracy. Calibration and validation measures as well as comparison of simulated and observed head indicate a substantial agreement. A spatial hydraulic conductivity was deduced from the transient simulation. Specific yield and porosity were initially estimated based on previous studies and calibrated from the transient simulation. The annual water balance reflects the correlation between seawater intrusion and net aquifer replenishment, which was negative throughout the simulation period except in 2004/05 (a wet hydrological year). Combined with a comprehensive approach of recharge estimation, the long-term forecasting (2010–2030) of underlying spatial patterns in the groundwater levels provides realistic and sustainable urban as well as water resource planning and decision making. Inputs were modified to fulfil the expected population growth and its influence on water supply quantities, built-up area, water

and wastewater leakage and reduction of average recharge from rainfall. A marked decline in the average groundwater level across the Gaza aquifer domain was detected over the whole simulation period 2004–2030. Considering the current management situation, the average annual groundwater levels correlate negatively with the increasing built-up area; the regression slope is estimated at -0.056 m/km^2. Linking the increasing built-up area with the potential impacts of urban expansion relating to water supply quantities and recharge components strengthened the inferred interrelation between the groundwater level and the built-up area. Taking into account potential planning alternatives, the optimum alternative should show a minimum negative regression slope, which would support decision makers in urban planning and water resources management. The derived groundwater-level trend index could be used as a spatial indicator for the sustainability of the Gaza coastal aquifer. Increasing recharge by treated wastewater reuse and decreasing groundwater depletion by storm water harvesting and/or desalination are highly recommended. Groundwater quality which may be related to urbanization expansion could be evaluated utilizing the presented results on simulated groundwater flow in combination with applying a contaminant transport engine in MODFLOW.

5.3 Third part: Integrated hydrologic modeling as a key for sustainable urban water resources planning

A coupling of surface water (SWAT), groundwater (MODFLOW) and solute transport (MT3DMS) models was performed to quantify surface-groundwater and quantity-quality interactions due to the impacts of urbanization. The calibration and validation results indicate a good fit between measured and simulated nitrate (NO_3) concentrations, while a good predictive capability with respect to the Cl concentrations was detected by the model during the simulation period. A low denitrification rate in the Gaza coastal aquifer was concluded during the calibration period that was supported by the porous media aquifer. This part of study provides insight in the use of non-conventional water resources within the urban water system. Three scenarios, inferred from the decision-making agenda, were investigated, namely desalination, stormwater harvesting, and treated wastewater (TWW) reuse. Spatial variety of the groundwater level as well as quality was assessed for the targeted scenarios (S1, S2, and S3) compared to the baseline scenario (S0). The deterioration cycle index was estimated as the ratio between the amounts of low and high quality recharge components predicted for year 2030. Based on the groundwater level differences between the scenarios

and the baseline scenario, the improvement index for the groundwater level (IIL) was calculated. The improvement index for the groundwater quality (IIQ) was derived by three ranking steps regarding the NO_3 and Cl concentrations. The main findings of the quality deterioration index, scenarios, and sustainability indexes can be summarized as follows. Firstly, even though the desalination (S1) and TWW reuse (S3) scenarios reflect a noticeable improvement in the groundwater level, the desalination scenario (S1) shows a stronger tendency toward sustainable groundwater quality. Secondly, decision makers should embed decision making into the overall context of further dimensions related to the TWW reuse scenario; however, changing cropping patterns could pose a threat to the groundwater quality (IIQ) in certain parts of the proposed TWW irrigation areas. Thirdly, the stormwater harvesting scenario (S2) shows a slight improvement in both groundwater quality and quantity, which raises the question whether this scenario is feasible as a strategic and effective approach towards sustainable groundwater in the Gaza Strip. Considering the spatial assessment approach, this part of study also provides insights into the opportunities for (1) increasing the planned desalinated water supply quantities for the northern part of the Gaza Strip (has the best groundwater quality and quantity), (2) using combined infiltration basins for TWW and harvested stormwater from catchments areas inside or/and outside the Gaza Strip boundary, (3) increasing the ratio of the artificially infiltrated TWW to the reused TWW for irrigation in parallel with a continuous quality improvement, and (4) improving irrigation efficiency and optimizing fertilizers in the targeted areas in the TWW reuse scenario. The results indicate a potential decline in groundwater level and increase in seawater intrusion in areas that are more sensitive to the reduction of water and wastewater leakage than to the corresponding reduction in pumping water supply. The enhancement of the NO_3 level in the groundwater in the infrastructure scenario indicates that it could be more important to improve the sewage system than the water distribution system, which could restore this importance with the implementation of the desalination systems to reduce desalinated water losses through distribution systems.

In General, *this study demonstrates the strength of using integrated hydrologic modeling in the sustainable urban water planning process. It provides a complete view of the urban water system of the watersheds intersecting with the Gaza Strip, quantifies the surface and groundwater interaction with sufficient spatial and temporal details, exhibits novel indexes related to urban area expansion as well as sustainability measures, and supports realistic scenarios inferred from the decision-making agenda. This study provides a 'corridor of options', which could facilitate future studies focusing on developing a micro-level assessment of the above scenarios and their trade-offs and synergies among the socio-economic and environmental aspects within the urban water system.*

References

Abbaspour, K., Johnson, C., and Genuchten, M., 2004. Estimating Uncertain Flow and Transport Parameters Using a Sequential Uncertainty Fitting Procedure. *Vadose Zone Journal*, 1352, 1340–1352.

Abbaspour, K. C., Yang, J., Maximov, I., Siber, R., Bogner, K., Mieleitner, J., … Srinivasan, R., 2007. Modelling hydrology and water quality in the pre-alpine/alpine Thur watershed using SWAT. *Journal of Hydrology*, 333(2-4), 413–430. doi:10.1016/j.jhydrol.2006.09.014

Aish, A., Batelaan, O., and De Smedt, F., 2010. Distributed recharge estimation for groundwater modelling using WETSPASS, Case study: Gaza Strip, Palestine. *The Arabian Journal for Science and Engineering*, 35(1B), 155–164.

Ajjur, S. and Mogheir, Y., 2012. Effect of climate change on the groundwater resources (Gaza Strip case study). *International Journal of Sustainable Energy and Environment*, 1(8), 136–149.

Al-Khatib, I. and Arafat, H., 2009.Chemical and microbiological quality of desalinated water, groundwater and rain-fed cisterns in the Gaza strip, Palestine. *Desalination*, 249(3), pp.1165–1170. Available at: http://linkinghub.elsevier.com/retrieve/pii/S0011916409009072 [Accessed January, 2014].

Almahallawi, K., 2005. *Modeling interaction of landuse, urbanization and hydrological factors for the analysis of groundwater quality in Mediterranean zone (example the Gaza Strip, Palestine)*. Ph.D dissertation, University of Lille for science and technology.

Almasri M. and Ghabayen S., 2008. Analysis of Nitrate Contamination of Gaza Coastal Aquifer, Palestine. *ASCE Journal of Hydrologic Engineering*, 13(3).

Almasri, M. and Kaluarachchi, J., 2007. Modeling nitrate contamination of groundwater in agricultural watersheds. *Journal of Hydrology*, 343, 211–229.

Arnold, J. and Fohrer, N., 2005. SWAT2000: current capabilities and research opportunities in applied watershed modelling. *Hydrological process*, 19(13), 563–572.

Austrian Development Coorperation and Palestinian Water Authority (ADA & PWA), 2011. *Stormwater infiltration plan for Gaza Governorates*. Project: Technical Assistant on Use of Non-Conventional Water Resources – Reuse of Treated Wastewater, management of Storm water Harvesting in Gaza Strip, Gaza QCBS/01/09. Consultant: Enfra and Almaden.

Baalousha, H., 2005. Using CRD Method for Quantification of Groundwater Recharge in the Gaza Strip, Palestine. *Environmental Geology*, 48, 889–900.

Baaloush, H., 2008. Analysis of nitrate occurrence and distribution in groundwater in the Gaza Strip using major ion chemistry. *Global NEST Journal*, 10(3), 337–349.

Baalousha H., 2010. Mapping groundwater contamination risk using GIS and groundwater modeling, a case study from the Gaza Strip, Palestine. *Arabian Journal of Geosciences*, doi:10.1007/s1257-010-0135-0.

Barron, O., Barr, A., and Donn, M., 2013. Effect of urbanization on the water balance of a catchment with shallow groundwater. *Journal of Hydrology*, 485, 162–176. doi:10.1016/j.jhydrol.2012.04.027

Bear, J., 1972. Dynamics of Fluids in Porous Media. Dover Publications, New York, 764pp.

Benhamiche N., Sahi L., Tahar S., Bir H., Madani K., and Madani B., 2014. Spatial and temporal variability of groundwater quality of an Algerian aquifer: the case of Soummam Wadi. *Hydrological Sciences Journal*. doi:10.1080/02626667.2014.966723.

Bhatt, G., Kumar, M. and Duffy, C.J., 2014. A tightly coupled GIS and distributed hydrologic modeling framework. *Environmental Modelling & Software*, 62, 70–84. URL: http://linkinghub.elsevier.com/retrieve/pii/S1364815214002266.

Carlson, M., Lohse, K., McIntosh, J., and McLain, J., 2011. Impacts of urbanization on groundwater quality and recharge in a semi-arid alluvial basin. *Journal of Hydrology*, 409(1-2), 196–211. doi:10.1016/j.jhydrol.2011.08.020.

Castronova, A., Goodall, J., and Ercan, M., 2013. Integrated modeling within a hydrologic information system: An OpenMI based approach. *Environmental Modelling & Software*, 39, 263–273. doi:10.1016/j.envsoft.2012.02.011.

Center for Engineering and Planning (CEP), Finnish Consulting Group International Ltd. (FCG), 2010. *Special Report Concerning Irrigation Scheme*, Contract Number: NGEST/AF-QCBS01-08/DD, PWA, Gaza, Palestine.

Chaudhuri, S. and Ale, S., 2014. Long-term (1930-2010) trends in groundwater levels in Texas: Influences of soils, land cover and water use. *Science of the Total Environment*, 490, 379–90. doi:10.1016/j.scitotenv.2014.05.013

Chen, C., Wang, C., Hsu, Y., Yu, S., and Kuo, L., 2010. Correlation between groundwater level and altitude variations in land subsidence area of the Choshuichi Alluvial Fan, Taiwan. *Engineering Geology*, 115(1-2), 122–131.

Childers, D., Pickett, S., Grove, J., Ogden, L. and Whitmer, A., 2014. Advancing urban sustainability theory and action: Challenges and opportunities. *Landscape and Urban Planning*, 125, 320–328. doi:10.1016/j.landurbplan.2014.01.022.

Cho, J., Barone, V., and Mostaghimi, S., 2009. Simulation of land use impacts on groundwater levels and streamflow in a Virginia watershed. Agric. *Water Management*, 96(1), 1–11. doi:10.1016/j.agwat.2008.07.005.

Chu, J., Zhang, C., and Zhou, H., 2010. *Study on interface and frame structure of SWAT And MODFLOW models coupling*. Geophysical Research–EGU General Assembly Conference Abstracts, 12, 4559.

Chung I., Lee J., Kim N., Na H., Chang S., Kim Y., and Kim G., 2014. Estimating exploitable amount of groundwater abstraction using an integrated surface water-groundwater model: Mihocheon watershed, South Korea. *Hydrological Sciences Journal*. doi:10.1080/02626667.2014.980261.

Costal Municipalities Water Utility (CMWU), 2013. Archived data, Gaza–Palestine, (CMWU).

Costal Municipalities Water Utility (CMWU), 2010. *Water Status in the Gaza Strip and Future Plans*. Annual report, CMWU, Gaza–Palestine. URL: http://www.cmwu.ps [Accessed August 2013].

Dan, J., Yaalon, D., Koyumdjisky, H., and Raz, Z., 1976. *The soil of Israel (Historical Palestine) with map 1:500,000*. Ministry of Agriculture, Division of scientific publications.

Delin, G., Healy, R., Lorenz, D., and Nimmo, J., 2006. Comparison of local- to regional-scale estimates of ground-water recharge in Minnesota, USA. *Journal of Hydrology*, 334(1–2), 231–249.

Dong, W., Cui, B., Liu, Z., and Zhang, K., 2013. Relative effects of human activities and climate change on the river runoff in an arid basin in northwest China. *Hydrological Processes*, doi:10.1002/hyp.9982.

Du, J., Qian, L., Rui, H., Zuo, T., Zheng, D., Xu, Y., and Xu, C., Y., 2012. Assessing the effects of urbanization on annual runoff and flood events using an integrated hydrological modeling system for Qinhuai River basin, China. *Journal of Hydrology*, 464-465, 127–139. doi:10.1016/j.jhydrol.2012.06.057.

Dudeen, B., 2001. The soils of Palestine (The West Bank and Gaza Strip) current status and future perspectives. *Options Méditerranéennes : Série B. Etudes et Recherches*, 34, 203–225.

Fadil, A., Rhinane, H., Kaoukaya, K., Kharchaf, K., and Alami Bachir, O., 2011. Hydrologic modeling of the Bouregreg watershed (Morocco) using GIS and SWAT Model. *Journal of Geographic Information System*, 3(4), 279–289.

Food and Agriculture Organization of the United Nations FAO, 2006. Guidelines for soil description. ISBN 92-5-105521-1.

Franke, O., Reilly, T., Bannett G., 1987. *Definition of boundary and initial conditions in the analysis of saturated groundwater flow systems; an introduction*. USGS, Techniques of water resources investigations, 03-B5, 15P.

Geron, R., Amit, R., and Grossman, S., 1985. *Dust availability in desert terrains, a study in the deserts of Israel and the Sinai.* Institute of Earth Sciences-the Hebrew University of Jerusalem, project for: the US Army Research, and Development and Standardization Group-UK. Contract No. DAJA45-83-C-0041.

Ghabayen, S., Nassar, A., El-Dirawi, S., Rashwan, H., and Sarsour, H., 2013. Enhancement of Artificial Infiltration Capacity in Low Permeability Soils for Gaza Coastal Aquifer. *Environment and Natural Resources Research*, 3(4), 155–166. doi:10.5539/enrr.v3n4p155.

Ghabayen, S., 2001. Archived data about Gaza Strip, Utah State University, URL: http://hydrology.neng.usu.edu/giswr/archive00/termpa-pers/ghabayen.htm [Accessed May 2010]

Ghabayen, S. and Salha, A., 2013. Crop Water Requirements (CWR) Estimation in Gaza Strip Using ArcMap-GIS Model Builter. *International Journal of Emerging Technology and Advanced Engineering*, 3(10), 291–299.

Goldfarb, O. and Kislev, Y., 2009. A sustainable salt regime in the Israeli coastal aquifer. In: Ayal Kimhi and Israel Finkelshtain (eds.) *The Economics of Natural and Human Resource.* Nova Science Publishers, 7–29.

Government portal–Israel, 2013. Metrological data, URL: http://data.gov.il/ims [Accessed August 2013].

Hamad, J., Eshtawi, T., Abushaban, A., and Habboub, M., 2012. Modeling the impact of land-use change on water budget of Gaza Strip. *Journal of Water Resource and Protection*, 4, 325–333.

Hamdan, S., Troeger, S., and Nassar, A., 2007. Stormwater availability in the Gaza Strip, Palestine. *International Journal of Environment and Health*, 1(4), 580–594.

Harbaugh, A, W., 2005. *MODFLOW-2005, The U . S .Geological Survey Modular Ground-Water Model — the Ground-Water Flow Process*. U.S. Geological Survey Techniques and Methods. URL: http://pubs.usgs.gov/tm/2005/tm6A16/PDF/TM6A16.pdf.

Harbaugh, A., Banta, E., Hill, M., and McDonald, M., 2000. *MODFLOW-2000, The U.S. Geological Survey Modular Ground-Water Model User Guide to Modularization Concepts and the Groundwater Flow and Process*. U.S. Geological Survey, Water-Resources Investigations Report 00–92. URL: http://www.gama-geo.hu/kb/download/ofr00-92.pdf.

Hassan, S., Lubczynski, M., Niswonger, R., and Su, Z., 2014. Surface–groundwater interactions in hard rocks in Sardon Catchment of western Spain: An integrated modeling approach. *Journal of Hydrology*, 517, 390–410. doi:10.1016/j.jhydrol.2014.05.026.

Holland, J., Berger, R., and Schmidt, J., 1998. Finite Element Analyses in Surface Water and Groundwater: An Overview of Investigations at the U.S. Army Engineer Waterways

Experiment Station. *International journal of computational fluid dynamics*, 9(3-4), 237–247. doi:10.1080/10618569808940856.

House of water and Environment (HWE), 2010. *Ground Water Protection Plan for Gaza Coastal Aquifer project*, Final report. URL: http://www.hwe.org.ps/ [Accessed March 2011].

Isaac, J., Saad, S., Hrimat, N., Khair, L., Ghayyadah, A., and Latif, F., 2006. *Analysis of urban trends and landuse changes in the Gaza Strip*. Report, Applied Research Institute–Jerusalem (ARIJ). URL: http://www.arij.org/publications/books-a-atlases/[Accessed August 2013].

Ismail, M., Moghavvemi, M., and Mahlia, T., 2013. Energy trends in Palestinian territories of West Bank and Gaza Strip: Possibilities for reducing the reliance on external energy sources. *Renewable and Sustainable Energy Reviews*, 28, 117–129.

Kandulu, J., Connor, J., and MacDonald, D., 2014. Ecosystem services in urban water investment. *Journal of Environmental Management*, 145, 43–53. URL: http://dx.doi.org/10.1016/j.jenvman.2014.05.024.

Karcher, S., VanBriesen, J., and Nietch, C., 2013. Alternative land-use method for spatially informed watershed management decision making using SWAT. *Journal of Environmental Engineering*, 139(12), 1413–1423.

Kerns, G.J., 2010. Introduction to Probability and Statistics Using R, URL: papers2://publication/uuid/7AC444D3-E151-41DE-8521-51948F21A8EE.

Khalaf, A., Al-Najar, H., and Hamed, J., 2006. Assessment of rainwater run-off due to the proposed regional plan for Gaza governorates. *Journal of Applied Science*, 6 (13), 2693–2704.

Kim, Y., Band, L., and Song, C., 2013. The influence of forest regrowth on the stream discharge in the north Carolina piedmont watersheds. *Journal of the American Water Resources Association*. doi: 10.1111/jawr.12115.

Krause, P., and Boyle, D., 2005. Advances in Geosciences Comparison of different efficiency criteria for hydrological model assessment. *Advances in Geosciences*, 5, 89–97.

Lachaal, F., Mlayah, A., Bédir, M., Tarhouni, J., and Leduc, C., 2012. Implementation of a 3-D groundwater flow model in a semi-arid region using MODFLOW and GIS tools: The Zéramdine–Béni Hassen Miocene aquifer system (east-central Tunisia). *Computers & Geosciences*, 48, 187–198. doi:10.1016/j.cageo.2012.05.007.

Laronne, J., Alexandrov, Y. and Reid, I., 2004. Surface water characterization and utilization in the Middle East, respectively exemplified by Nahal Eshtemoa (Wadi Samoa) and the Shiqma Besor (Wadi Gaza) reservoirs, Israel. In: Shuval, H. & Dwiek, H. (eds.) *Water for Life in the Middle East*, Israel/Palestine Center for Research and Information, Jerusalem, 2, 680–692.

Levick, L., Semmens, D., Guertin, D., Burns, I., Scott, S., Unkrich, C., and Goodrich, D., 2004. Adding global soils data to the automated geospatial Watershed Assessment Tool (AGWA). *The 2nd International Symposium on Transboundary Waters Management*, Tucson –Arizona. URL: http://www.tucson.ars.ag.gov/agwa/docs/pubs/sahra-global_soils.pdf [Accessed August 2013].

Liu, Y., Yamanaka, T., Zhou, X., Tian, F., and Ma, W., 2014. Combined use of tracer approach and numerical simulation to estimate groundwater recharge in an alluvial aquifer system: A case study of Nasunogahara area, central Japan. *Journal of Hydrology*, (accepted manuscript). doi:10.1016/j.jhydrol.2014.08.017.

Marlow, D., Moglia, M., Cook, S. and Beale, D., 2013. Towards sustainable urban water management: a critical reassessment. *Water Research*, 47(20), 7150–61. doi:10.1016/j.watres.2013.07.046

McCuen R., 2004. Hydrology analysis and design. 4th edition. Prentice Hall.

McDonald, M. and Harbaugh, A., 1988. *A Modular Three-Dimensional Finite- Difference Ground-Water Flow Model*. US Geological Survey Techniques of Water-Resources Investigations, Book 6, Washington, USA (Chapter A1).

McNider, R., Handyside, C., Doty, K., Ellenburg, W., Cruise, J., Christy, J., … Hoogenboom, G., 2014. An integrated crop and hydrologic modeling system to estimate hydrologic impacts of crop irrigation demands. *Environmental Modelling & Software*, 1–15. URL: http://dx.doi.org/10.1016/j.envsoft.2014.10.009.

Melloul A. and Collin M., 2000. Sustainable Groundwater management of the stressed Coastal Aquifer in the Gaza region. *Hydrological Sciences*, 45(1).

Memarian, H., Balasundram, S., Abbaspour, K., Talib, J., Sung, C., and Sood, A., 2014. SWAT-based Hydrological Modelling of Tropical Land Use Scenarios. *Hydrological Sciences Journal*. doi:10.1080/02626667.2014.892598.

Metcalf & Eddy Inc., 2000. *The Gaza Costal Aquifer Management Program CAMP, Integrated Aquifer management Plan.* Final report prepared under USAID, Contract No. 294-C-99-00038-00. Palestinian Water Authority (PWA), Palestine.

Meteorological Service database, 2013. Archived data, URL: http://www.ims.gov.il/ims [Accessed August 2013].

Ministry of Agriculture (MoA), 2013. Archived data, Gaza–Palestine, (MoA).

Ministry of Planning (MoP), 2007.Archived data, Gaza – Palestine, (MoP).

Moe H., Hossain R., Banna M., Mushtaha A., and Yaqubi A., 2001. Application of a 3-Dimensional coupled flow transport model in the Gaza Strip. In: Ouazar, E., Cheng, A. (Ed.), *Proceedings 1st International Conference on Saltwater Intrusion and Costal*

Aquifer – Monitoring, Modeling, and Management, Morocco. URL: http://olemiss.edu/sciencenet/saltnet/swical.

Mogheir Y., De Lima J. and Singh V., 2005. Assessment of Informativeness of Groundwater Monitoring in Developing Regions (Gaza Strip Case Study). *Water Resources Management*, 19, 737–757.

Moriasi, D., Arnold, J., Liew, V., Bingner, R., Harmel, R., and Veith, T., 2007. Model evaluation guidelines for systematic quantification of accuracy in watershed simulations. *T.ASABE*, 50(3), 885–900.

Moukana, J. and Koike, K., 2008. Geostatistical model for correlating declining groundwater levels with changes in land cover detected from analyses of satellite images. *Computers & Geosciences*, 34(11), 1527–1540. doi:10.1016/j.cageo.2007.11.005.

Neitsch, S., Arnold, J., Kiniry, J., and Williams, J., 2011. *The soil and water assessment tool theoretical documentation version 2009, technical report*. Texas water resources institute, No. 406, URL: http://twri.tamu.edu/reports/2011/tr406.pdf [Accessed August 2013].

Niraula, R., Norman, L., Meixner, T., and Callegary, B., 2012. Multi-gauge calibration for modeling the semi-arid Santa Cruz watershed in Arizona-Mexico border area using SWAT. *Air, Soil and Water Research*, 5, 41–57.

Northeast Region Certified Crop Adviser (NRCCA), Cornell University–New York–US, 2013. Soil hydrology, URL: http://nrcca.cals.cornell.edu/soil/CA2/CA0212.1-3.php [Accessed August 2013].

Obuobie, E., Diekkrueger, B., Agyekum, W., and Agodzo, S, 2012. Groundwater level monitoring and recharge estimation in the White Volta River basin of Ghana. *Journal of African Earth Sciences*, 71-72, 80–86.

Palestinian Water Authority (PWA), 2011. *The Comparative Study of Options for an Additional Supply of Water for the Gaza Strip (CSO-G)*. The Updated Final Report, [Report 7 of the CSO-G], 31 July 2011.

Palestinian Water Authority (PWA), 2013. Archived data, Gaza–Palestine, (PWA).

Panagopoulos, Y., Gassman, P., Jha, M., Kling, C., Campbell, T., Srinivasan, R., …Arnold, J., 2015. A refined regional modeling approach for the Corn Belt - experiences and recommendations for large-scale integrated modeling. *Journal of Hydrology*, doi:10.1016/j.jhydrol.2015.02.039.

Panday, S., Langevin, C., Niswonger, R., Ibaraki, M., and Hughes, J., 2013, *MODFLOW-USG version 1: An unstructured grid version of MODFLOW for simulating groundwater flow and tightly coupled processes using a control volume finite-difference formulation,* U.S. Geological Survey Techniques and Methods, book 6, chap. A45. URL: http://pubs.usgs.gov/tm/06/a45.

Pandey, V., Shrestha, S., Chapagain, S., and Kazama, F., 2011. A framework for measuring groundwater sustainability. *Environmental Science & Policy*, 14(4), 396–407. doi:10.1016/j.envsci.2011.03.008

PCBS (Palestinian Central Bureau of Statistics), 2006. Palestinians at the end of year 2006, Ramallah–Palestine, URL: http://www.pcbs.gov.ps. [Accessed March 2013].

PCBS (Palestinian Central Bureau of Statistics), 2013. Palestinians at the end of year 2013, Ramallah–Palestine, URL: http://www.pcbs.gov.ps. [Accessed March 2014].

PCBS (Palestinian Central Bureau of Statistics), 2015. Palestinians at the end of year 2014, Ramallah–Palestine, URL: http://www.pcbs.gov.ps. [Accessed March 2015].

Peng, T., Lu, W., Chen, K., Zhan, W., and Liu, T., 2014. Groundwater-recharge connectivity between a hills-and-plains' area of western Taiwan using water isotopes and electrical conductivity. *Journal of Hydrology*, 517, 226–235. doi:10.1016/j.jhydrol.2014.05.010.

Penman, H., 1961. Weather, plant and soil factors in hydrology. *Weather*, 16, 207–219.

Potchter, O. and Ben-Shalom, H., 2013. Urban warming and global warming: Combined effect on thermal discomfort in the desert city of Beer Sheva, Israel. *Journal of Arid Environments*, 98, 113–122.

Qahman, K. and Larabi, A., 2006. Evaluation and numerical modeling of seawater intrusion in the Gaza aquifer (Palestine). *Hydrogeology Journal*, 14(5), 713–728. URL: http://link.springer.com/10.1007/s10040-005-003-2.

Quessar, M., Bruggeman, A., Abdelli, F., Mohtar, R., Gabriels, D., and Cornelis, W., 2009. Modeling water- harvesting systems in the arid south of Tunisia Using SWAT. *Hydrology and Earth System Sciences*, 13, 2003– 2021.

Rabah F, 1997. *Quantification of nitrate pollution to groundwater resources of Rafah (Gaza Strip)*. Unpublished M.Sc. Thesis, S.E.E. 10, IHE, Delft, the Netherlands.

Rahman, M., Rusteberg, B., Uddin, M., Lutz, A., Saada, M., and Sauter, M., 2013. An integrated study of spatial multicriteria analysis and mathematical modelling for managed aquifer recharge site suitability mapping and site ranking at Northern Gaza coastal aquifer. *Journal of Environmental Management*, 124, 25–39.

Rapport, D., 2007. Sustainability science: An eco-health perspective. *Sustainability Science*, 2, 77–84

Rassam, D., Peeters, L., Pickett, T., Jolly, I. and Holz, L., 2013. Accounting for surface–groundwater interactions and their uncertainty in river and groundwater models: A case study in the Namoi River, Australia. *Environmental Modelling and Software*, 50, 108–119. doi:10.1016/j.envsoft.2013.09.004.

Ross, M., Geurink, J., Aly, A., Tara, P., Trout, K., and Jobes, T., 2004. *Integrated Hydrologic Model (IHM) Volume 1: Theory Manual*. Water Resource Group, Dept. of Civil and

Environmental Engineering, University of South Florida. URL: http://hspf.com/pub/him/IHM_Theory_Manual.pdf.

Rozos, E. and Makropoulos, C., 2012. Assessing the combined benefits of water recycling technologies by modelling the total urban water cycle, *Urban Water Journal*, 9 (1), 1–10.

Saleh A., 2007. *The Impact of Pumping on Saltwater Intrusion in Gaza Coastal Aquifer, Palestine*. Unpublished M.Sc. Thesis, An-Najah National University, Nablus, Palestine.

Santhi, C., Arnold, J., Williams, J., Dugas,W., Srinivasan, R., and Hauck, L., 2001. Validation of the SWAT model on a large river basin with point and nonpoint sources. *Journal of the American Water Resources Association*, 37(5), 1169–1188.

Science for a changing world (USGS), EarthExplorer, URL: http://earthexplorer.usgs.gov [Accessed March 2012].

Shadeed, S. and Almasri, M., 2010. Application of GIS-based SCS-CN method in West Bank catchments, Palestine. *Water Science and Engineering*, 3(1), 1–13.

Shomar, B., Osenbrück, K. and Yahya, A., 2008. Elevated nitrate levels in the groundwater of the Gaza Strip: distribution and sources. *The Science of the total environment*, 398(1-3), 164–74. URL: http://www.ncbi.nlm.nih.gov/pubmed/18407316 [Accessed January 20, 2014].

Shu, Y., Villholth, K., Jensen, K., Stisen, S. and Lei, Y., 2012. Integrated hydrological modeling of the North China Plain: Options for sustainable groundwater use in the alluvial plain of Mt. Taihang. *Journal of Hydrology*, 464-465, 79–93. doi:10.1016/j.jhydrol.2012.06.048

Siegkas, P., Tagarielli, V., and Petrinic, N., 2014. Modelling Stochastic Foam Geometries for FE Simulations Using 3D Voronoi Cells. *Procedia Materials Science*, 4(2003), 212–217. doi:10.1016/j.mspro.2014.07.604.

Singh, A., Imtiyaz, M., Isaac, R., and Denis, D., 2014. Assessing the performance and uncertainty analysis of the SWAT and RBNN models for simulation of sediment yield in the Nagwa watershed, India. *Hydrological Sciences Journal*, 59 (2), 351–364.

Singh, V. and Woolhiser, D., 2002. Mathematical Modeling of Watershed Hydrology. *Journal of Hydrologic Engineering*, 7, 270–292.

Sirhan, H. and Koch, M., 2013. Numerical Modeling of the Effects of artificial Recharge on hydraulic Heads in constant-Density Ground Water Flow to manage the Gaza Aquifer, Coastal Palestine, South. *In: Proceeding 6th International Conference on Water Resources and Environment Research*, 114–147. doi:10.5675/ICWRER.

Soil and water assessment tool (SWAT). Model website, URL: http://swat.tamu.edu/ [Accessed August 2013].

Spruill, C., Workman, R., and Taraba, J., 2000. Simulation of daily and monthly stream discharge from small watersheds using SWAT model. *American Society of Agricultural Engineers*, 43(6), 1431–1439.

Srinivasan, V., Seto, K., Emerson, R., and Gorelick, S., 2013. The impact of urbanization on water vulnerability: A coupled human–environment system approach for Chennai, India. *Global Environmental Change*, 23(1), 229–239. doi:10.1016/j.gloenvcha.2012.10.002.

Srivastava, V., Graham, W., Muñoz-Carpena, R. and Maxwell, R., 2014. Insights on geologic and vegetative controls over hydrologic behavior of a large complex basin – Global Sensitivity Analysis of an integrated parallel hydrologic model. *Journal of Hydrology*, 519, 2238–2257. doi:10.1016/j.jhydrol.2014.10.020.

Sun, D., Zhao, C., Wei, H., and Peng, D., 2011. Simulation of the relationship between land use and groundwater level in Tailan River basin, Xinjiang, China. *Quaternary International*, 244(2), 254–263. doi:10.1016/j.quaint.2010.08.017.

Tang, F., Xu, H., and Xu, Z., 2012. Model calibration and uncertainty analysis for runoff in the Chao River Basin using sequential uncertainty fitting. *Procedia Environmental Sciences*, 13, 1760–1770. doi:10.1016/j.proenv.2012.01.170

The Central Bureau of Statistics (CBS), 2013, Agricultural Crop Areas, Natural Region 2012, Israel. URL: http://www1.cbs.gov.il/ [Accessed August 2013].

Tuinhof, A., Foster, S., Steenbergen, F., Talbi, A., and Wishart, M., 2011. *Sustainable Groundwater Management Contributions to Policy Promotion Appropriate Groundwater Management Policy for Sub-Saharan Africa*. The GW•MATE Strategic Overview Series published by the World Bank, Washington D.C., USA.

Turkeltauub, T., 2011. *Monitoring and modeling recharge-water fluxes in the deep vadose-zone under different land uses over the southern coastal aquifer, Israel*. Unpublished M.Sc. Thesis, Ben-Gurion University of the Negev, The Jacob Blaustein Institutes for Desert Research.

UN-ESCWA and BGR (United Nations Economic and Social Commission for Western Asia; Bundesanstalt für Geowissenschaften und Rohstoffe), 2013. *Inventory of Shared Water Resources in Western Asia*, Ch.20, Beirut. URL: http://waterinventory.org

United Nations (UN), 1956. *Methods for population projections by sex and age*, Manual III, United Nations publication. Sales No. 56.XIII.3.

Valdivieso, F. and Sendra, J., 2013. Semi-distributed hydrological model with scarce information: An application to a large south-American binational basin. *Journal of Hydrologic Engineering*. doi: 10.1061/(ASCE)HE.1943-5584.0000853.

Wang, D. and Hejazi, M., 2011. Quantifying the relative contribution of the climate and direct human impacts on mean annual streamflow in the contiguous United States. *Water Resources Research*, 47(10), W00J12. doi:10.1029/2010WR010283.

Wang, R., Kalin, L., Kuang, W., and Tian, H., 2013. Individual and combined effects of land use/cover and climate change on Wolf Bay watershed stream flow in southern Alabama. *Hydrological Processes*, doi: 10.1002/hyp.10057.

Water Authorities, Israel (WAI). *Hydrological annual reports*. URL: http://www.water.gov.il/hebrew/Pages/home.aspx [Accessed August 2013].

White, K. and Chaubey, I., 2005. Sensitivity analysis, calibration and validations for a multisite and multivariable SWAT model. *Journal of the American Water Resources Association*, 41(5), 1077–1089.

Wikipedia, 2013. Gaza Strip map, URL: http://en.wikipedia.org/wiki/File:Gaza_Strip_map2.svg [Accessed January 2014]

World Health Organization (WHO), 2010. *Guidelines for Drinking-water Quality*. Third edition incorporating the first and second addenda. Volume 1 - Recommendations, Geneva 2008, WHO.

Wu, P. and Tan, M., 2012. Challenges for sustainable urbanization: a case study of water shortage and water environment changes in Shandong, China. *Procedia Environmental Sciences*, 13(2011), 919–927. doi:10.1016/j.proenv.2012.01.085

Wu, Y. and Liu, S., 2013. Improvement of the R-SWAT-FME framework to support multiple variables and multi-objective functions. *Science of the Total Environment*, 466/467, 455–466.

Xu, X., Huang, G., Zhan, H., Qu, Z., Huang, Q., 2012. Integration of SWAP and MODFLOW-2000 for modeling groundwater dynamics in shallow water table areas. *Journal of Hydrology*, 412/413, 170–181. doi:10.1016/j.jhydrol.2011.07.002.

Yang, J., Reichert, P., Abbaspour, K., Xia, J., and Yang, H., 2008. Comparing uncertainty analysis techniques for a SWAT application to the Chaohe Basin in China. *Journal of Hydrology*, 358(1-2), 1–23. doi:10.1016/j.jhydrol.2008.05.012

Zhang, Y., 2005. Development of Study on Model-SWAT and Its Application. *Progress in Geography*, 24(5), 121–130.

Zheng C., 2009. Recent Developments and Future Directions for MT3DMS and Related Transport Codes. *Groundwater*, 47(5), 620–625.

Zheng, C. and Wang, P., 1999. *MT3DMS: A Modular Three-Dimensional Multispecies Transport Model for simulation of advection, dispersion and chemical reactions of contaminants in groundwater systems*. Documentation and user's guide, U.S. Army Corps of Engineers, Washington, DC20314-1000. URL: http://www.geo.tu-freiberg.de/hydro/vorl_portal/gw-modellierung/MT3DMS Ref Manual.pdf.

Appendix A

Table A.1 Monthly climatic data for study area

Beersheva (Meteorological Service database, 2013)												
Months	JAN	FEB	MAR	APR	MAY	JUN	JUL	AUG	SEP	OCT	NOV	DEC
Tmax ^{o}C	17.9	19.2	23.3	27.3	30.2	33.5	34.8	35.4	33.3	29.6	24.7	20.1
Tmin ^{o}C	7.0	8.3	10.3	13.2	15.8	19.3	21.4	21.9	20.4	16.8	12.0	8.4
Mean rainfall (mm/month)	29.8	43.2	16.0	12.1	1.0	0.0	0.0	0.0	0.8	10.9	21.7	28.0
Dew ^{o}C	4.0	6.0	6.8	7.9	11.4	15.3	17.7	19.1	17.3	14.3	8.8	5.1
Mean relative humidity %	64.7	66.9	60.8	54.4	56.3	58.3	60.6	63.1	62.5	63.7	60.8	62.4
Wind (m/s) (10m height)	2.4	2.5	2.5	2.7	2.6	2.6	2.4	2.3	2.4	2.2	2.1	2.2
Pan evaporation (mm/day)*	2	2.6	3.8	5.9	7.6	8.6	8.4	7.8	6.6	5	3.4	2.1
Global solar radiation, (MJ/m^2/day)	10.7	13.6	18.1	22.8	26.3	28.9	27.9	25.6	22.0	16.8	12.5	10.1

(*) Average value, 1988–2000

Lahav (Meteorological Service database, 2013)												
Months	JAN	FEB	MAR	APR	MAY	JUN	JUL	AUG	SEP	OCT	NOV	DEC
Tmax ^{o}C	15.8	17.0	20.8	25.2	28.5	31.8	33.1	33.6	31.4	27.5	22.5	18.0
Tmin ^{o}C	7.4	8.2	10.0	12.6	14.5	17.7	19.6	20.4	19.4	16.7	13.2	9.4
Mean rainfall (mm/month)	53.7	54.1	28.8	11.7	0.6	0.0	0.0	0.0	0.0	5.8	64.7	54.4
Dew ^{o}C	2.9	5.0	6.0	7.4	10.4	14.3	17.3	18.2	16.5	13.5	8.3	4.4
Mean relative humidity%	60.9	64.2	59.4	53.9	52.4	54.8	59.0	60.2	62.0	62.2	57.8	59.5
Wind (m/s) (10m height)*	2.3	2.6	2.8	2.5	2.6	2.8	2.9	2.6	2.3	1.9	4.9	2.8
Global solar radiation, (MJ/m^2/day)**	10.0	12.9	17.5	21.9	25.5	28.0	27.1	24.8	21.3	16.0	11.8	8.92

(*) Wind speed data for Hebron (Ismail *et al.*, 2013)
(**) Calculated based the interpolation between Negba station and Beersheva station

Ein-Habsor (Meteorological Service database, 2013)												
Months	JAN	FEB	MAR	APR	MAY	JUN	JUL	AUG	SEP	OCT	NOV	DEC
Tmax ^{o}C	18.0	19.2	22.7	26.1	27.9	30.9	32.2	32.5	31.1	28.0	24.2	20.1
Tmin ^{o}C	7.6	8.6	10.3	12.6	15.1	18.5	20.7	21.5	20.2	17.2	12.8	9.3
Mean rainfall (mm/month)	40.1	51.7	21.2	10.6	0.4	0.0	0.0	0.0	0.0	31.3	42.1	62.6
Dew ^{o}C	5.9	7.6	8.5	10.6	13.8	17.5	19.8	20.8	18.7	15.8	11.3	7.3
Mean relative humidity%	70.3	73.3	68.8	66.7	68.4	69.6	70.9	72.6	68.9	71.0	69.7	69.0
Wind (m/s) (10m height)	2.7	2.8	2.7	2.8	2.5	2.4	2.3	2.1	2.2	2.2	2.2	2.4
Pan evaporation (mm/day)*	2.4	2.9	4.1	6.1	7.1	7.8	7.7	7.1	6.2	4.8	3.5	2.5
Global solar radiation, (MJ/m^2/day)	9.6	12.8	16.9	21.2	25.6	27.6	26.7	24.0	21.0	15.5	11.6	9.0

(*) Average value, 1988–2000

Cont., Table A.1 Monthly climatic data for study area

Negba (Meteorological Service database, 2013)												
Months	JAN	FEB	MAR	APR	MAY	JUN	JUL	AUG	SEP	OCT	NOV	DEC
Tmax ^{o}C	17.5	18.3	21.4	25.2	27.2	30.0	31.5	31.9	30.8	27.6	23.9	19.6
Tmin ^{o}C	7.8	8.5	10.0	12.4	14.9	18.7	21.2	22.1	21.0	17.9	13.2	9.5
Mean rainfall (mm/month)	99.9	71.9	33.3	12.9	3.1	0.0	0.0	0.0	0.0	53.4	47.0	71.9
Dew ^{o}C	6.1	8.0	9.1	10.7	13.9	17.7	20.1	20.9	18.5	15.6	10.6	7.2
Mean relative humidity%	70.3	75.0	70.9	66.8	68.2	69.7	71.1	71.6	66.5	67.4	64.9	67.7
Wind (m/s) (10m height)	2.9	3.1	3.0	3.1	2.9	2.9	2.9	2.8	2.8	2.7	2.6	2.6
Pan evaporation (mm/day) *	1.9	2.5	3.4	5.2	6.3	7.2	7.3	6.8	6.1	4.6	3.1	2.1
Global solar radiation, (MJ/m^2/day)	9.4	12.2	16.8	21.1	24.8	27.2	26.3	24.0	20.5	15.3	11.2	8.9

(*) Average value, 1988–2000

Gaza												
Months	JAN	FEB	MAR	APR	MAY	JUN	JUL	AUG	SEP	OCT	NOV	DEC
Tmax ^{o}C [a]	18.0	18.4	19.6	24.7	24.8	27.1	29.8	31.9	30.0	27.6	24.2	20.8
Tmin ^{o}C [a]	10.3	11.4	11.9	15.8	18.6	21.6	23.2	25.0	22.7	20.4	17.4	12.7
Mean rainfall (mm/month) [c]	75.9	71.7	27.7	5.5	0.2	0.0	0.0	0.0	0.0	26.2	55.8	52.0
Dew ^{o}C [d]	8.0	9.0	9.0	14.0	17.0	20.0	22.0	23.0	20.0	17.0	16.0	10.0
Mean relative humidity % [a]	66.0	69.0	64.0	67.0	73.0	77.0	76.0	75.0	65.0	66.0	72.0	62.0
Wind (m/s) (10m height) [b]	2.7	2.8	2.72	2.8	2.52	2.4	2.3	2.1	2.2	2.2	2.24	2.4
Pan evaporation (mm/day) [e]	2.5	2.9	3.7	4.6	5.4	6.0	6.3	6.1	5.6	4.2	3.3	2.6
Global solar radiation, (MJ/m^2/day) [f]	9.5	12.5	16.9	21.2	25.2	27.4	26.5	24.0	20.8	15.4	11.4	9.0

(a) Ghabayen 2001, average values for 20 years
(b) Ein-Habsor station
(c) (PWA, 2013) archived data (from 2004 to 2010)
(d) Calculated based the relation between mean temperature and relative humidity
(e) Ministry of Agriculture-Gaza (average monthly value, 1996–2006)
(f) Calculated based the interpolation between Negba station and Ein-Habsor station

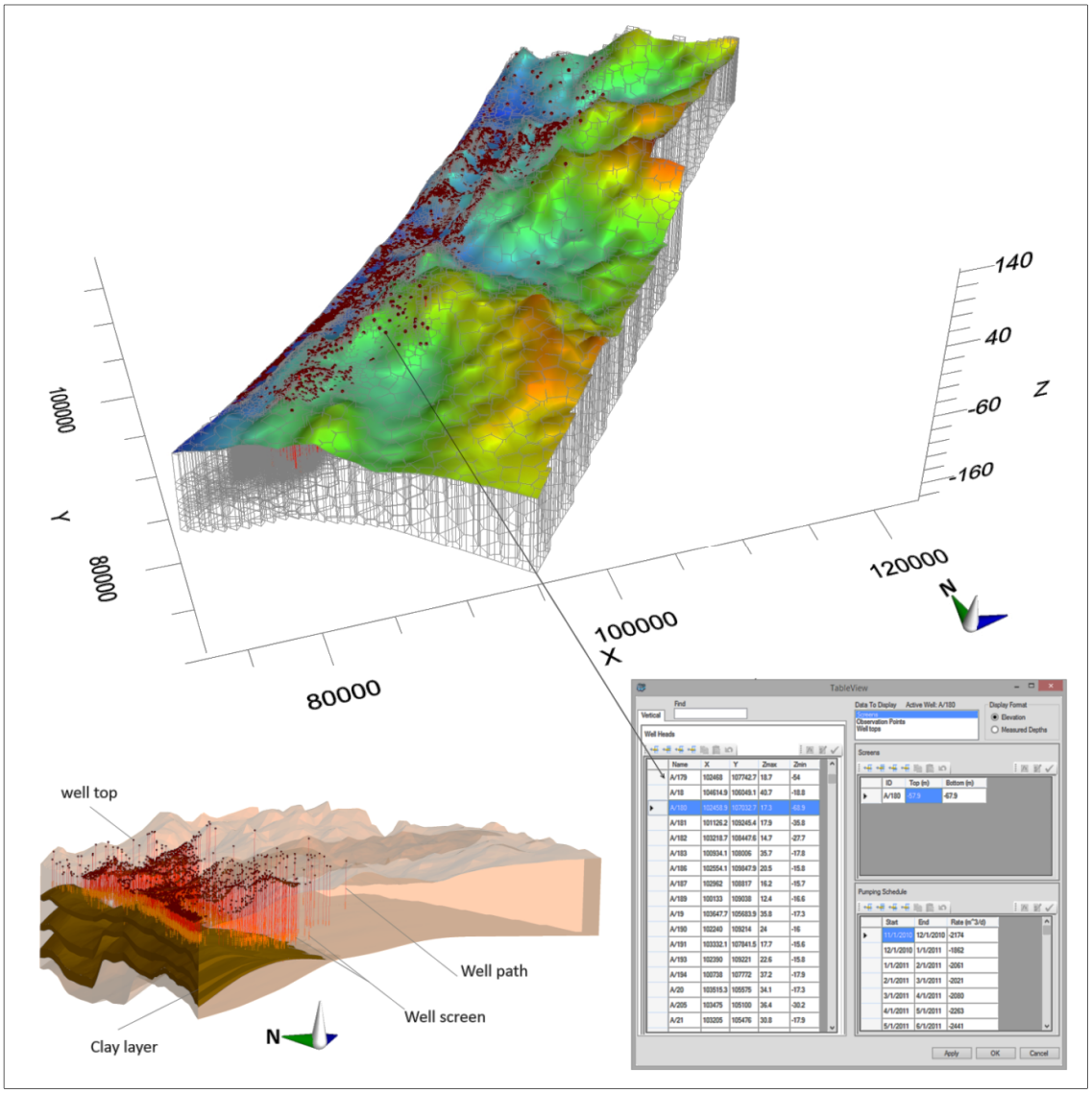

Figure A.1 Aquifer domain and more than 4000 water wells

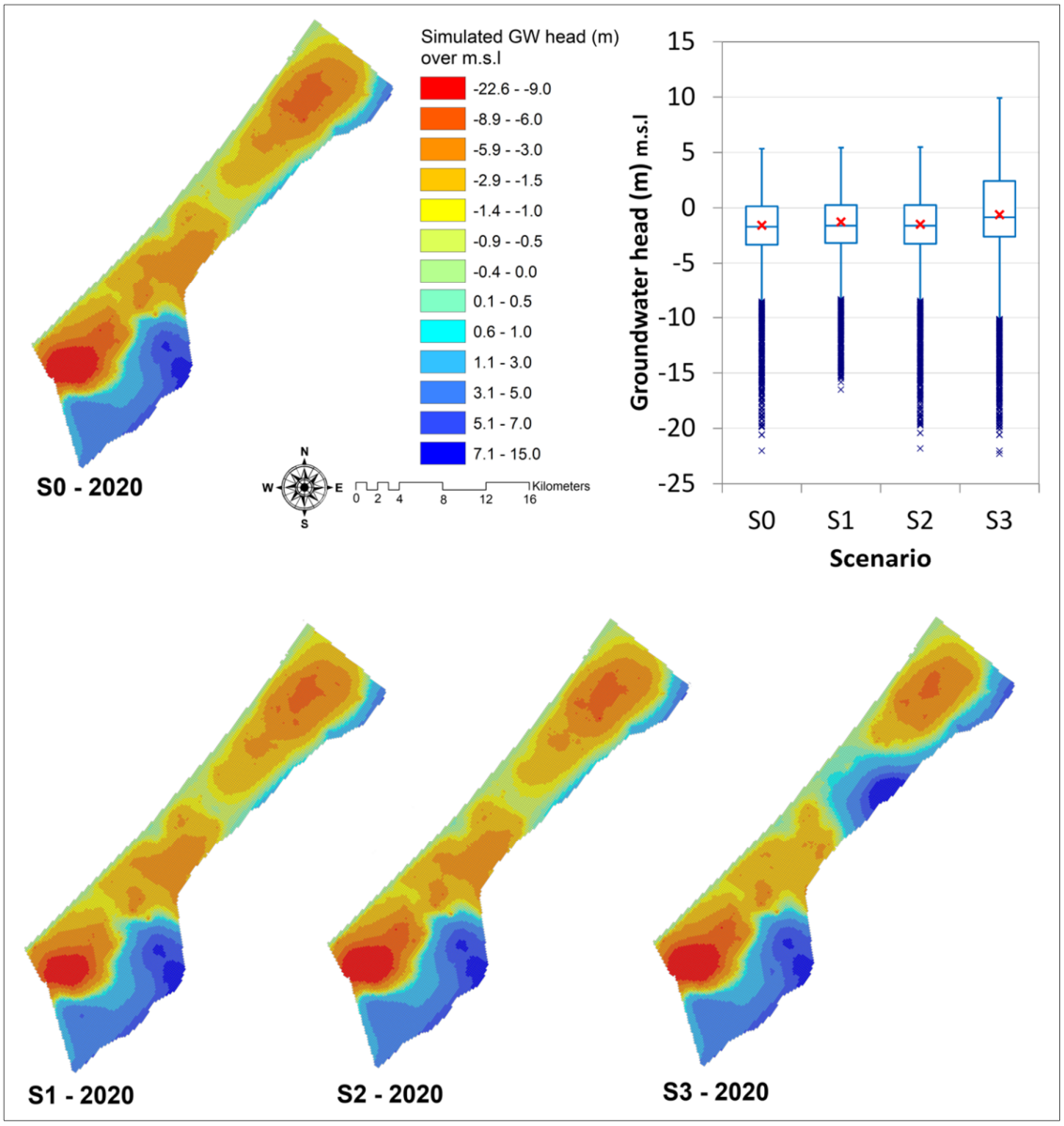

Figure A.2 Simulated groundwater levels in 2020 among scenarios

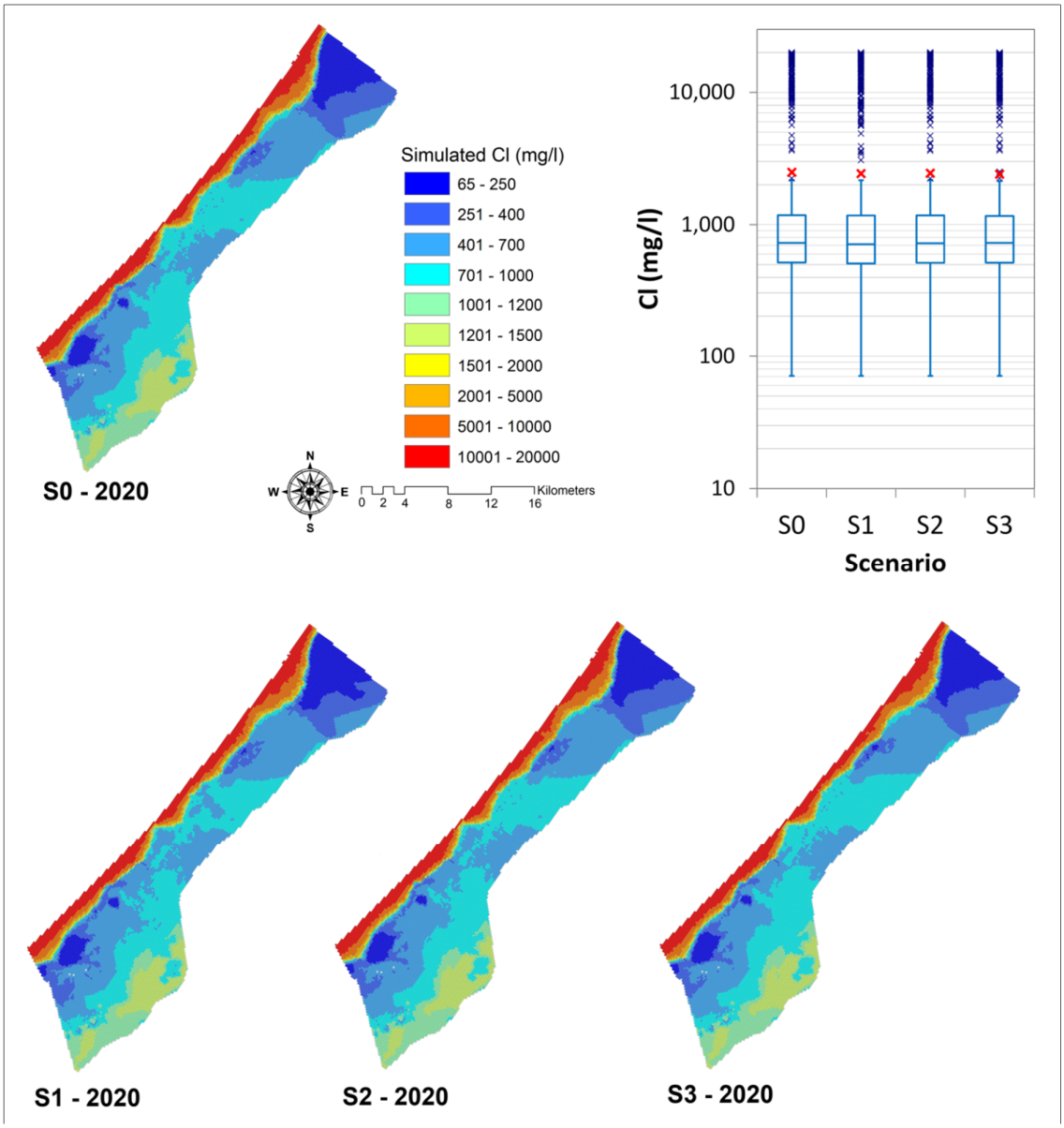

Figure A.3 Simulated chloride concentrations in 2020 among scenarios

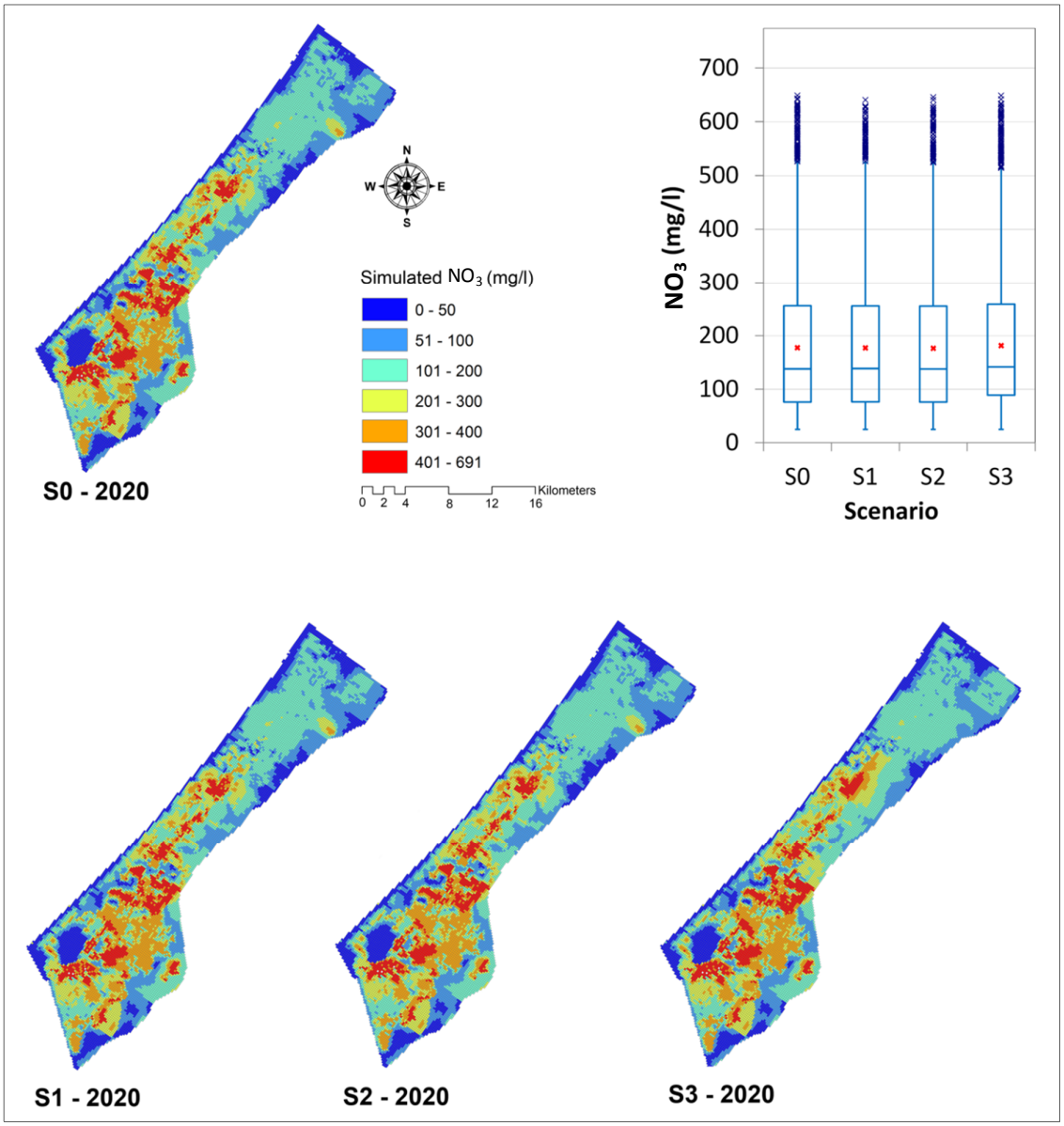

Figure A.4 Simulated nitrate concentrations in 2020 among scenarios